DESIGN AND PERFORMANCE EVALUATION OF MIXED FLOW PUMPS BY NUMERICAL EXPERIMENTATION AND AXIAL THRUST INVESTIGATION

A THESIS SUBMITTED TO
THE GRADUATE SCHOOL OF NATURAL AND APPLIED SCIENCES
OF
MIDDLE EAST TECHNICAL UNIVERSITY

BY

ALİ CİRİT

IN PARTIAL FULFILLMENT OF THE REQUIREMENTS
FOR
THE DEGREE OF MASTER OF SCIENCE
IN
MECHANICAL ENGINEERING

OCTOBER 2007

Approval of the thesis:

DESIGN AND PERFORMANCE EVALUATION OF MIXED FLOW PUMPS BY NUMERICAL EXPERIMENTATION AND AXIAL THRUST INVESTIGATION

submitted by **ALİ CİRİT** in partial fulfillment of the requirements for the degree of **Master of Science in Mechanical Engineering Department, Middle East Technical University** by,

Prof. Dr. Canan Özgen _____
Dean, Graduate School of **Natural and Applied Science**

Prof. Dr. S. Kemal İder _____
Head of Department, **Mechanical Engineering**

Prof. Dr. Kahraman Albayrak _____
Supervisor, **Mechanical Engineering Dept., METU**

Examining Committee Members

Prof. Dr. O. Cahit Eralp _____
Mechanical Engineering Dept., METU

Prof. Dr. Kahraman Albayrak _____
Mechanical Engineering Dept., METU

Prof. Dr. M. Haluk Aksel _____
Mechanical Engineering Dept., METU

Dr. A. Tahsin Çetinkaya _____
Mechanical Engineering Dept., METU

M. Sc. Onur Konuralp _____
Project and Quality Control Manager, Layne Bowler

Date: 17.10.2007

I hereby declare that all information in this document has been obtained and presented in accordance with academic rules and ethical conduct. I also declare that, as required by these rules and conduct, I have fully cited and referenced all material and results that are not original to this work.

Name, Last name: Ali Cirit

Signature :

ABSTRACT

DESIGN AND PERFORMANCE EVALUATION OF MIXED FLOW PUMPS BY NUMERICAL EXPERIMENTATION AND AXIAL THRUST INVESTIGATION

Cirit, Ali
M. S., Department of Mechanical Engineering
Supervisor : Prof. Dr. Kahraman Albayrak

October 2007, 117 pages

In this thesis a vertical turbine mixed flow pump that has a flow rate of 40 l/s and 16 mwc head at 2900 rpm is designed. Effect of design parameters are investigated and flow inside the pump is analyzed with the help of numerical experimentations. The designed pump is manufactured and tested in Layne Bowler Pumps Company and completed in TÜBİTAK – TEYDEB project. Pump is designed in the tolerance limits that are defined in the standard TS EN ISO 9906. Numerical experimentation results for performance characteristics show the same trend with the test results.

In addition, axial thrust measurements are done on the designed pump with using load cells. Effect of balancing holes and balancing ring are investigated. Balancing holes are drilled at various diameters at the back side of the impellers and its effect is analyzed on the pump performance characteristics. Test results are compared with different approaches.

Keywords: Vertical turbine mixed flow pump, CFD analysis, Pump performance test, Axial thrust, Balancing holes, Balancing ring

ÖZ

SAYISAL DENEYLER İLE KARIŞIK AKIŞLI POMPALARIN TASARIMI, PERFORMANS ANALİZİ VE EKSENEL İTME İNCELEMESİ

Cirit, Ali
Yüksek Lisans, Makina Mühendisliği Bölümü
Tez Yöneticisi: Prof. Dr. Kahraman Albayrak

Ekim 2007, 117 sayfa

Bu tezde, 40 l/s debi ve 16 mss basma yüksekliğine sahip karışık akışlı dik türbin pompa 2900 d/d'da tasarlanmıştır. Tasarım parametrelerinin etkisi ve pompa içerisindeki akış sayısal deneyler yardımıyla incelenmiştir. Tasarlanan pompa Layne Bowler Pompa Sanayi'nde üretilmiş, test edilmiş ve TÜBİTAK-TEYDEB projesi kapsamında tamamlanmıştır. Pompanın tasarımı TS EN ISO 9906 standartlarında belirtilen tolerans sınırları dahilinde yapılmıştır. Sayısal deneylere ait pompa performans karakteristikleri sonuçlarının test sonuçları ile aynı eğilime sahip olduğu görülmüştür.

Ayrıca, tasarlanan pompa üzerinde yük hücreleri yardımı ile eksenel yük ölçümleri yapılmıştır. Dengeleme delikleri ve dengeleme halkasının etkileri incelenmiştir. Çark arka tarafına açılan değişik çaptaki dengeleme deliklerinin pompa performansı üzerine olan etkileri gözlemlenmiştir. Test sonuçları değişik yaklaşımlarla karşılaştırılmıştır.

Anahtar kelimeler: Dik türbin karışık akışlı pompa, HAD analizi, Pompa performans testi, Eksenel itme, Dengeleme delikleri, Dengeleme halkası

to those who help me throughout my life

ACKNOWLEDGEMENTS

I wish to express my deepest gratitude to my supervisor Prof. Dr. Kahraman ALBAYRAK for his guidance, encouragement and invaluable help throughout this study.

This thesis is based on the project supported by TÜBİTAK – TEYDEB which is proposed by Layne Bowler Pumps Company. I would like to thank Mr. Onur KONURALP, manager of Layne Bowler Project and Quality Control Department, for his matchless support and advices throughout the thesis. The invaluable help of Mr. Ramazan ÖZCAN in any technical subject is gratefully acknowledged. I would like to thank Mr. Kayhan CENGİZ for his contributions in technical drawings. Special thanks go to Mr. Mehmet BEYAZÇİÇEK for his cooperation throughout the tests. I also want to thank all of the workers of Layne Bowler who help me during my study.

I wish to thank Mr. Onur ÖZGEN for his great help and encouragement throughout the thesis. His contributions to thesis are gratefully acknowledged.

I express my sincere appreciation to Mr. Alper ALP for his never-ending support and friendship throughout the life.

Finally, I would like to thank my parents Bekir CİRİT and Neşe CİRİT for their endless support, sacrifice and love.

TABLE OF CONTENTS

LIST OF TABLES

TABLES

LIST OF FIGURES

LIST OF SYMBOLS

SYMBOLS

b	breadth
d	diameter
e	blade thickness, vane thickness
g	gravitational acceleration
h	pressure head
k	number of parameters
l_m	length of midstreamline
m	mass
mwc	meters water column
n	rotational speed in revolutions per minute
r	radius, number of primary dimensions
s	safety of coefficient , standard deviation
t	arc length, collet thickness
x	value of measured quantity
$\overline{x}$	average of measured quantity
z	number of blades, number of vanes
A	area
BEP	best efficiency point
CC	constriction coefficient
C_P	Pfliederer correction factor
D	diameter
DR	diffusion rate
H	pump head
Hdyn	dynamic water level
Hm	head measured by manometer
Ht	total head
K	empirical coefficient

L	length
K_T	thrust coefficient
M	static moment, mass
N_S	specific speed
P	power, pressure
PS	pressure side
Re	Reynolds Number
SS	suction side
Q	flow rate
T	thrust, time
Th	thrust (in dimensional analysis)
U	tangential component of velocity, uncertainty
V	absolute velocity
W	relative velocity
α	fluid angle, power margin, axial thrust coefficient, relaxation factor
β	blade angle
λ	angle between breadth and streamline
η	efficiency
η_S	system efficiency of pump
μ	dynamic viscosity
π	pi number
ρ	density of fluid
ω	angular speed
τ	torsionalst ress
σ	yield strength
ϕ	flow coefficient, flow property
ψ	head coefficient
Γ	circulation
ζ	velocity loading
Π	Buckingham Pi number

INDICES

0	inlet eye of the impeller
1	inlet of the blade
2	outlet of the blade before slip
3	outlet of the blade after slip
4	inlet of bowl
dyn	dynamic
f	fluid
h	hydraulic
i	inlet
m	meridional, mechanical
n	number of measurements
p	Pfleiderer, pump, pipe
s	shaft
t	total
th	theoretical
wr	wearing ring
θ	tangential direction
v	volumetric
A	mid streamline
M	motor
P	power
Q	flow rate
R	random
S	shaft, systematic, system
T	total
V	volume
η	efficiency
ρ	density of fluid
∞	infinity

CHAPTER 1

INTRODUCTION

1.1. Brief History of Pump

Water plays an important role in human life from the existence of the human being. Throughout the history human want to raise and transport water from one place to another. By the time, cities grew and potential energy of the water became insufficient to transport it so there is a need for giving energy to water and carrying it to further distances.

From the engineering point of view invention of Denis Papin, which was found in 1689, is regarded as the first centrifugal pump. Water enters axially to the machine and it is accelerated by two straight blades. Then it exits from the machine in circumferential direction. The machine is driven by hand. It was used to remove water from mines. In 1875, Osborne Reynolds obtained patent of the first vaned diffuser and these types of pumps were began to be produced in 1878. His invention looks like a turbine and these types of pumps are named as turbine pump after his invention.

Today, increasing of population, expansion and development of cities, becoming widespread of irrigation make demand to water more than before. However, the water resources are limited. On the other hand, distances between resources and consumption areas are increasing. These situations cause constructing of pump stations, reservoirs, long pipelines which result in high operation costs.

Pumps are the most important equipments when transportation of limited underground and surface resources to the consumers. Dimensions of pumps are expanding due to requirement of pumps with high flow rate and head. As a result

power requirements also increase. Besides, pumps consume 20% of electric production all over the world. This necessitates designing of efficient, lightweight and robust pumps.

1.2. General Information about Vertical Turbine and Mixed Flow Pumps

A vertical turbine pump is made up from four main assemblies. These are driver, discharge assembly (discharge head or discharge elbow), column assembly and pump assembly, [1].

Vertical turbine pumps are used for drainage, irrigation, sewage pumping, service water storage and boosting, pipeline boosting, fire fighting and water pumping from canal, river, sea or lake, [2]. Vertical turbine pumps are generally driven by electric motors. Electric motors are submersible motors, vertical hollow shaft (VHS) motors and vertical solid shaft (VSS or V1) motors. Diesel engine motors, turbines, tractors, vertical pulleys can also drive pumps with a right angle gear.

"A submersible pump is a pump which has a hermetically sealed motor close-coupled to the pump body", [3]. Both motor and pump are submerged into the water. Since electric motor is coupled to the pump there are no long shafts, bearings and bearing retainers. Submersible pumps are generally installed in a borehole and used in water wells. When VHS and V1 motors are considered, motor is installed on the ground over the discharge head. Torque is transmitted to the pump with line shafts whose total length changes with installation depth.

Discharge heads are used with VHS and V1 motors to support the motor body, while discharge elbows are used with submersible motors. Discharge heads are cast parts for most of the pump applications, with increasing dimension of pumps steel constructions are manufactured and used. Discharge assembly also holds the whole pump assembly. It is connected to the column assembly and the discharge line. It is fixed to the ground with anchorage bolts and base plate.

Column assembly includes pipes, intermediate shafts, bearings, bearing retainers and couplings. Its length increases with installation depth. Pipes are connected to each other with bolts and nuts. Intermediate shafts are used to transmit torque from head shaft to pump shaft. Couplings make the connection between shafts. Bearings and bearing retainers compensate dynamic radial forces which appear while the pump operates. There can be changes in the column assembly according to the type of lubrication. Water lubrication or oil lubrication can be applied on shafts in pump applications. In water lubrication, shafts and bearings are lubricated with water. Generally, it is used in the applications which the static water level is not high because at start-up bearings could not be lubricated with water. However in oil lubrication, shafts and bearings are always lubricated with oil so wear in these parts is minimized. Also, enclosed shaft do not face with abrasive particles such as sand or others, [2].

Last of all, pump assembly contains the main parts which are impellers, bowls (return passages), suction intake, strainer, collets, pump shafts and bearings, Figure 1.1. Pump assembly is designed according to requirements of the client. These are capacity, total head and revolution speed of the pump.

Impellers are categorized according to their specific speed as radial, mixed flow or axial, Figure 1.2. "The specific speed of an impeller is defined as the revolutions per minute at which a geometrically similar impeller would run if it were of such a size as to discharge one unit flow rate against one unit head", [4].

$$N_S = \frac{\omega\sqrt{Q}}{(gH)^{0.75}} \tag{1.1}$$

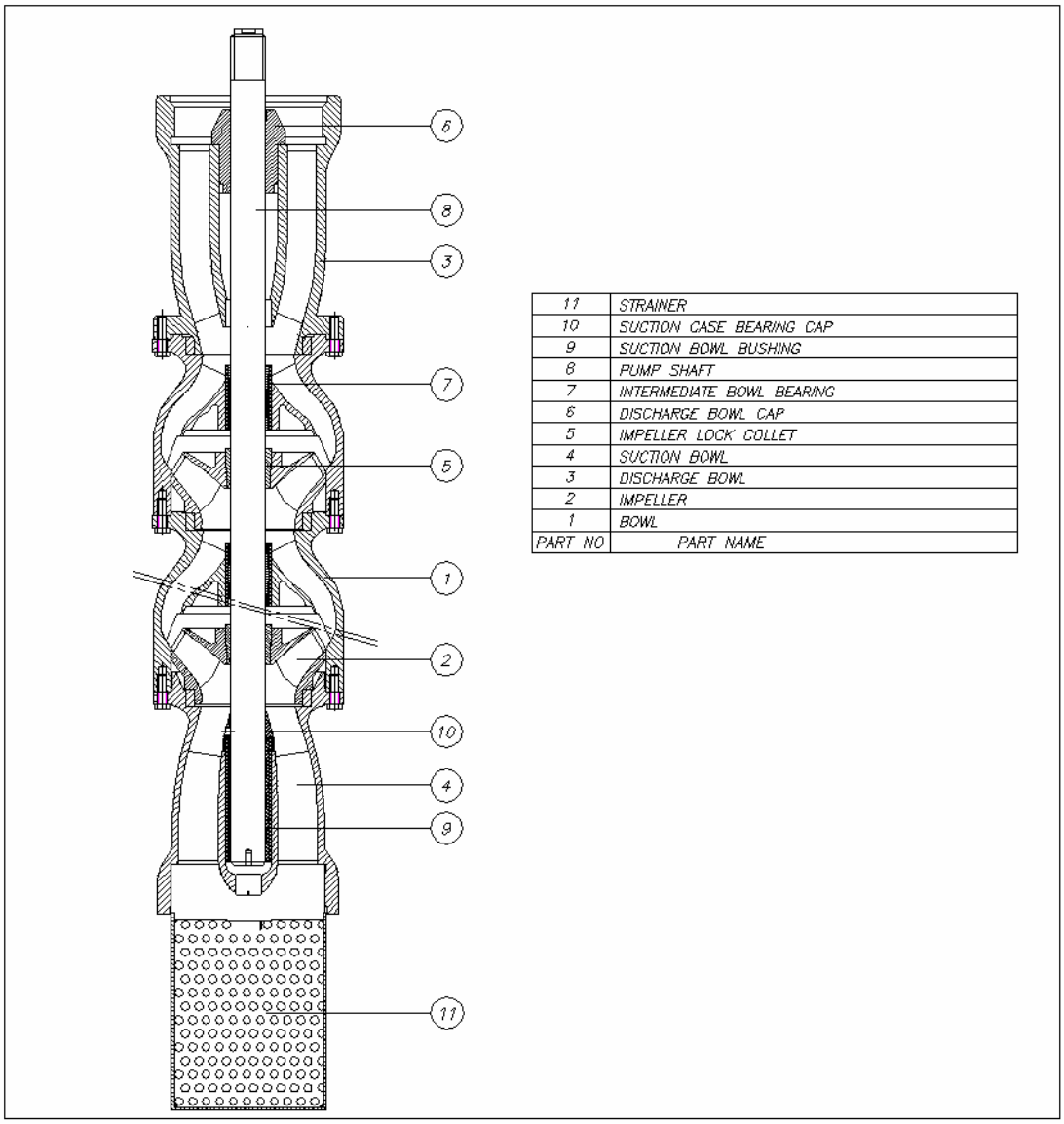

PART NO	PART NAME
11	STRAINER
10	SUCTION CASE BEARING CAP
9	SUCTION BOWL BUSHING
8	PUMP SHAFT
7	INTERMEDIATE BOWL BEARING
6	DISCHARGE BOWL CAP
5	IMPELLER LOCK COLLET
4	SUCTION BOWL
3	DISCHARGE BOWL
2	IMPELLER
1	BOWL

Figure 1.1 Vertical turbine pump assembly, (Layne Bowler)

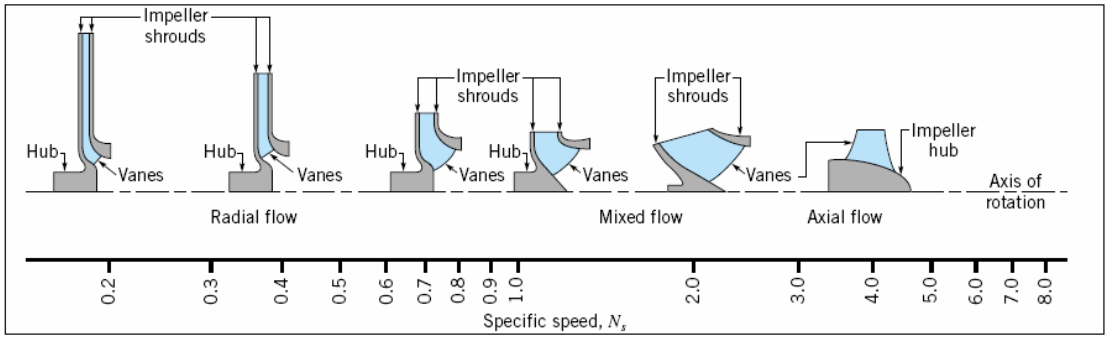

Figure 1.2 Profiles of impellers according to specific speed, [5]

ω is the angular speed in rad/s, Q is the capacity (flow rate) in m^3/s, H is the head in m and g is the acceleration of gravity in m/s^2 in ISO units. Specific speed N_S is dimensionless. For radial pumps it changes from 0.2 to 0.7, for mixed flow pumps it changes from 0.6 to 2.7 and for axial flow pumps specific speed changes from 2.5 to 7. It gives an idea about how shape of the impeller and bowl may be for a given flow rate, head and angular speed, [5]. Pumps are designed for required flow rate and efficiency of the pump assembly is maximum at this flow rate. This point is called as best efficiency point. Pumps operate flow rates near best efficiency point for energy savings and other mechanical considerations. Efficiency of the pump changes with dimension and specific speed of the pump, Figure 1.3. In the figure specific speed (N_{sQ}) is calculated with Equation 1.2 where n is in revolutions per minute. Specific speed of mixedflow pumps is changed between 4 0 and 150 in this scale.

$$N_{sQ} = \frac{n\sqrt{Q}}{(H)^{0.75}} \tag{1.2}$$

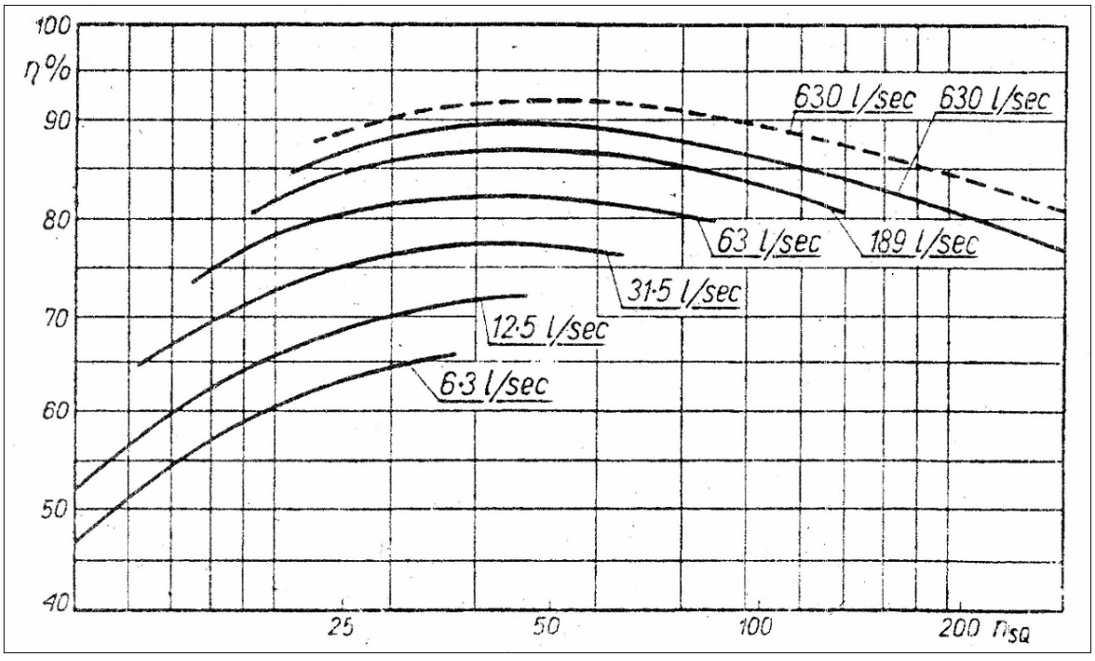

Figure 1.3 Pump efficiency versus specific speed (Worthington), [6]

Overall pump efficiency is calculated by multiplying hydraulic, mechanical and volumetric efficiencies.

Hydraulic efficiency is defined as the ratio of the effective head to the internal head. Hydraulic losses happen due to friction between the fluid and the walls in all flow passages (including suction, impeller and bowl) acceleration and deceleration of the fluid, [4], [6]. It has an upper limit related with specific speed of the impeller, design parameters and manufacturing abilities.

Mechanical efficiency is defined as the ratio of the internal power to the power input of the motor to the pump shaft. The losses at the bearings, couplings, seals, stuffing box and shafts decrease the mechanical efficiency. Also disk friction, the loss between impeller shrouds and stationary walls, affects the mechanical efficiency, [6].

Volumetric efficiency is defined as the ratio of the discharge to the internal discharge. A leakage occurs from high pressure (exit of the impeller) to low pressure (inlet of the impeller) at wearing rings, labyrinths, balancing holes and glands.

These efficiencies also depend on manufacturing techniques, operating position of impeller in bowl (lateral clearance), dimensional tolerances, materials of the pump parts, fluid to be pumped and operating conditions. Lifetime costs, permanent and optimum efficiency can be assessed taking into account all of these efficiencies.

1.3. General Information about Axial Thrust

Higher pressure exists at the exit of the impeller rather than the suction of the impeller while the pump is operating. On the other hand, back surface of the impeller, where higher pressure exists, is larger than the bottom surface of the impeller. Momentum of the fluid changes after passing through the impeller. Therefore, an unbalanced force occurs on the shaft while the pump is operating. This force is named as axial thrust and transmitted from impeller to the pump shaft, line

shaft, head shaft, adjusting nut, clutch of the motor and bearings of the motor respectively (when a vertical hollow shaft – VHS motor is used). For vertical turbine pumps, axial thrust is calculated approximately multiplying pump head with axial thrust coefficient of the pump assembly in practice. The unit of axial thrust coefficient is kilogram per meter. When axial thrust is too high to compensate from motor bearings, additional bearings are mounted on the head shaft of the pump. This assembly is called as thrust bearing assembly. Thrust bearing assembly is generally used with V1 electric motors. On the other hand in submersible pumps, axial thrust is compensated with journal bearings of the motor. If journal bearings are damaged, submersible motor could not work properly and windings of motor may burn.

For vertical turbine pumps axial thrust has a significant effect on the mechanical and volumetric efficiencies. The methods used to lower axial thrust such as balancing holes and balancing disks affect mechanical and volumetric efficiencies of the pump. High axial thrust makes it necessary to use high capacity bearings to compensate these forces. Mechanical losses increase with axial thrust and cause to decrease lifetime of the system.

Axial thrust plays important role on selection of shafts, bearings and couplings. Costs of these components can be reduced with measurement of these forces. The obtained results can be used from motor manufacturers, which use bearings to compensate these forces in submersible and vertical hollow shaft (VHS) type motors. For vertical solid shaft (V1) motors, cost of additional thrust bearings and lubrication of these components can be reduced. All of these works lead to designing of efficient electric motors and pumps.

Yücel (1999) [7] investigated axial thrust on a radial pump. He used an axial thrust transducer on a special designed bearing cover and measured the forces, acted on the bearings. In addition, he opened pressure taps on casing of the pump and measured the pressures at those locations. With the help of the pressure measurements he

calculated the axial thrust acting on the pump shaft. He investigated the effects of balancing holes on the axial thrust.

To measure axial thrust in multistage vertical turbine pumps, load cell equipment is used in this study. Special assembling parts are manufactured for this purpose. Axial thrust is tried to minimize without decreasing overall pump efficiency. Approaches, used to decrease axial thrust, which are balancing holes and balancing disks are analyzed systematically. This includes application of different diameter of balancing holes with or without balancing disk. Axial thrust is measured on every combination with prepared test equipment.

1.4. General Layout of the Thesis

In this thesis, a vertical turbine pump is designed, manufactured and tested. The objectives of the study are to analyze design parameters effect on the pump performance, to understand the flow inside the pump better, to compare test results with numerical experiment results and to investigate axial thrust balancing techniques.

In Chapter 1, general information about vertical turbine pumps is given. In Chapter 2, hydraulic designs of the pump components are explained and manufacturing steps are mentioned. Chapter 3 includes information about axial thrust, theoretical approaches to calculate axial thrust, parameters that affect the axial thrust and axial thrust measurement test setup. In Chapter 4 numerical experimentation process of the designed pump are introduced. Test setup and test procedure for pump performance tests are presented in Chapter 5. Finally, in Chapter 6 discussions on the results and conclusions are done. Also results of numerical experimentation and tests are given and compared in this chapter.

CHAPTER 2

HYDRAULIC DESIGN AND MANUFACTURING OF THE PUMP

In this study a vertical turbine pump with a specific speed of 1.37 is to be designed, manufactured and tested. It has a design capacity of 40 l/s and 16 mwc head at 2900 revolutions per minute. Pump efficiency is assumed to be 77% from Figure 1.3., volumetric efficiency is assumed as 95% and mechanical efficiency is assumed as 96%.

A vertical turbine pump has mainly three components which affect the hydraulic performance of the pump. These are impeller, bowl and suction. Impellers are the heart of the pumps. The energy of the rotating parts is exerted on the fluid particles by impeller blades. Design process of the impeller includes developing the meridional profile and forming the blades from leading edge to trailing edge after determining of the blade inlet and outlet angles. Bowls are named as return passages for vertical turbine pumps sometimes, because they guide the fluid through its way from impeller exit to inlet of next impeller. It is generally designed as a diffuser to gain pressure recovery from the kinetic energy of the fluid to be pumped. The main approach for designing bowl vanes includes changing the velocity components (circumferential and meridional) gradually from bowl inlet to bowl outlet. Suction intake is another important part as it has a significant effect on performance of the pump. A bad designed suction may cause cavitation which will reduce the performance of the pump. However, most of the vertical turbine pumps are installed in wells, so they do not suck water with a suction line which causes pressure of the fluid to drop. Main design criterion is to constitute an acceptable fluid velocity at suction intake. On the other hand when the requirements become large by means of capacity and head mechanical considerations also become important. Selection and design of these parts necessitate a great attention to reduce mechanical losses.

2.1. Impeller Design

The main feature thataffects the impeller performance is the meridional profile. The literature is so limited for meridional profile effect on pump performance characteristics and developing the meridional profile greatly depends on know-how or evaluation of good previous designs. Impeller shape is determined by specific speed of the pump, Figure 1.2. Change in direction of the fluid after leaving the impeller makes the impellers to be named as radial, mixed flow or axial. In radial (centrifugal) pumps fluid leaves the impeller in a direction approximately perpendicular to the shaft axis. The blade design is done using single curvature method, [6]. Impeller creates pressure by means of the velocity of the fluid derived from centrifugal force. In mixed flow pumps fluid changes its direction in both radial and axial ways. Pressure is created both by diffusion and centrifugal effect of the impeller rotational speed. Double curvature method is used for forming of the blades. Finally, in axial flow pumps fluid enters axially and exits axially from impeller parallel to the pump shaft axis. Centrifugal effect does not play role to increase pressure of the fluid, [8]. Profiles are selected and used at different sections of blades in the design process of axial impellers.

2.1.1. Impeller Profile

“To design a new impeller for which no model is available designers use ‘design factors’ established experimentally from successful designs that give direct relationship between the impeller total head and capacity at the design point and several elements of Euler’s velocity triangles.”, [9]. General shapes are given in Reference [1] for several specific speeds Figure 2.1. In the figure specific speed is calculated with Imperial units.

Beginning with specific speed calculation development of the impeller meridional profile begins,

$$N_S = \frac{\omega\sqrt{Q}}{(gH)^{0.75}} \tag{2.1}$$

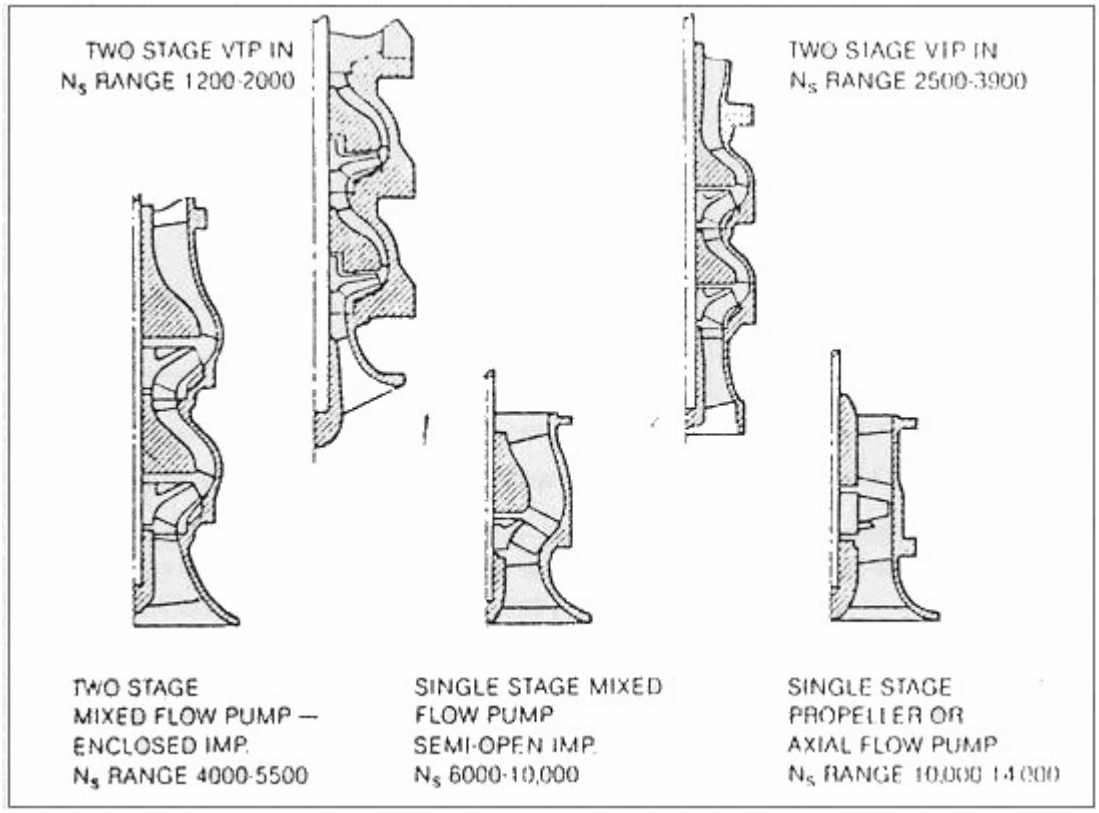

Figure 2.1 Development of assembly design for several specific speeds, [1]

According to specific speed several non dimensional numbers and design charts are used while creating impeller meridional profile.

These non dimensional numbers, derived with Buckingham Pi theorem, are, [10]

$$\pi_1 = \frac{Q}{\omega D_2^3} \text{ or } \varphi = \frac{Q}{U_2 A} = \frac{V_{m2}}{U_2} \tag{2.2}$$

$$\pi_2 = \frac{gH}{\omega^2 D_2^2} \text{ or } \Psi = \frac{gH}{U_2^2} \tag{2.3}$$

$$\pi_3 = \frac{P}{\rho\omega^3 D_2^2} \tag{2.4}$$

$$\pi_4 = \frac{\rho \omega D_2^2}{\mu} \text{ or } Re = \frac{\rho U_2 D_2}{\mu} \tag{2.5}$$

where P is the pump power (W), ρ is the fluid density (kg/m^3), μ is the dynamic viscosity (Pa.s), D is the impeller outlet diameter (m) and U is the circumferential velocity (m/s)

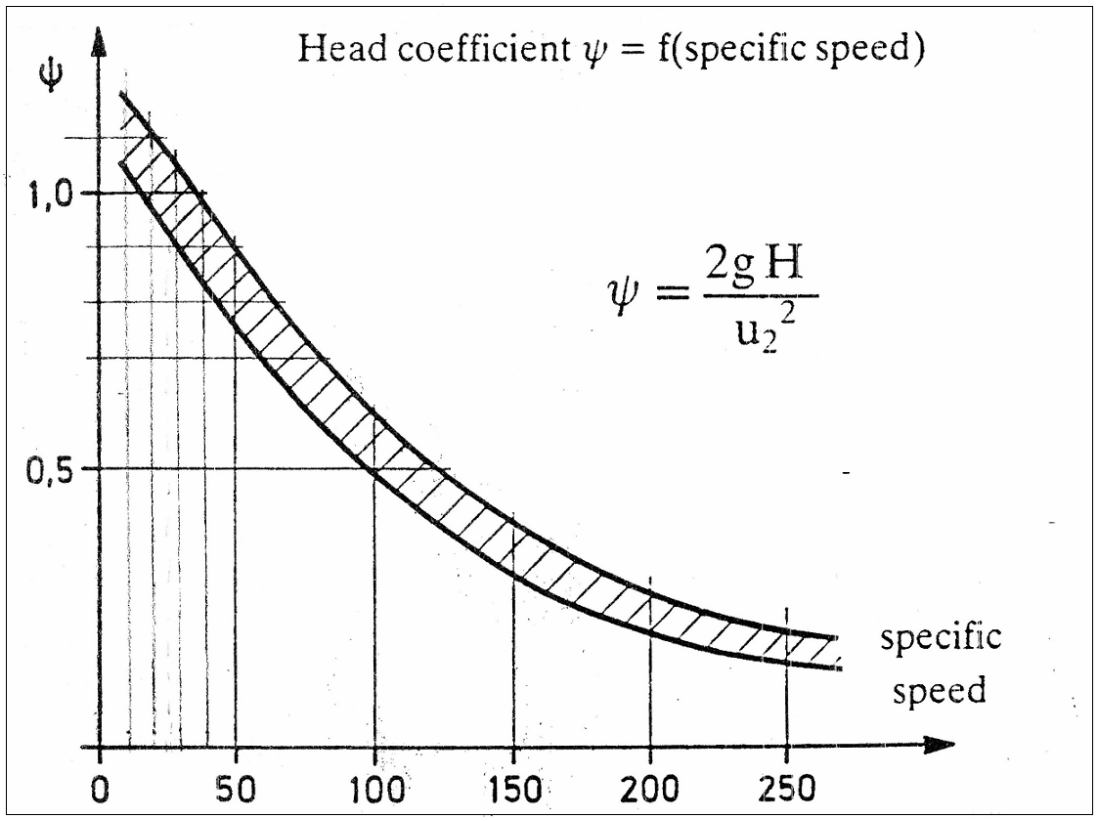

Figure 2.2 Head coefficient versus specific speed, [11]

First equation is for flow coefficient, second one is for head coefficient, third one is for power coefficient and fourth one is for Reynolds number.

Also there exist some other design charts which give geometrical relations between dimensions of the impeller, Figure 2.3.

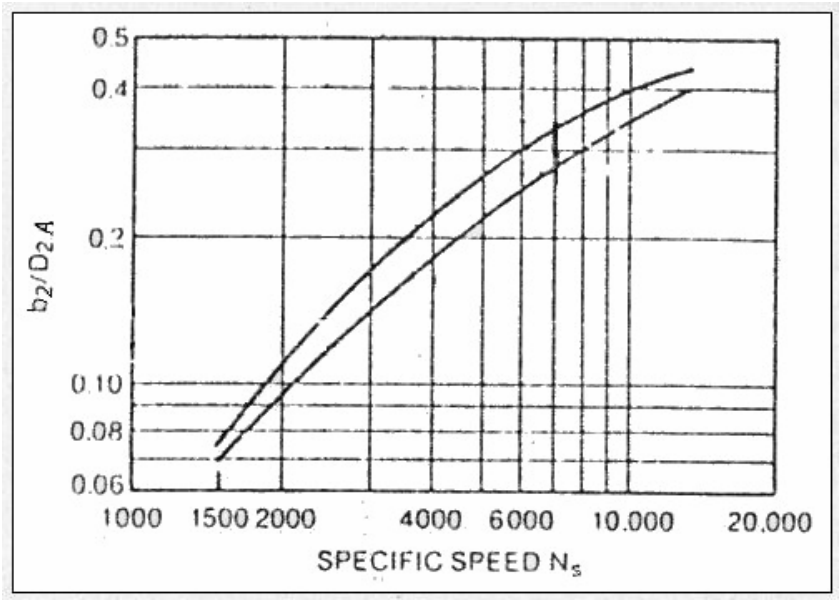

Figure 2.3 Design chart showing b_2/D_{2A} ratio, [1]

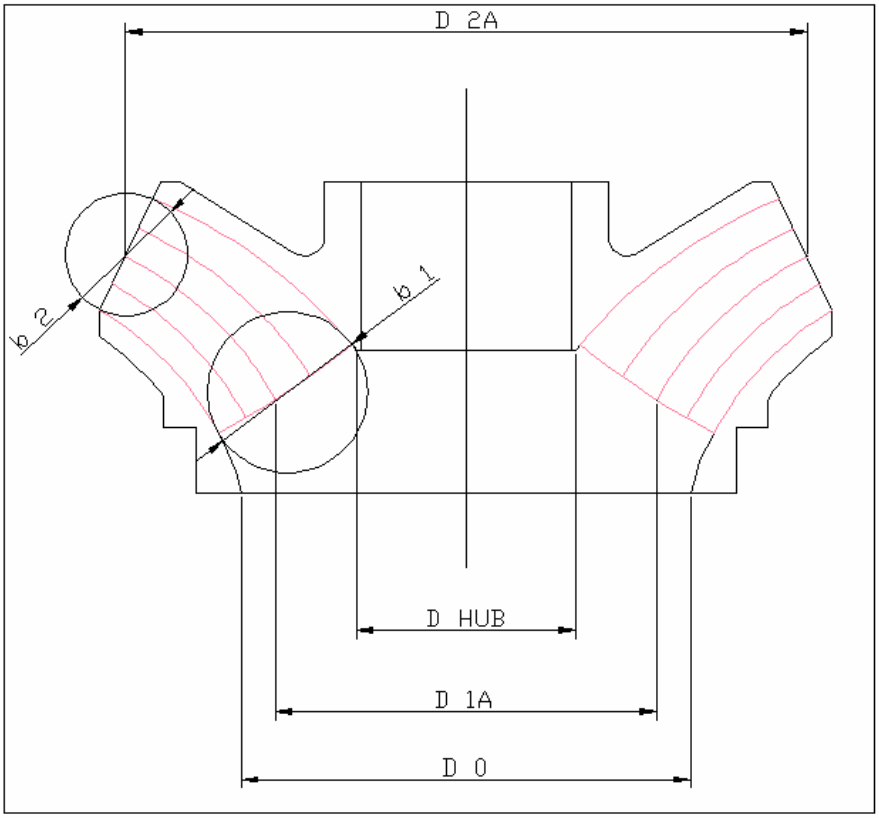

Figure 2.4 Main dimensions of an impeller

Firstly, to determine shaft diameter, shaft power is to be calculated first, [8]. It is clearly seen that shaft diameter is not calculated for single stage pump and must be selected for the head value of multistage vertical turbine pump. Otherwise pump shaft may fail.

$$P_S = \frac{P_{HYDRAULIC}}{\eta} = \frac{\rho g Q H}{\eta} \tag{2.6}$$

η is the overall pump efficiency estimated using Figure 1.3, which is obtained from experimental data. To find the required motor power P_M, power margin is multiplied with calculated shaft power. These values that change with shaft power are given in Table 2.1

$$P_M = \alpha P_S \tag{2.7}$$

Table 2.1 Power margins for different shaft powers

Shaft Power – P_S [kW]	**α**
$P_S < 1.5$	$1.4 < \alpha < 1.5$
$1.5 < P_S < 4$	$1.25 < \alpha < 1.4$
$4 < P_S < 35$	$1.15 < \alpha < 1.25$
$P_S > 35$	$1.10 < \alpha < 1.15$

Shaft diameter d_S is found in millimeters with the formula given as;

$$d_s = \sqrt[3]{\frac{16 P_M}{\tau \pi \omega}} \tag{2.8}$$

$$\tau = \tau_{yield} / s \tag{2.9}$$

$$\tau_{yield} \approx 0.5\sigma \tag{2.10}$$

Here s is the coefficient of safety, τ is the torsional stress in N/m^2, σ is the yield strength of the shaft material in N/m^2, and ω is the rotational speed in rad/s.

Yield strength of several shaft materials are given in the Table 2.2. For most of the vertical turbine pump applications stainless steel AISI 420 is selected as shaft material.

Table 2.2 Yield strength for shaft materials

Material	**σ [N/mm^2]**
St-50	290
St-70	360
C-35	320-420
C-45	370-480
AISI 420	500

Then thickness of the impeller lock collet t is added on calculated shaft diameter to find the minimum hub diameter of the impeller.

$$d_{hub} = d_s + 2t \tag{2.11}$$

2.1.2. Flow Inside the Impeller

Flow can be separated into two components for representation. These are "meridional flow, in which the liquid particles move with velocities V_m in planes passing through the impeller axis and circumferential flow, in which the liquid particles move with velocities V_θ on circles lying in planes perpendicular to the impeller axis.", [6]. V_m velocities are proportional to capacity of the pump and V_θ velocities are proportional to the head of the pump.

Meridional velocities in the impeller are calculated as follows,

$$V_O = \frac{4Q_{IMPELLER}}{\pi\left(D_O^2 - D_{SHAFT}^2\right)} \text{ (Meridional velocity at impeller inlet eye)} \quad (2.12)$$

$$V_{m1} = \frac{Q_{IMPELLER}}{A_{INLET}} \text{ (Meridional velocity at impeller blade inlet)} \quad (2.13)$$

$$V_{m2} = \frac{Q_{IMPELLER}}{A_{OUTLET}} \text{ (Meridional velocity at impeller blade exit)} \quad (2.14)$$

Areas are the net values after considering constriction of the blades and the recommended values for velocity ratios are, [6]

$$0.8 < \frac{V_O}{V_{m1}} < 1.0 \quad (2.15)$$

$$0.70 < \frac{V_{m2}}{V_{m1}} < 0.75 \quad (2.16)$$

Modifications should be made on the meridional profile if these ratios could not be achieved. On the contrary, Figure 2.5 can be used to construct impeller meridional profile by means of calculating meridional velocities at first with Equation 2.17. Inlet and outlet areas and impeller main dimensions, Figure 2.4, can be found respectively with the help of these velocities. Velocity coefficients k_{Vm1} and k_{Vm2} come from experimental data. In the design, velocities are found after determination of impeller main dimensions and Figure 2.5 is not used for calculations.

$$V_{m1\text{-}2} = k_{V_{m1\text{-}2}}\sqrt{2gH} \quad (2.17)$$

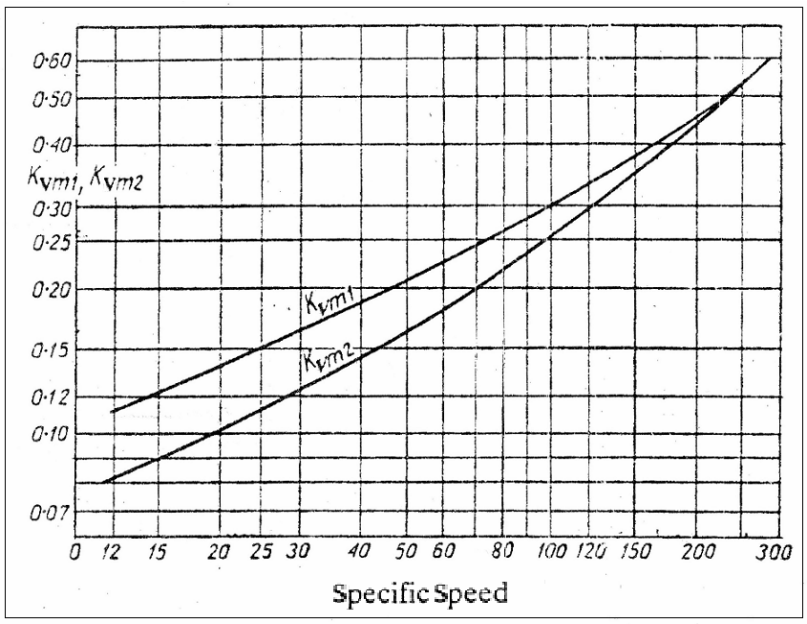

Figure 2.5 Graph of velocity coefficients according to specific speed, [6]

Other meridional velocities at any point are calculated with formula, [6]

$$V_m = \frac{Q_{IMPELLER}}{A_{NET}} CC \tag{2.18}$$

$$Q_{IMPELLER} = \frac{Q}{\eta_{VOLUMETRIC}} \tag{2.19}$$

CC is the constriction coefficient and given with formula,

$$CC = \frac{\frac{\pi D}{z}}{\left(\frac{\pi D}{z} - \frac{e}{sin\beta}\right)} \tag{2.20}$$

Here D is the diameter, z is the blade number and e is the blade thickness at the point which calculations are made. $Q_{IMPELLER}$ is the total flow rate, passes through the impeller, which portion of Q is delivered to next stage of the pump and $Q_{LEAKAGE}$ returns to the inlet of the same impeller.

Since blade angle β is used in calculating constriction coefficient CC, iterations are made until convergence is achieved. Then point by point method is followed to form the blades between leading edge and trailing edge. Calculation of β is given in section 2.1.6.

2.1.3. Impeller Inlet Eye

Impeller inlet eye diameter can be calculated with the following U.S.S.R. empirical formula, [6].

$$D_o = (4.0 - 4.5)\left(\frac{Q}{n}\right)^{1/3} \tag{2.21}$$

D_o is the net inlet diameter in m, Q is the flow rate in m^3/s, and n is the rotational speed in revolutions per minute. Coefficient is selected as 4.0 for better pump efficiency and 4.5 for better cavitation characteristics, [8]. While designing a vertical turbine pump impeller cavitation phenomena is not one of the main criterion. However in centrifugal impellers, design begins with net positive suction head (NPSH) calculations.

2.1.4. Impeller Blade Inlet (Leading Edge)

Inlet diameter D_1 and inlet breadth width b_1 can be calculated with a trial and error procedure to satisfy recommended design velocity ratios inside the impeller. Inlet diameter can be calculated with Equation 2.22

$$D_1 = kD_O \tag{2.22}$$

Coefficient k is selected between 0.8 and 0.95. It is recommended to take smaller values of k with increasing specific speed, [8].

Next step is to find impeller inlet breadth b_1.

$$b_1 = \frac{Q_{IMPELLER}}{\pi V_{m1} D_1 ICC} \tag{2.23}$$

ICC is the inlet constriction coefficient given by the following formula, [6].

$$ICC = \frac{1}{1 - e_1/t_1 \sqrt{1 + \frac{1}{\tan^2(\beta_1)\sin^2(\lambda)}}} \tag{2.24}$$

t_1 is the arc length between adjacent blades, e_1 is the blade thickness, β_1 is the blade inlet angle and λ is the angle between mid-streamline and inlet breadth. Since constriction coefficient and blade inlet angle depend on each other, calculation procedure is iterative.

2.1.5. Impeller Blade Outlet (Trailing Edge)

Impeller exit diameter D_{2A} can be found with the help of head coefficient ψ, Figure 2.2.

$$\psi = \frac{2gH}{U_2^2} \Rightarrow U_2 = \sqrt{\frac{2gH}{\psi}} \tag{2.25}$$

$$D_{2A} = \frac{60U_2}{\pi n} \tag{2.26}$$

Outlet breadth width b_2 is also determined after calculating peripheral velocity U_2 and using flow coefficient ϕ,

$$\varphi = \frac{V_{m2}}{U_2} \tag{2.27}$$

$$b_2 = \frac{Q_{IMPELLER}}{\pi V_{m2} D_2 OCC} \tag{2.28}$$

Here OCC is the outlet constriction coefficient given by the following formula, [6].

$$\lambda = t_2/(t_2 - e_2') \tag{2.29}$$

t_2 is the arc length between adjacent blades and e'$_2$ is the thickness of the impeller blade along circumferential arc, [6], Figure 2.6.

$$e_2' = e_2/sin\beta_2 \tag{2.30}$$

e_2 is the perpendicular blade thickness at the impeller exit and β_2 is the blade outlet angle.

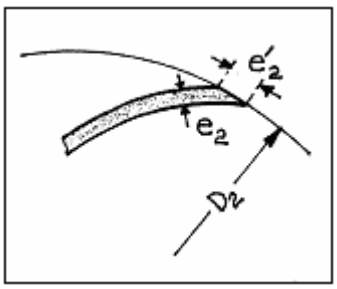

Figure 2.6 Blade thicknesses, [8]

Calculation of impeller breadth width b_2 and selection of the impeller exit angle from Layne Bowler impeller data table according to specific speed of the impeller make it possible to determine endpoints of the hub and shroud profiles at the impeller exit. A circle, whose diameter is b_2 and center lies on the diameter of D_{2A} is drawn with a line inclined from horizontal about selected exit angle. Intersection of the circle and the inclined line gives the endpoints of the hub and shroud profiles, Figure 2.7.

"Outlet edge should be as little inclined as possible, since large differences in diameter increase the tendency to form secondary currents at just below maximum discharge, which lowers the efficiency of the pump", [6]. On the other hand, if exit angle is too low it is difficult to design a low-diameter bowl. Exit angle increases with specific speed.

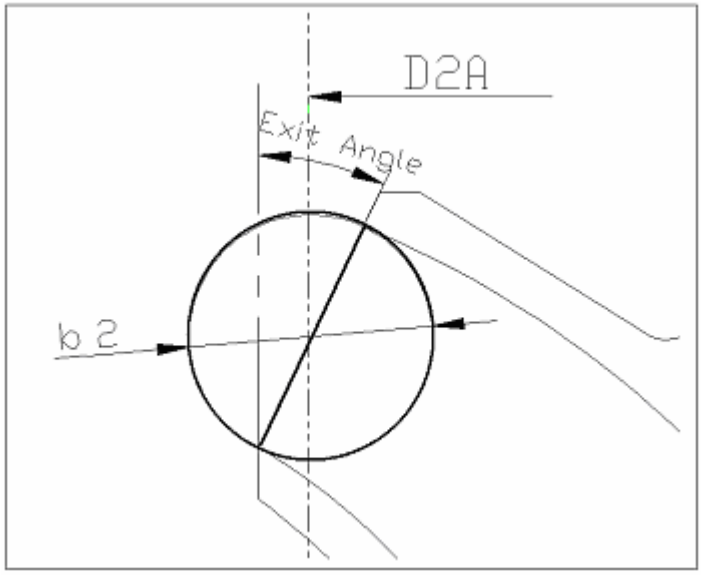

Figure 2.7 Constructing of meridional profile at exit of the impeller

Impeller exit diameter D_{2A} which is calculated from head coefficient ψ, impeller outlet width b_2 which is calculated from flow coefficient ϕ and impeller exit angle β_2 play an important role on the performance characteristics of the pump. Calculating D_{2A} and β_2 correctly lead to have the desired head from impeller and b_2 affects the best efficiency point of the pump to be at the desired capacity.

To complete the meridional profile last step is to find the length of the bladed region. Meridional profile length (l_m) of the impeller can be found with an iterative procedure using blade number check formula;

$$z = 13\frac{r}{l_m}sin\left(\frac{\beta_1 + \beta_2}{2}\right) \tag{2.31}$$

z is the blade number, r is the mean radius of the mid-streamline, β_1 and β_2 are blade inlet and outlet angles respectively and M_{st} is the moment of the mid-streamline.

$$r = M_{ST}/l_m \tag{2.32}$$

Then, outline of the impeller could be drawn according to calculated values. Smooth arcs are drawn while forming hub and shroud profiles. Trailing and leading edges are tried to be perpendicular to these profiles. Next step is to determine the streamlines where blade angles are to be calculated. Drawings of these streamlines are similar to dividing the blade passage into pumps which are parallel in operation and have same flow rate, Figure 2.8. A visual basic computer code is written in order to draw these streamlines. Then iso-velocity splines (potential splines) are drawn. Along these splines meridional velocity is assumed to be constant and they are proportional to streamlines. Potential splines are revolved along axis to find flow passage areas. These areas then divided into blade constriction coefficient of that location to find net flow passage area. Generally five streamlines are plotted for calculations, for small pumps three streamlines are also sufficient which are hub profile, shroud profile and mid streamline. Afterwards design process continues with calculation of blade angles at the outlet of the impeller.

Finite number of blades causes two phenomenons on the flow. One of them is blockage or constriction of the flow and the other one is slip effect, Figure 2.9, which means deviation of fluid flow angle from outlet blade angle, [12].

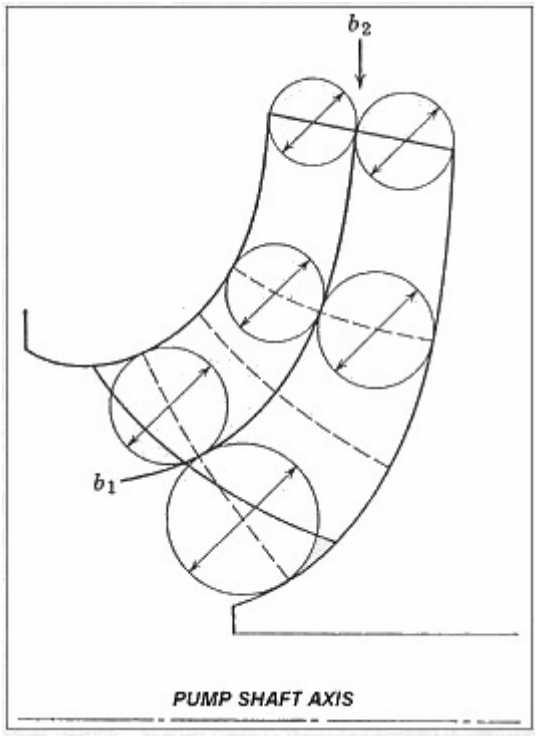

Figure 2.8 Development of streamlines, [6]

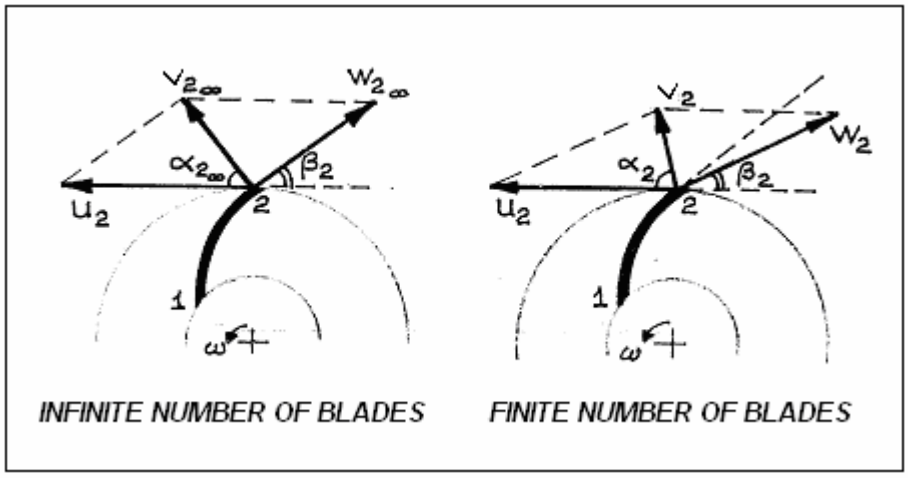

Figure 2.9 Effect of finite number of blades on the velocity triangle at the impeller trailing edge, [8]

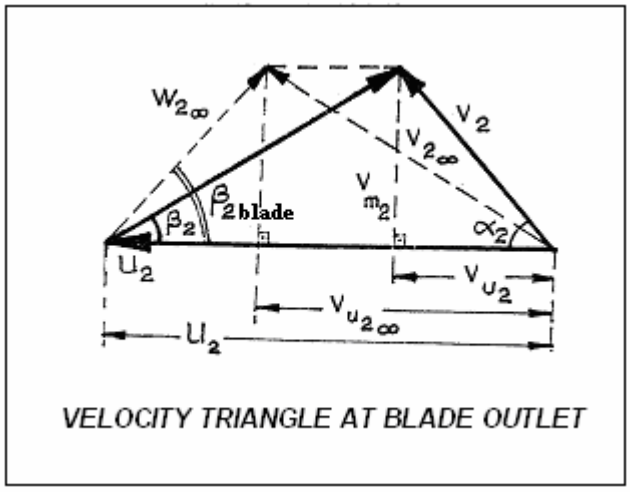

Figure 2.10 Velocity triangles at the trailing edge of the impeller, [8]

Pfleiderer correction factor (C_P) is described for a representation to slip effect of finite number of blades. This factor is determined for all plotted streamlines. C_P is between 0.25 and 0.40 for mixed flow impellers at mid-streamline.

Theoretical head of the pump is calculated with Equation 2.33 and used in C_P calculations,

$$H_{th} = \frac{H}{\eta_{HYDRAULIC}} \tag{2.33}$$

On the contrary, using simplified Stepanoff Master Chart, Figure 2.11, with calculated C_P, blade outlet angle β_2 can be determined easily. First of all, Pfleiderer correction factor is found for specific speed and meridional characteristics of the pump. $(1-C_P)$ value is marked on vertical axis and a line is drawn between $(0, 1-C_P)$ and (ϕ, ψ) points. This line is lengthened until it intersects horizontal axis. Intersection point gives tangent of the blade outlet angle. $\phi = 0.16$, $\psi = 0.31$ and $C_P = 0.35$ for the mid-streamline of the impeller.

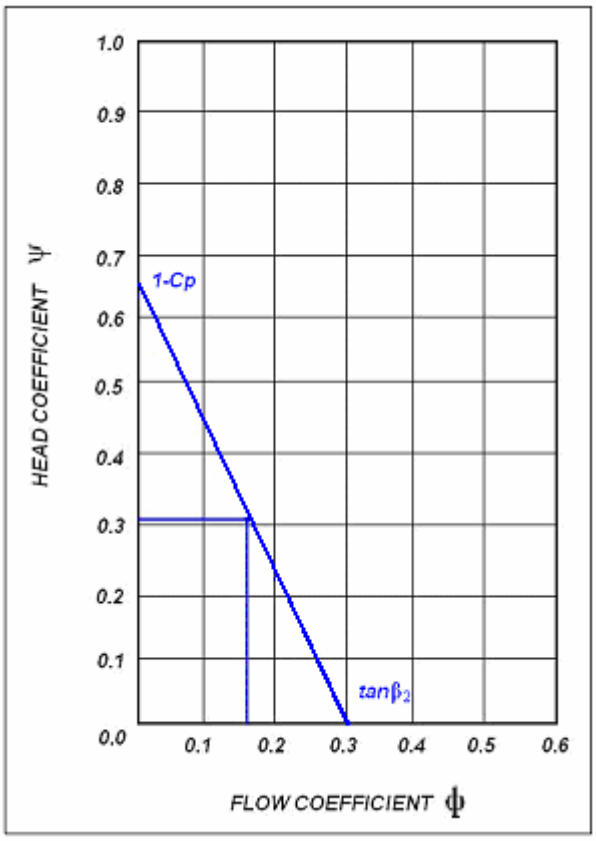

Figure 2.11 Determination of blade outlet angle β_2 for mid-streamline

This calculation is done for all streamlines. C_P values are different for streamlines so different outlet angles are obtained for each streamline. Blade outlet angle β_2 has a significant effect on the performance and head of the pump so calculation of β_2 is one of the key points of impeller design.

Theoretical head H_{th}, which is the head of the pump when there are finite number of blades, no hydraulic resistance and no mechanical friction, can be calculated using Euler Turbine equation. The turning moment exerted on the fluid by the impeller blades is,

$$M = \frac{\rho g Q(r_2 V_2 \cos\alpha_2 - r_1 V_1 \cos\alpha_1)}{g} \qquad (2.34)$$

On the other hand, moment times angular speed is equal to hydraulic power of the pump.

$$M\omega = \rho g Q H_{th} \tag{2.35}$$

Using Equation 2.34 and Equation 2.35 H_{th} is found as,

$$H_{th} = \frac{V_{\theta 2} U_2 - V_{\theta 1} U_1}{g} \tag{2.36}$$

For no inlet whirl condition, Figure 2.12, Equation 2.36 reduces to

$$H_{th} = \frac{V_{\theta 2} U_2}{g} \tag{2.37}$$

Here V_θ denotes for tangential component of absolute velocity and U is the peripheral velocity.

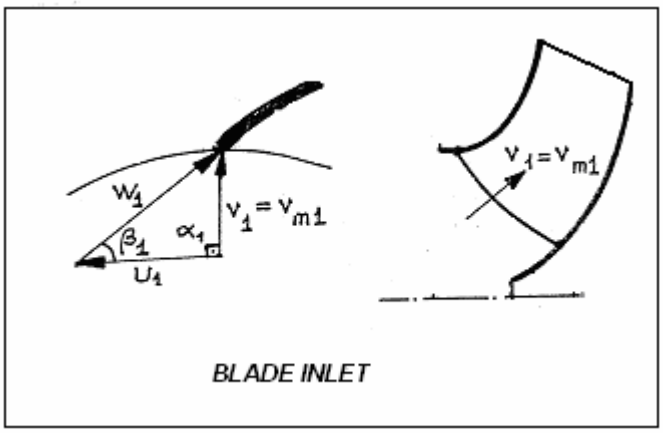

Figure 2.12 Inlet velocity triangle, [8]

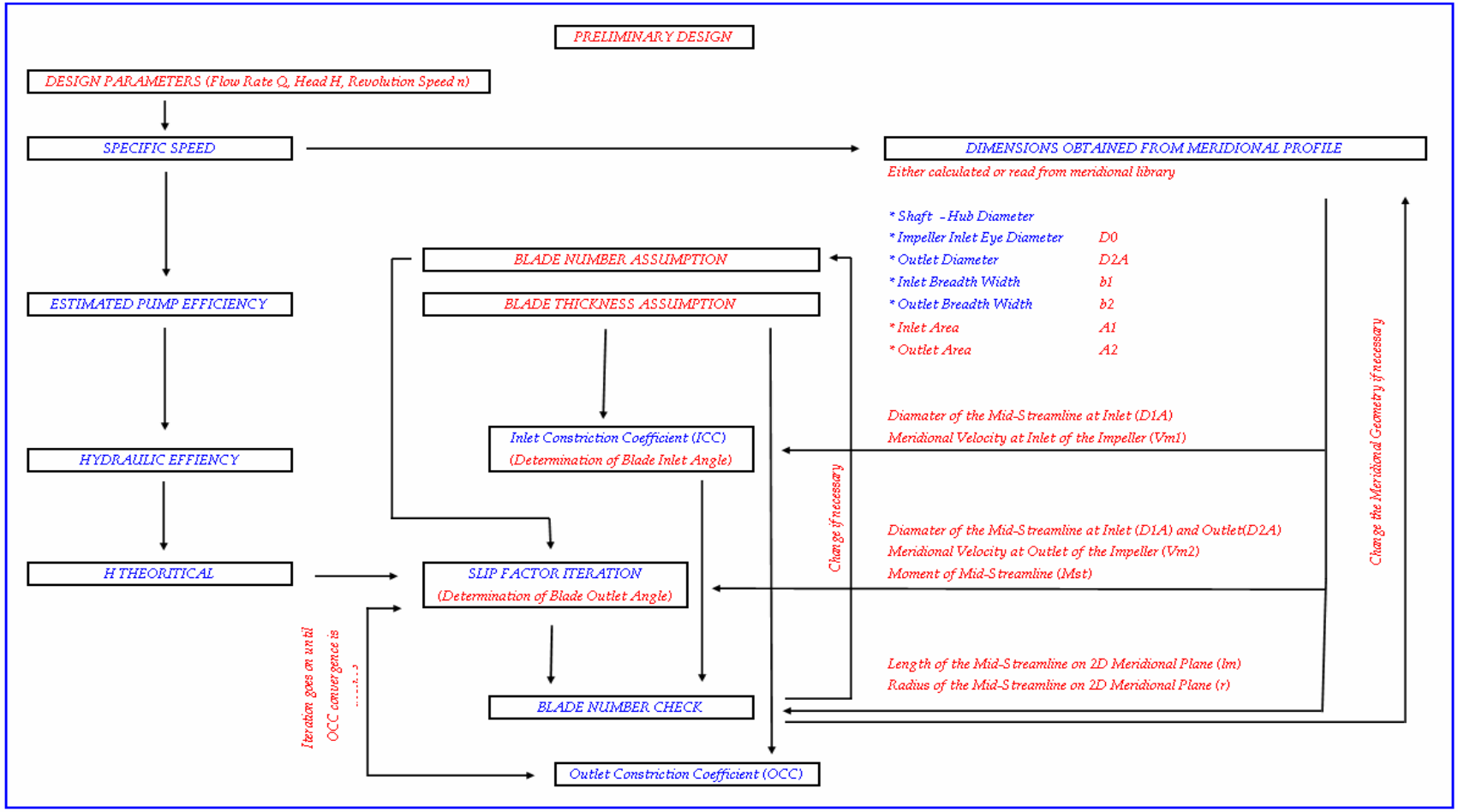

Figure 2.13 Preliminary design chart

2.1.6. Impeller Blading

Since $r_1 V_{\theta 1} = \frac{\Gamma_1}{2\pi}$ and $r_2 V_{\theta 2} = \frac{\Gamma_2}{2\pi}$, Figure 2.14, Equation 2.36 can be written,

$$H_{th} = \frac{\omega}{2\pi g}\left(\Gamma_2 - \Gamma_1\right) \tag{2.38}$$

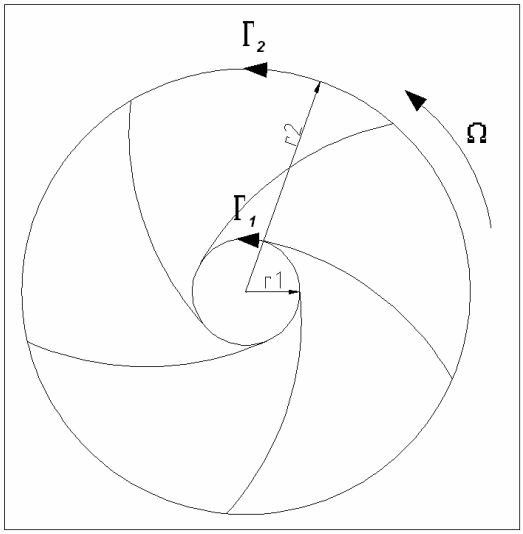

Figure 2.14 Circulation of velocity in impeller

Γ is the circulation at the inlet and outlet of the blades. Change of Γ (radius*circumferential velocity) from leading edge to trailing edge gives the shape and curvature of the blade on the streamlines which calculations are carried on. This design method is mentioned in References [13], [14], [15], [16] in detail with small differences. Using smooth blade angle distribution does not always guarantee good flow fields, so this method is a good alternative in design process. It is seen that there is direct relation between circulation distribution and the head of the pump. Distribution of Γ has to meet four requirements along the non-dimensional meridional length of streamlines, Figure 2.15. Since meridional streamlines have

different lengths they are non-dimensionalized. At the leading edge ($\dot{m} = 0$) and at the trailing edge ($\dot{m} = 1$) there are two requirements.

1. $\Gamma = 0$ at $\dot{m} = 0$
2. $\frac{d\Gamma}{d\dot{m}} = 0$ at $\dot{m} = 0$
3. $\Gamma = 1$ at $\dot{m} = 1$
4. $\frac{d\Gamma}{d\dot{m}} = 0$ at $\dot{m} = 1$

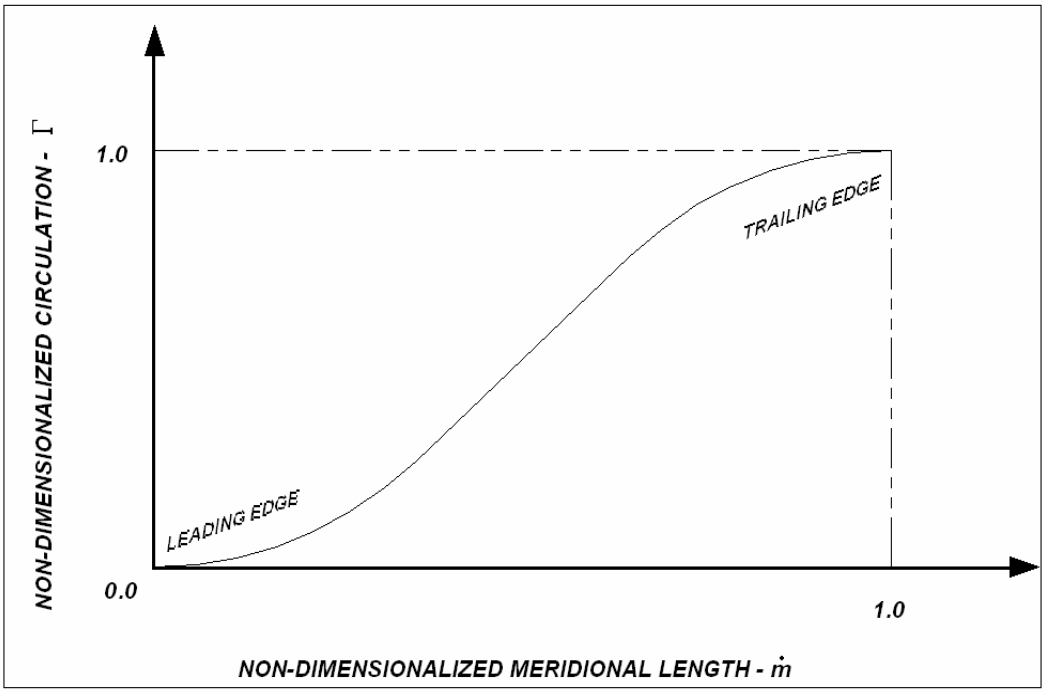

Figure 2.15 Non-dimensionalized circulation distribution through non-dimensionalized meridional length

First requirement denotes for there is no pre-whirl at the leading edge. Second one indicates that derivative of the circulation along dimensionless meridional length is zero at the leading edge which means there is shockless entry. Shockless entry states

that there are no eddy and separation losses at the impeller inlet and flow angle is same with blade angle. Therefore angle of incidence is zero, [9]. Circulation distribution is also non-dimensionalized with its maximum value which is at the trailing edge composes the third equation. Finally the last one, derivative of the circulation along dimensionless meridional length is zero at the trailing edge, is required to satisfy Kutta condition. Kutta condition defines the amount of circulation in airfoils where the trailing edge is sharp and a stagnation point. In impellers, flow is assumed to leave smoothly from trailing edge of the impeller blades, [17]. In other words relative velocity is proportional to blade surface normal. However, in the real situation flow leaves with an angle smaller than blade angle due to effect of finite number of blades (slip effect), Figure 2.9, Figure 2.10. This undesired effect is tried to be minimized with removing material from suction side of the blade and named as underfiling, Figure 2.16. Since circumferential component of the absolute velocity ($V_{\theta 2}$) increases, underfiling cause an increase on the head of the pump. Underfile is a must to increase head and efficiency of the pump. It also affects the best efficiency point of the pump; an underfiled impeller's best efficiency point goes to higher flow rates. Figure 2.17 and Figure 2.18 show the effect of underfile on the head rise at the best efficiency point and at the same head respectively.

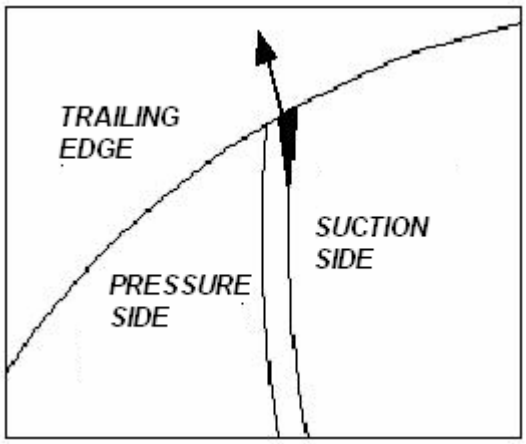

Figure 2.16 Hatched area shows the underfiled region (removed material)

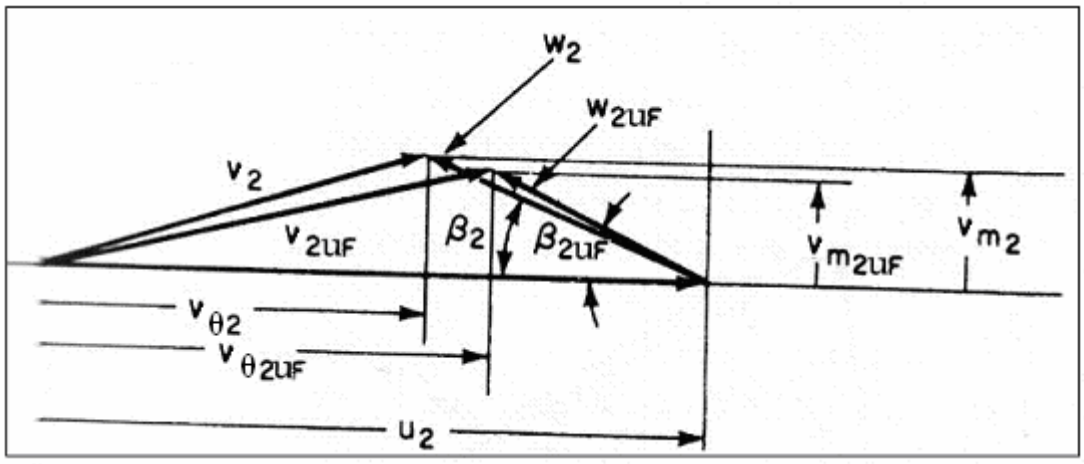

Figure 2.17 Underfile effect for best efficiency point, [4]

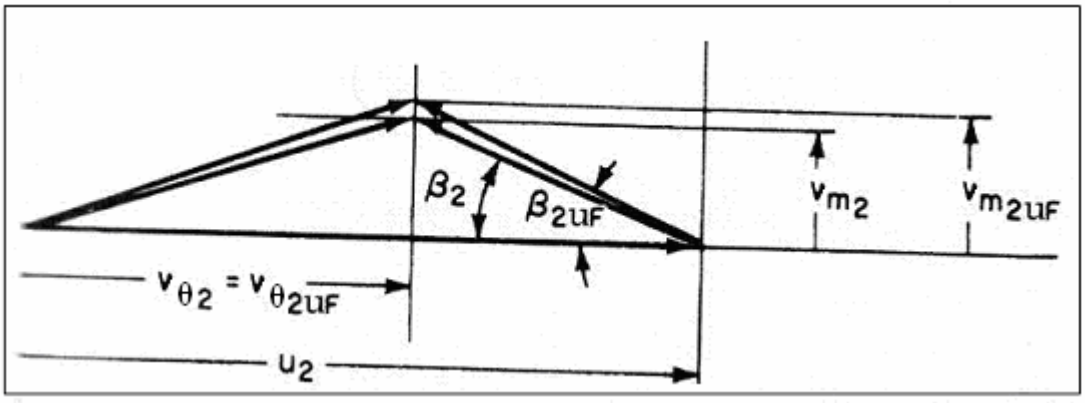

Figure 2.18 Underfile effect at the same head, [4]

Since four conditions are prescribed for Γ distribution, the simplest function for this purpose will be a third order polynomial. A cosines type function is proposed in Reference [14] for this purpose. The fact that various numbers of functions can be determined for Γ distribution from leading edge to trailing edge, the criterion which determines the best one (or the coefficients of the polynomial) is the swirl angle of the blade. Swirl angle depends on the blade angle and meridional length of the streamline, calculated with the Equation 2.39, [6]. Performance of the pump and cavitation also play an important role on the selection of the Γ distribution, [16]. Modifications can be made if the desired characteristics are not achieved after numerical experimentations.

$$swirl = \Sigma\left[\Delta l\left[\frac{1}{2}\left(\frac{1}{r_n tan\beta_n}+\frac{1}{r_n tan\beta_{n-1}}\right)\right]\right] \tag{2.39}$$

Here Δl denotes for the length between two stationary points on the streamline where the blade angles are to be found. r_n and β_n are the radius and blade angle at that point respectively. $\Sigma\Delta l$ gives the total length of the streamline. "In impellers with 5 to 9 blades, the angle of overlap is $30^o - 45^o$", [6].

Swirl angle of the streamline also determines the stacking of the blade. Stacking defines the position of the blade at the trailing edge of the impeller. "If the blades are leaned against the direction of rotation the result is a blade force which will increase the pressure at the shroud endwall and reduce the pressure at the hub endwall", [16]. This type of blade lean helps to suppress secondary flows in mixed flow turbomachines at the trailing edge of the impeller due to reduction of relative velocity at the shroud and increase of relative velocity at the hub profile, Figure 2.19, [16]. However, blade lean and blade swirl angle is limited with manufacturing and structural considerations. More swirled and leaned blades make it difficult to get together of the impeller cores. If blade number is low more swirled blades can be designed and manufactured.

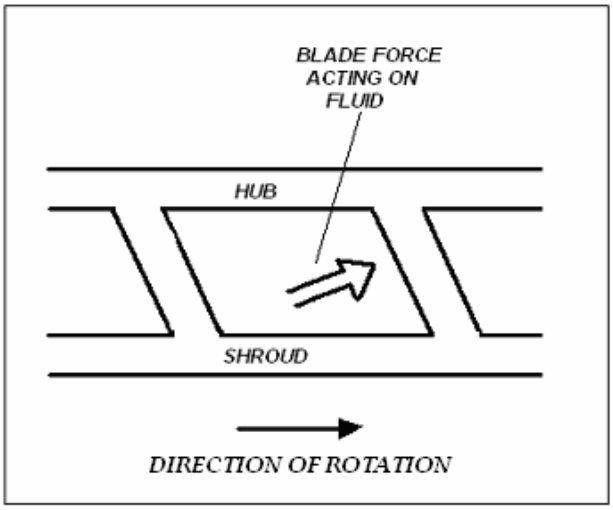

Figure 2.19 Stacking of the impeller blades

Circumferential velocities V_θ can be determined after calculation of $V_{\theta 2}$ from Euler Equation 2.37 at the impeller exit. Then using Γ distribution across the non-dimensional meridional length, Figure 2.15, other V_θ values can be found. Finally, blade angles β are calculated throughout the blade.

$$\beta = arctan\left(\frac{V_m}{U - V_\theta}\right) \tag{2.40}$$

Another way to specify the circulation distribution could be done by defining pressure distribution along the meridional length of the streamlines. When "Newton's Second Law for Moments of Forces" is considered along a strip of fluid between pressure and suction sides of the impeller blades, Figure 2.20, [4], [16];

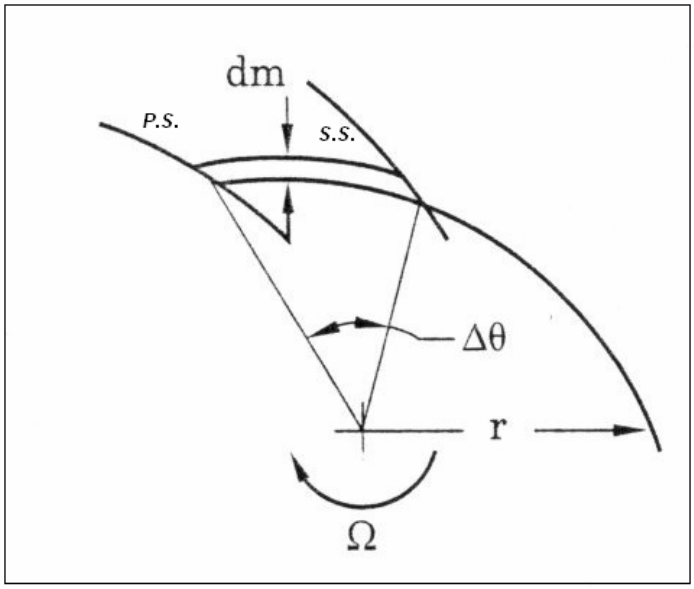

Figure 2.20 Blade static pressure difference, [4]

$$r\left(p_P - p_S\right)bdm = \rho V_m br\Delta\theta d(rV_\theta) \tag{2.41}$$

Substituting $\frac{2\pi}{z}$ instead of $\Delta\theta$ assuming blade thickness is zero,

$$\left(p_P - p_S\right) = \rho V_m \frac{2\pi}{z} \frac{d(rV_\theta)}{dm} \tag{2.42}$$

Then Γ distribution could be found by integrating the value from leading edge ($\dot{m} = 0$) to the trailing edge($\dot{m} = 1$)

$$\Gamma = rV_\theta = \int_{\dot{m}=0}^{1} \left[\frac{\left(p_P - p_S\right)}{\rho V_m \frac{2\pi}{z}} \right] dm \tag{2.43}$$

"For a given impeller profile, there are virtually a thousand ways a blade can be designed between inlet and outlet angles", [13]. Due to this situation, some flow properties should be checked with the help of the numerical experimentation. These criteria are given as, Figure 2.21,

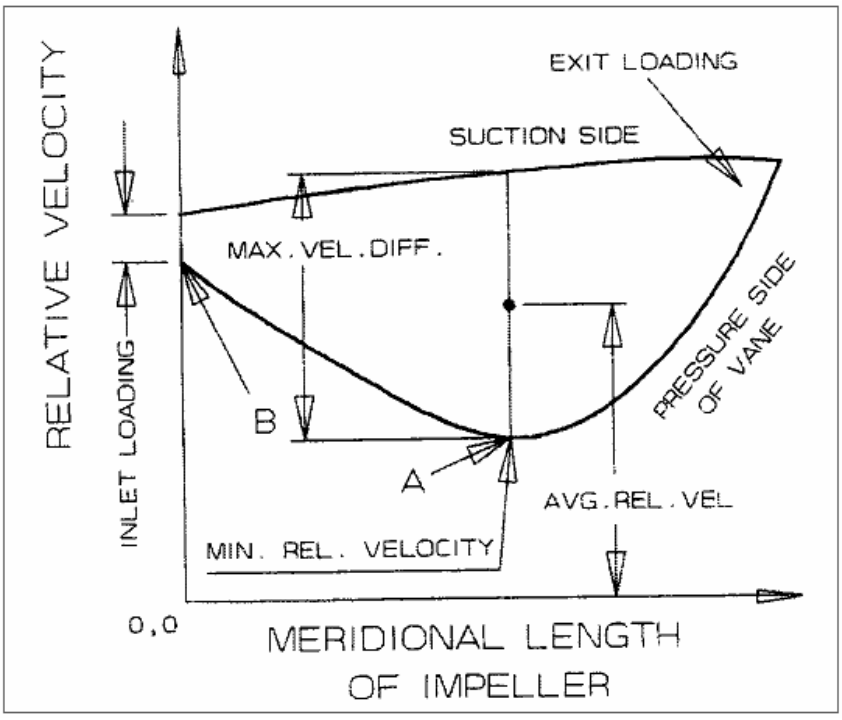

Figure 2.21 Sample relative velocity distribution along meridional length, [18]

Diffusion Rate, DR, [18]

$$DR = \left(\frac{W_{Min,Pt.A}}{W_{Max,Inlet,Pt.B}} \right)_{PRESSURE.SIDE} \tag{2.44}$$

Velocity Loading, [15]

$$\zeta = \left[\frac{W_{SS} - W_{PS}}{\frac{1}{2}\left(W_{SS} + W_{PS}\right)} \right]_{AT.MAXIMUM.VELOCITY.DIFFERENCE} \tag{2.45}$$

For pumps whose specific speed is in the area of 1.0 to 1.7, DR should not be less than 0.7 and ζ should remain below 1.0, [15], [18]. "These are all widely used experienced based rules that cannot be independently corroborated. Nonetheless, they are useful to check in all cases", [10]. If the cavitation is a concern inlet loading should be as small as possible and this region should be lightly loaded, [18].

Relative velocity is generally assumed as decreasing gradually while designing blade and calculating blade angles from leading edge to trailing edge, [4], [6]. However, it could be seen that flow inside the impeller is different from what is assumed, Figure 2.20. Numerical experimentation results are given in section 4.3.

To summarize the whole impeller design, impeller hub diameter is found with shaft diameter and impeller collet thickness considering torsion of the pump shaft, impeller inlet eye diameter is found using Equation 2.21, impeller inlet diameter D_{1A} and inlet breadth width are found with Equations 2.22 and 2.23 respectively, impeller outlet diameter D_{2A} is found using head coefficient graph, Figure 2.2, impeller outlet width b_2 is found with Equation 2.27 and 2.28 using flow coefficient and length of the streamline is controlled with blade number check formula, Equation 2.31. Hub and shroud profiles are drawn as smooth arcs from leading edge to trailing edge.

Area of the meridional flow passage is increased gradually from inlet breadth to outlet breadth. Then inlet and outlet blade angles are determined. Between inlet and outlet angles of the blade, blade angles are determined using circulation (Γ) distribution, if required another distribution is specified. Finally, design checks are done with analyzing performance characteristics with the help of the numerical experimentation results (head, efficiency, best efficiency point, cavitation, blade loading, diffusion rate, velocity loading) and considering manufacturing considerations. (blade number, swirl angle of the blade, stacking condition)

2.2. Bowl Design

Bowl design consists of developing meridional profile, determining of vane inlet angle and shaping the vane, which is similar to impeller design. Main function of the bowl is to guide to fluid flow from exit of the impeller to the inlet of the next impeller. In other words, it turns the swirling flow at the impeller exit into the axial flow at the impeller inlet, [14]. Pressure recovery is also concerned, from this point of view bowl can be regarded as diffuser. Bowl slows down the velocity of the fluid in the flow passage. However, meridional velocity increases due to contraction of the meridional passage. Velocity decreases because of vanishing of the circumferential component of the velocity. It is also essential to circumferential velocity be zero at the exit of the bowl to provide an acceptable inflow for the next impeller.. Lastly, friction losses are also tried to be minimized by changing length of the bowl and swept of the bowl vanes.

Meridional profile formation of the bowl is similar to impeller meridional profile formation. Design is made on three streamlines (hub, shroud, mid-streamline) Mid-streamline is drawn dividing the flow passage into two equal passages, Figure 2.22. Inlet area of the bowl should be designed larger than impeller exit area in order to make efficiency increase possible when underfile is applied at the trailing edge of the impeller. Inlet breadth of the bowl should be selected at least 1.1 times of the impeller exit breadth for this purpose, [6]. On the other hand, throat area of the bowl

has a great effect on best efficiency point of the pump. To minimize losses in the bowl, width of the meridional flow passage should be increased through the direction of the flow, [14] and flow passage area should be decreased gradually from inlet to exit, Figure 2.23.

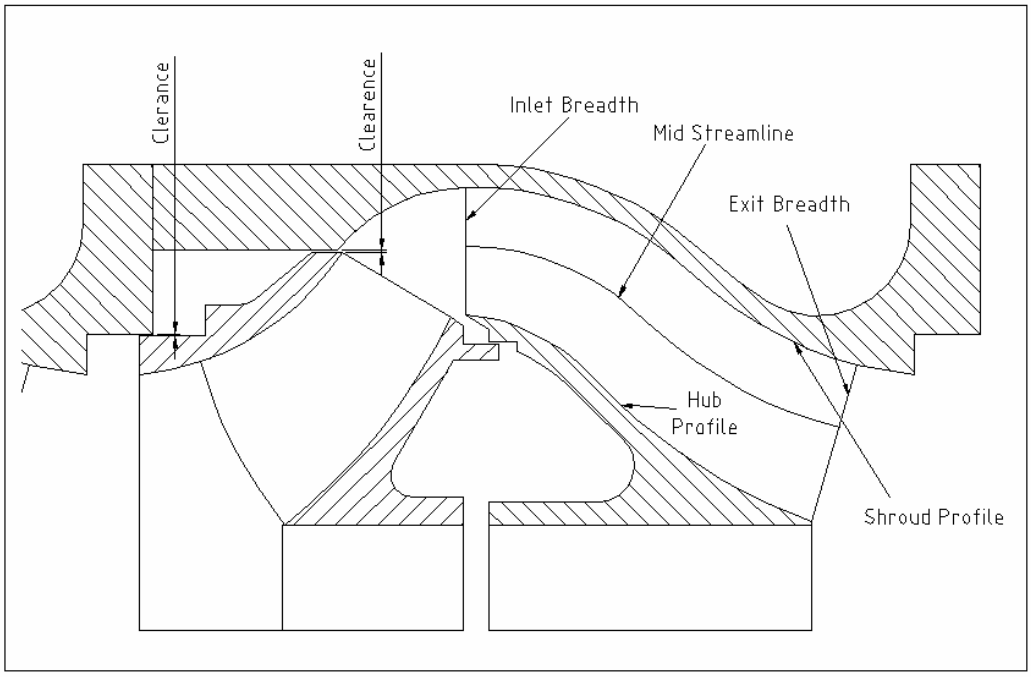

Figure 2.22 Bowl meridional profile

Next step is to determine the vane number of the bowl. Acoustic considerations take place while choosing number of the vanes. Due to interaction of the static bowl vanes and rotating impeller blades, pressure pulsations and resonance occur, [4]. To prevent strong pressure pulsations and resonance, same numbers of vane and blade combinations should be strictly avoided. Also, diffuser vanes multiples and impeller blade multiples should not be equal in first three orders, [4]. Interaction area between bowl vanes and impeller blades should not be so small to prevent a torque ripple which can cause due to interaction.

Inlet angle of the bowl is another important parameter for design process. If inlet angle is not calculated correct, leading edge separation may occur, which will result

in a great head loss in the bowl. After fluid exits from the impeller, slip makes happen due to finite number of blades situation. Fluid angle, which leaves the impeller, is calculated with Equation 2.46.

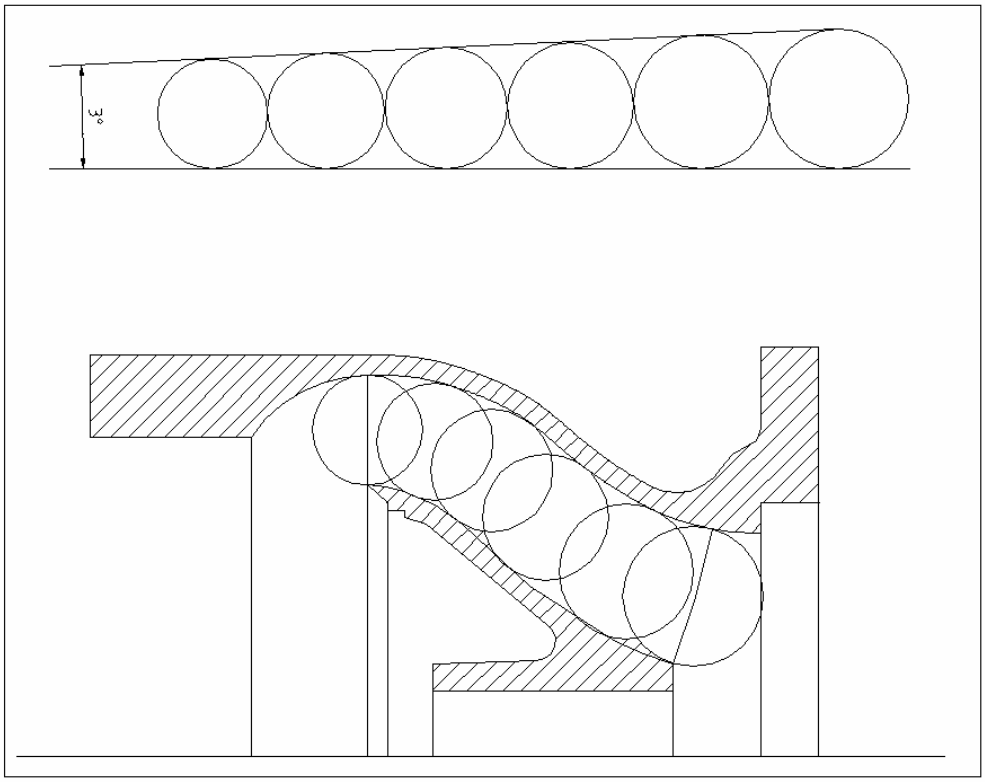

Figure 2.23 Development of meridional profile

$$\alpha_3 = tan^{-1} \frac{V_{m2}}{\left(\frac{gH_{th}}{U_2}\right)} \tag{2.46}$$

Inlet angles should be increased, considering constriction of the bowl vanes, [6]

$$\alpha_4 = tan^{-1} \left(tan\alpha_3 \frac{t_4}{t_4 - \frac{e}{sin\alpha_3}} \right) \tag{2.47}$$

Here, t is the arc length between adjacent vanes calculated with Equation 2.48 and e is the thickness of the vane. Angle α_4 can be increased 4 to 5 degrees in order to use same bowl for impellers with larger discharges, [6].

$$t_4 = \frac{\pi D_4}{z_{Bowl}} \tag{2.48}$$

z_{Bowl} is the number of bowl vanes and D_4 is the diameter of the streamline where the calculations are carried on. Meridional velocities inside the bowl are calculated as;

$$V_m = \frac{Q}{A_{NET}} CC \tag{2.49}$$

$$CC = \frac{\frac{\pi D}{z}}{\left(\frac{\pi D}{z} - \frac{e}{sin\alpha}\right)} \tag{2.50}$$

Circumferential velocity at the inlet is calculated with Equation 2.51 and assumed to be decreasing gradually to zero at the bowl exit. V_{m4} is the meridional velocity at the bowl inlet.

$$V_{\theta 4} = \frac{V_{m4}}{tan\alpha_4} \tag{2.51}$$

Vane angles are found by dividing meridional velocity to circumferential velocity at any location of the bowl. Vane swept is important for manufacturing and its calculation is done using vane angles with Equation 2.53.

$$\alpha = \frac{V_m}{V_\theta} \tag{2.52}$$

$$swept = \Sigma \left[\Delta l \left[\frac{1}{2} \left(\frac{1}{r_n tan\alpha_n} + \frac{1}{r_{n-1} tan\alpha_{n-1}} \right) \right] \right] \tag{2.53}$$

Swept angle of the hub and shroud streamlines are equalized to swept angle of mid-streamline to obtain a straight vane exit. In order to adjust swept angle, circumferential velocity distribution is changed on hub and shroud streamlines. Different swept angles cause a curved shape vane end and make gathering of cores difficult. Vane number together with swept angle is another factor which defines the manufacturability of the bowl.

Diametral clearance, the distance between bowl and impeller, is determined according to Figure 2.24. This figure is given for diameter of the leakage joint and assumed as equal to the diameter of impeller. Machining tolerances are also given in the figure. Generally, wearing rings are used at these close surfaces. “Wearing rings provide an easily and economically leakage joint between the impeller and the casing”, [4]. It is better to use wearing rings on the stationary parts (bowl) because unbalance may occur on the rotating parts (impeller) if the ring wears in course of time. Radial clearance has an important effect on the volumetric efficiency of the pump. It also affects the mechanical efficiency when the disk friction is considered between rotating and stationary parts. On the other hand, if the fluid to be pumped includes abrasive materials or solid particles like sand, clearance should be increased.

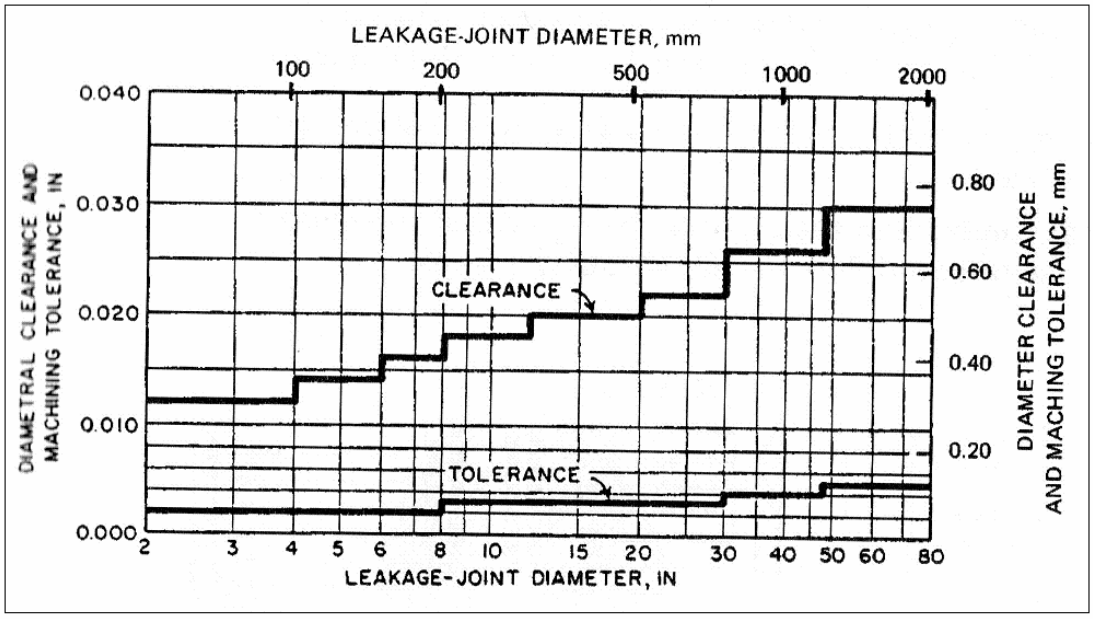

Figure 2.24 Clearance, [4]

2.3. Manufacturing

Manufacturing of the pump consists of design, casting, machining and preparing of technical drawings. Hydraulic design and mechanical design are integrated processes that determine the final product. Mechanical design of the pump is generally based on calculation of strength of materials. Torsion calculations are made to determine the shaft diameter. Wall thickness of the impeller is determined by calculating of the strength of the material. On the other hand, wall thickness of the bowl is found considering the bowl as a pressure vessel and minimum wall thickness, which is available for casting, is found. Machining tolerances are added and shrinkage ratio is applied on the final models to scale it up respectively.

Pump parts are cast except shafts, collets, bolts and nuts. Cores, core boxes, impeller model, bowl model and suction model of the pump must be prepared at first for casting. CAM (Computer Aided Machining) process and numerical codes are used during machining of the wooden core boxes. Cores should not be swirled (twisted) so much in order to pull them from the mold. Blade number is another criterion for

easiness of pulling cores from the mold after casting. Taper angles should be given to the surfaces in the direction of pulling. Individual cores are assembled and core assembly is acquired before casting, Figure 2.25, Figure 2.26. Great care should be taken while assembling of the cores and during casting process to prevent shift of any of the cores. Sand is packed around wooden model of the impeller, bowl and suction intake to form a cavity after models are pulled from the mold. Then core assembly is placed inside the mold and molten metal is poured inside of this cavity from risers.

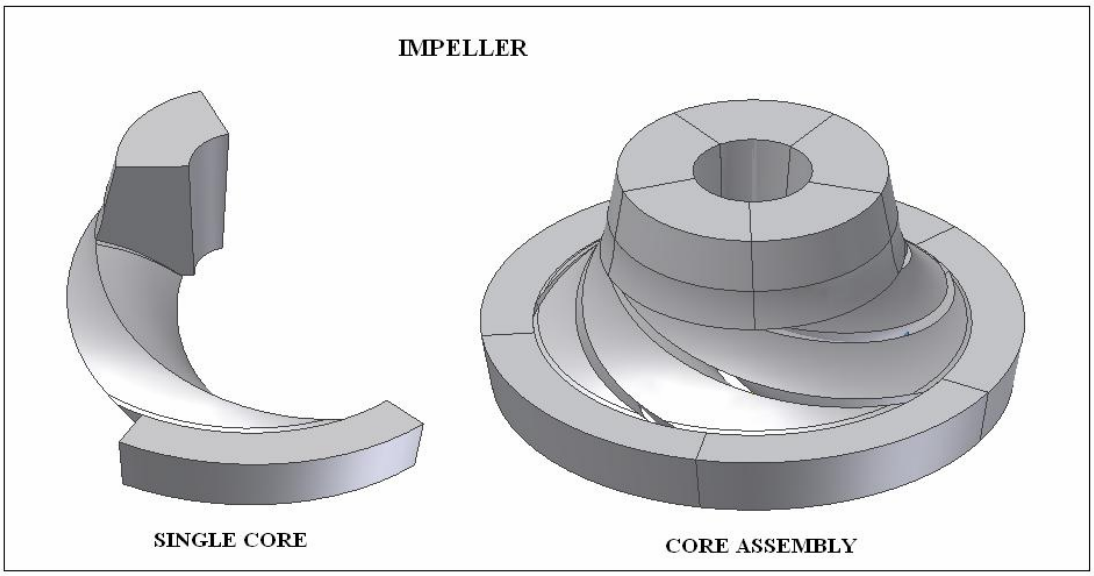

Figure 2.25 Single core and core assembly of impeller

Blade thickness is so essential for hydraulic performance of the pump. Pumps with low blade thicknesses have low blockage, occurred by blades, which will result in a rise in performance characteristics of the pump. Casting process determines the minimum blade thicknesses which can be cast. Gravity die casting is used during manufacturing process. However, processes such as investment casting give the opportunity to cast lower blade thicknesses. A whole wax model of the desired part is placed inside the sand and when the metal is poured, wax is melted out and the desired part is achieved. Its high cost makes it the second choice in the casting step.

Technical drawings of the parts are prepared for machining with desired tolerances on the dimensions of the pump. Finally, balancing of the impellers is done in order to minimize vibration and radial forces on shaft. The photographs of the manufactured pump parts can be found in the Appendix A.

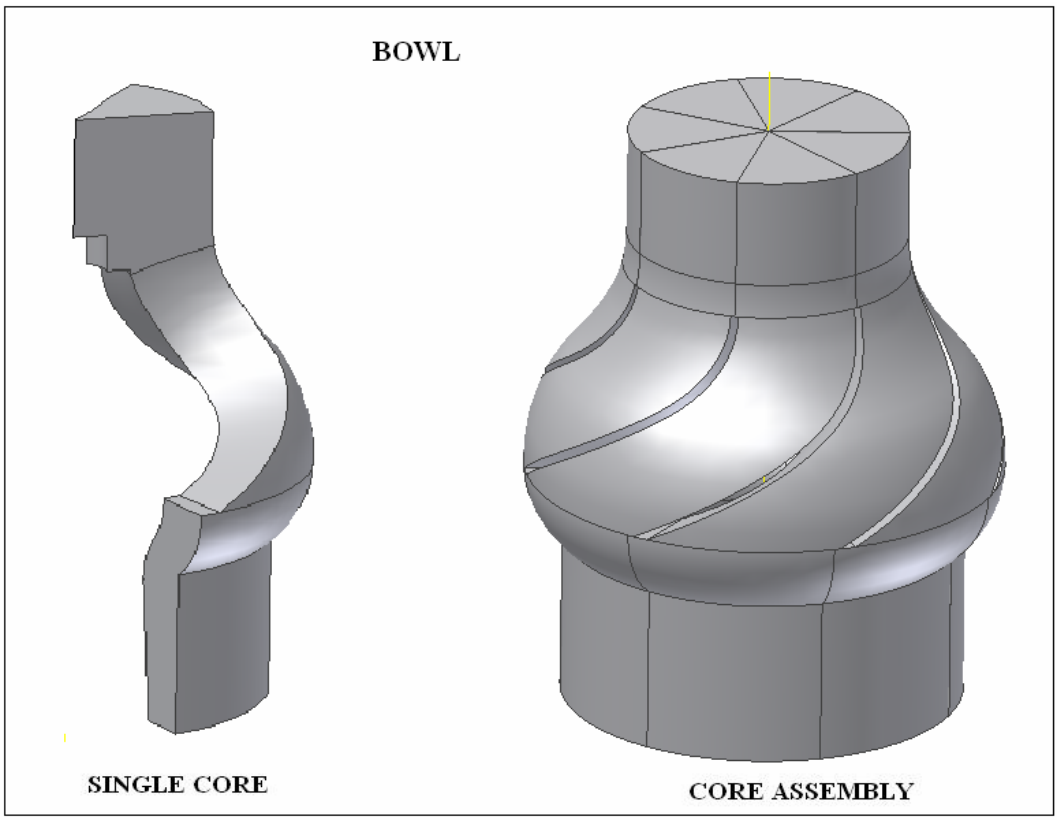

Figure 2.26 Single core and core assembly of bowl

CHAPTER 3

AXIAL THRUST BALANCING TECHNIQUES AND MEASUREMENT SYSTEM

Axial thrust is the resultant force which occurs in the direction of shaft. Its act of direction is upwards at the start up due to accelerating and entering of water to the impellers and downwards while the pump is operating, [4]. Pressure differences between upper and lower surfaces of the impeller cause a force (named as hydrostatic force) whose direction is to the suction of the pump or downwards when the pump is operating in vertical position. Upper surface area of the impellers, which the higher pressure is acting on, is also larger than lower surface area of the impellers. This situation also increases the magnitude of the axial thrust. Hydrostatic force acting on the blades of impellers and axial momentum change of the fluid constitute a small amount of axial thrust when compared with hydrostatic forces, [7]. Axial thrust is mainly proportional to head of the pump has several effects on the pump. It causes shafts to elongate. Elongation of shafts changes the position of impellers in the bowls and a second adjusting should be required for impellers. It is the main factor when bearings are selected to compensate these loads. Bearings also compensate the weight of the rotating parts (impellers, shafts, collets).

Axial thrust is either compensated with driver components or another thrust assembly. It is compensated in different ways according to type of the pump driver. Vertical solid shaft motors (V1 motors), which are the first electric drivers used in vertical turbine pump operations, have a limited capability to balance high axial thrust. Therefore, thrust bearing assemblies are used with V1 motor driver applications. This is closed assembly, filled with lubrication oil and consists of the bearings. Ratchet type pins with non-reversing plate are also mounted on this assembly to prevent the motor drive in counter direction. Development of vertical hollow shaft (VHS motor) pump drivers reduces the usage of V1 motors and thrust

bearing assemblies. VHS motors include high capacity thrust bearings and they provide simplifications in assembling of the motor and adjusting of the impellers positions in bowls. However, thrust capacities of VHS motors are also limited. In pump applications thathave high flow rate and head, V1 motors are use d with thrust bearing assembly to compensate high axial thrust that occurred due to hydraulic forces. In submersible pumps load carrying bearings are at the bottom of the submersible motor driver. The axial thrust capacities of the submersible motors are lower than VHS motors and thrust bearing assembly applications. High axial thrust may cause damage in bearings which will result in failure of the motor windings. In these situations power consumption of the motor increases and relay on the electrical panel must cut out the electricity to prevent burning of the windings of the motor, [19].

Bearings have a limited service life. Dynamic load capacity of a bearing is defined as the number of revolutions or operating hours without being fatigue on the bearing, [11]. “At a particular rotating speed, the useful life of a ball or roller bearing varies inversely with the third power of the imposed thrust load”, [1]. For example, 50% reduction in the thrust increases the life of the bearing to eight times as much. On the contrary, a low-capacity bearing can be used instead to lower costs. Reduction of axial thrust also lowers the losses that happen at the thrust bearings. Therefore, mechanical efficiency of the pump increases with decreasing axial thrust. Rotating speed, operating temperature, lubrication type and dimensions of the bearing are other criteria that affect the friction losses at the bearings, [1].

Angular contact ball bearings are the most common type that are used in drivers and thrust bearings assemblies. If necessary, another bearing is mounted in thrust bearing assemblies and with greater thrust spherical roller bearings are used instead. These types of bearings are oil-lubricated and require much more cooling. They are generally water cooled with a small pipe connected to the discharge of the pump, [1]. Both bearing types need continuous downthrust to ensure stable operation. On the other hand, upthrust of the pump should not exceed the upthrust capacity of the

bearing. Approximately, upthrust capacity of the bearings is equal to 30% of its downthrust capacity, [1].

In brief, high axial thrust causes high thrust bearing temperatures, short bearing life, shaft failures and it lowers the mechanical efficiency. For not to use high diameter shafts and high load carrying capacity bearings, axial thrust should be reduced to acceptable degrees. It is also necessary to minimize the cost of the pump.

In this study, balancing holes with balancing ring are used to reduce axial thrust. Pumps are tested with special designed axial thrust measurement system and axial thrust is measured throughout the pump operation. Four main impeller combinations are used during the tests.

- Impeller with ring and holes are not drilled
- Impeller without ring and holes are not drilled
- Impeller with ring and holes are drilled
- Impeller without ring and holes are drilled

Different size holes are drilled at the back side of the impeller. Reduction of the efficiency and other structural – mechanical considerations determine the maximum hole diameter. Number of holes is five because blade number of the impeller is five. After the tests, axial thrust measurements are compared with theoretical calculations and numerical experimentation results.

3.1. Approaches to Calculate Axial Thrust

Axial thrust can be calculated with different theoretical approaches proposed in several references. It cannot be determined exactly due to complexity of the flow inside the pump. Besides downwards axial thrust, momentum change of the fluid, which enters the impeller axially and leaves in semi-radial direction according to

specific speed and exit angle of the impeller, causes a reduction in axial thrust, [1]. Here are some calculation procedures for calculating axial thrust.

Dicmas, [1] proposed a formula to calculate thrust coefficient. Thrust coefficient K_T is found with Equation 3.1, [1].

$$K_T = C\rho A \tag{3.1}$$

Here C is an experimental coefficient, which changes with specific speed of the pump accordingly, Figure 3.1 (Specific speed is calculated with Imperial units in the figure). When balancing ring is used at the backside of the impeller to reduce impeller area subjected to differential pressure, A' is used instead of A in the Equation 3.1, [1].

$$A = \frac{\pi}{4}\left[D_{wr}^2 - D_{SHAFT}^2 \right] \tag{3.2}$$

$$A' = \frac{\pi}{4}\left[D_{wr}^2 - D_{RING}^2 \right] \tag{3.3}$$

Then total axial thrust is calculated by multiplying head of the pump at operating point with thrust coefficient.

$$T = K_T H \tag{3.4}$$

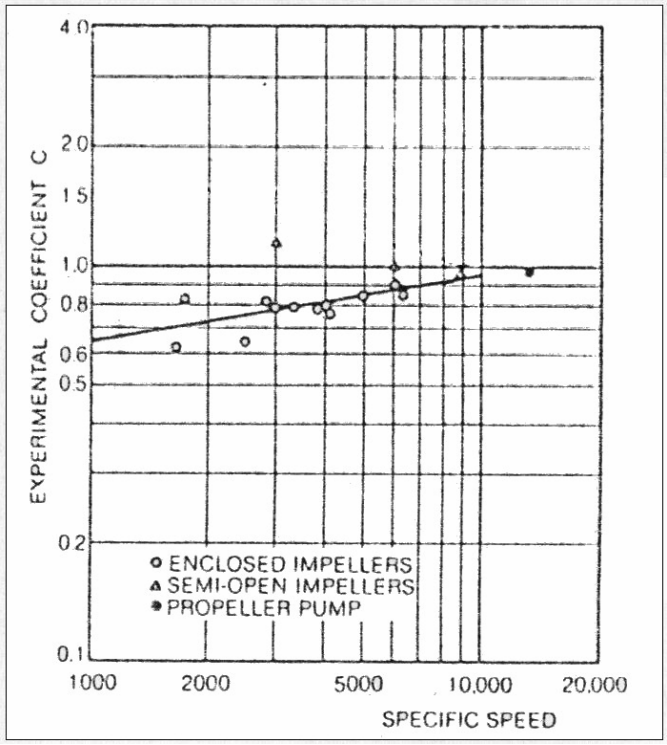

Figure 3.1 Experimental coefficient C, [1]

Lazarkiewicz and Troskolañski, [6] claimed that surface of the pressure distribution at the back face of the impeller is a shape of a paraboloid revolution whose axis coincides with the impeller axis, Figure 3.3. The pressure head, h, on a circular area of radius at a speed of $U = \omega \cdot r$ is,

$$h = H_P - \frac{\left(\frac{U_2}{2}\right)^2 - \left(\frac{U}{2}\right)^2}{2g} = H_P - \frac{\omega^2}{8g}(r_2^2 - r^2) \qquad (3.5)$$

where H_P is the static pressure head at the periphery of the impeller.

Force T_1, acting on the back surface of the impeller between the shaft diameter d_s and the outer diameter of the wearing ring d_{wr} is defined by the formula,

$$T_1 = \rho g \int_{r_s}^{r_{wr}} 2\pi r dr h = 2\pi\rho g \int_{r_s}^{r_{wr}} r dr \left[H_p - \frac{\omega^2}{8g}(r_2^2 - r^2) \right] \tag{3.6}$$

After integration;

$$T_1 = \pi\rho g(r_{wr}^2 - r_s^2)\left[H_p - \left(r_2^2 - \frac{r_{wr}^2 + r_s^2}{2} \right)\frac{\omega^2}{8g} \right] =$$

$$= \rho g(A_{wr} - A_s)\left[H_p - \frac{1}{8}\left(\frac{U_2^2}{g} - \frac{U_{wr}^2 + U_s^2}{2g} \right) \right] \tag{3.7}$$

Static pressure rise can be found as;

$$H_p \approx \eta_h^{'} H_{th}\left(1 - \frac{gH_{th}}{2U_2^2} \right) \tag{3.8}$$

$\eta_h^{'}$ is the impeller hydraulic efficiency and accounts for the only hydraulic losses of impeller.

The change of direction of flow also causes an axial thrust on the impeller, whose direction is upwards (to the exit of the impeller).

$$T_2 = \rho Q_{IMPELLER}(V_o - V_{m2}\cos\theta) \tag{3.9}$$

Finally the resultant force, whose direction is to the suction of the pump, is;

$$T = T_1 - T_2 \tag{3.10}$$

KSB, [11], proposes an approximation for axial thrust calculations between flow rates of $0.8 \cdot Q_{BEP}$ and $1.0 \cdot Q_{BEP}$

$$T = \alpha \rho g H \frac{\pi D_{2A}^2}{4} \tag{3.11}$$

where coefficient α is calculated with Equation 3.12

$$\alpha = 0.5 \left(\frac{D_{wr}}{D_{2A}} \right)^3 + 0.09 \tag{3.12}$$

Axial thrust T should be increased 8% if the clearance between rotating and stationary parts is greater than 0.2 mm, [11].

Axial thrust measurement approaches of Dicmas and Lazarkiewicz – Troskolañski base on calculation of the unbalanced force that is shown in the Figure 3.2. They are assumed the forces acting on the shrouds of the impeller equal. Moreover, KSB introduce an axial thrust coefficient which is substantially dependent on the specific speed of the pump.

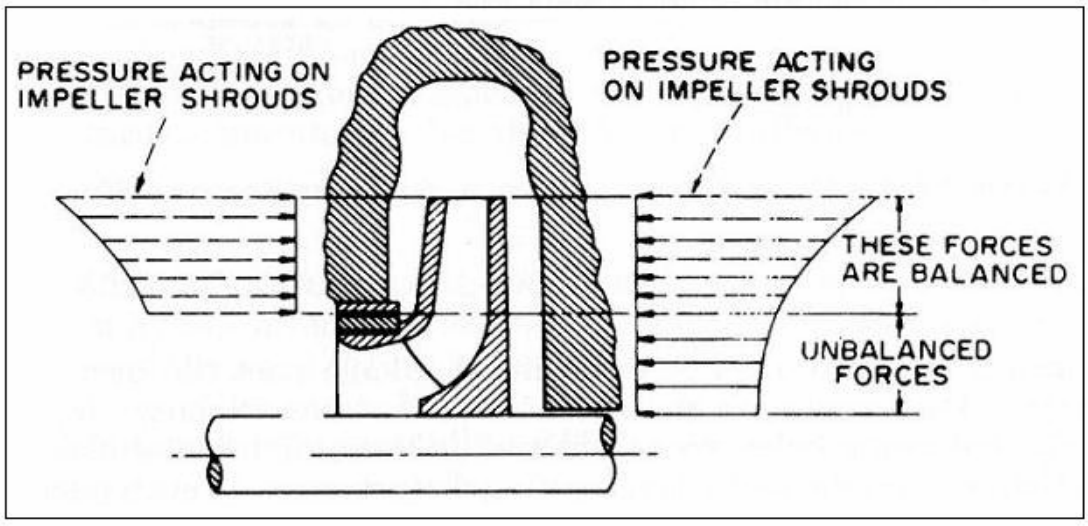

Figure 3.2 Axial thrust calculation approach, [4]

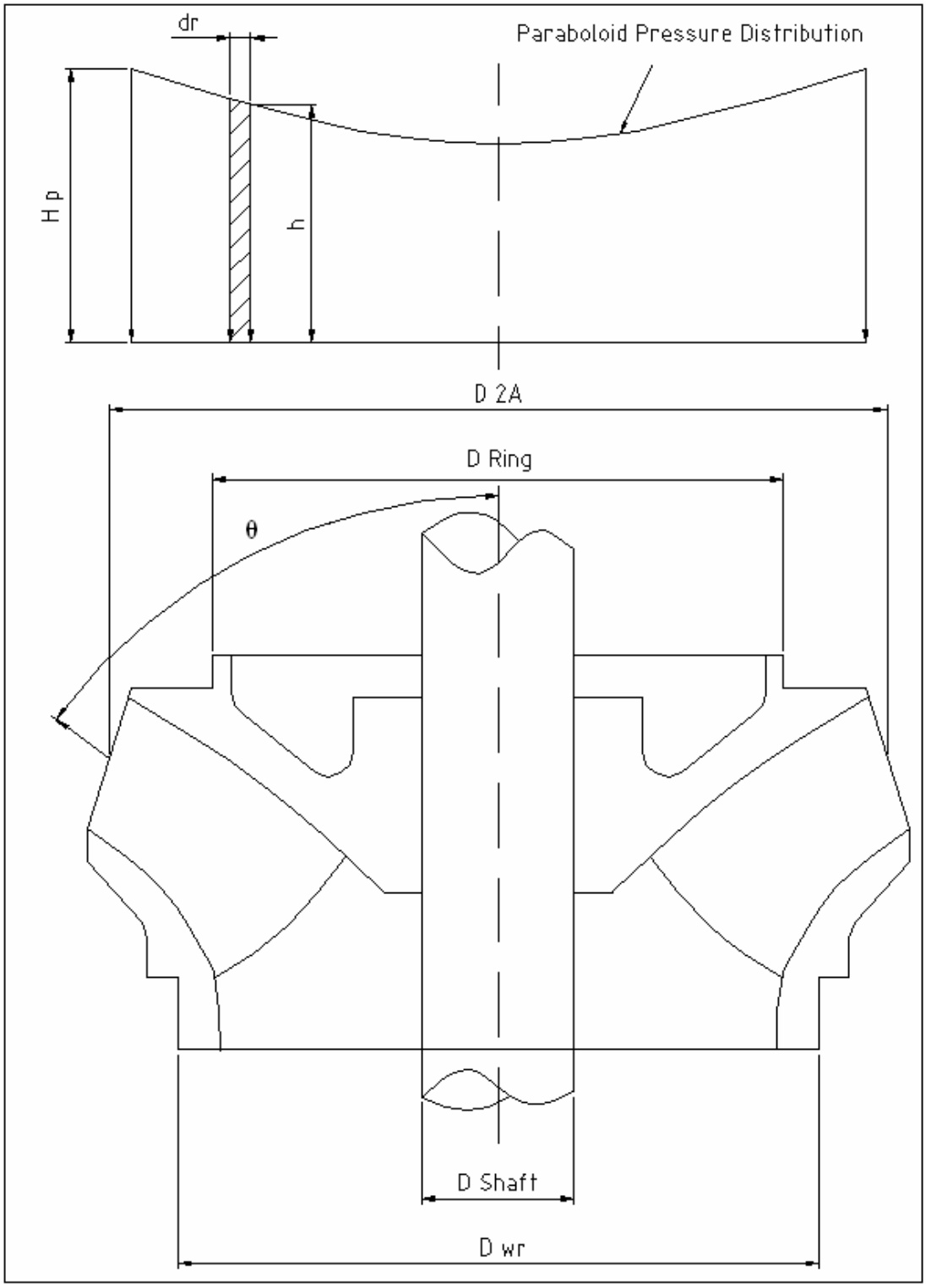

Figure 3.3 Dimensions that are used in axial thrust calculations

3.2. Axial Thrust Balancing Techniques

Axial thrust balancing techniques change with pump (impeller) type, mechanical considerations, economical considerations and desired performance characteristics of pumps. Hydraulic balancing devices used in pumps are balancing drums, balancing disks, balancing holes with back wearing rings, simple radial back vanes, opposed impellers or combination of these. Axial thrust should be reduced in order to minimize cost of the pump and to prevent mechanical failures (shaft or bearings) with one of these methods.

Balancing drum is a device fixed on the pump shaft with a key or a screw, Figure 3.4. There is a small radial clearance between stationary and rotating parts of the drum. It causes leakage between drums' stationary and rotating parts to the back side. At the back side of the drum, there is a balancing chamber. This chamber is connected to the suction of the pump so the pressure is so close to the suction pressure of the pump. Since the pressure at the discharge of the last impeller is considerably higher than the pressure of the balancing chamber, a resultant force occurs on the drum whose direction is to the discharge of the pump, [4]. The diameter of the drum is determined as to reduce axial thrust 90-95% at the operating point of the pump Leakage losses are higher in this application, [6].

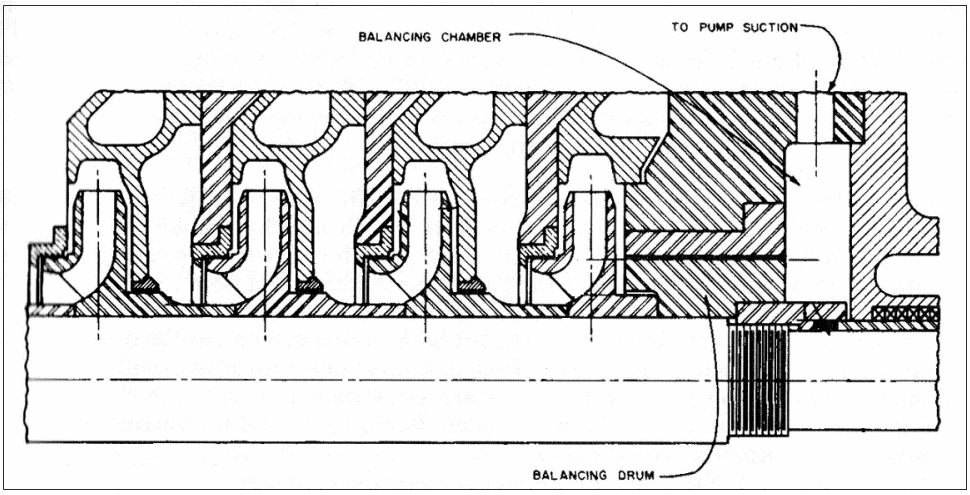

Figure 3.4 Balancing drum, [4]

Balancing disk is a simple disk which rotates with pump shaft. The main difference of balancing disk from balancing drum is self-adjusting its axial position. Axial clearance between the balancing disk head and balancing disk changes while the pump is operating with variable axial thrust on shaft. When axial thrust tends to increase, axial clearance gets smaller and back pressure of the balancing disk reduces. This situation automatically increases the force acting on the disk and it begins to move away from disk head. Therefore, back pressure of the disk begins to increase again and disk is getting closer to the disk head. Movement of the disk continues until a balance is achieved. Restricting orifices should be used to position balancing disc in the axial direction for a proper operation, [4]. It has advantages of simplicity of construction and ability to balance quite large thrusts. On the contrary, its usage for only clean liquids, requiring continuous observance of axial clearance to prevent wear and drop in efficiency due to leakage are disadvantages. Disc diameter is 0.7-0.8 times of the impeller diameter. Volumetric loss is approximately 3% to 6% depending on axial clearance. If disk head wears, it should be renewed to lower the leakage, [6].

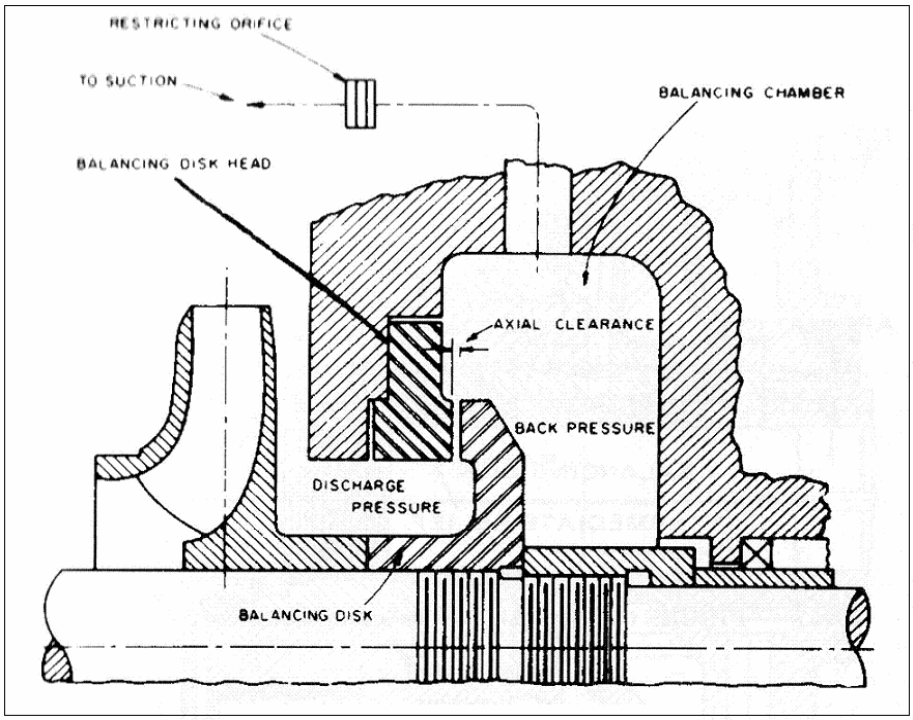

Figure 3.5 Balancing disk, [4]

Combination of balancing drum and balancing disk are used more than single applications of balancing disk and balancing drum. It overcomes the disadvantages of balancing disk with having advantage of automatic positioning of the disk. Rotating parts are a combination of long cylindrical drum and a disk. In this method, radial clearance does not change while operating, but axial clearance depends on balance of the system as described in balancing disk operation. Intermediate relief chamber pressure, which changes with the resultant force acting on the system, plays role in axial movement and proper operation of the balancing disk – drum system, [4]. Increased surface joints also reduce the amount of leakage which results in small drop in volumetric and overall efficiency. On the other hand, acting of pump discharge pressure on the balancing drum gives the opportunity of reducing of disk diameter, [6].

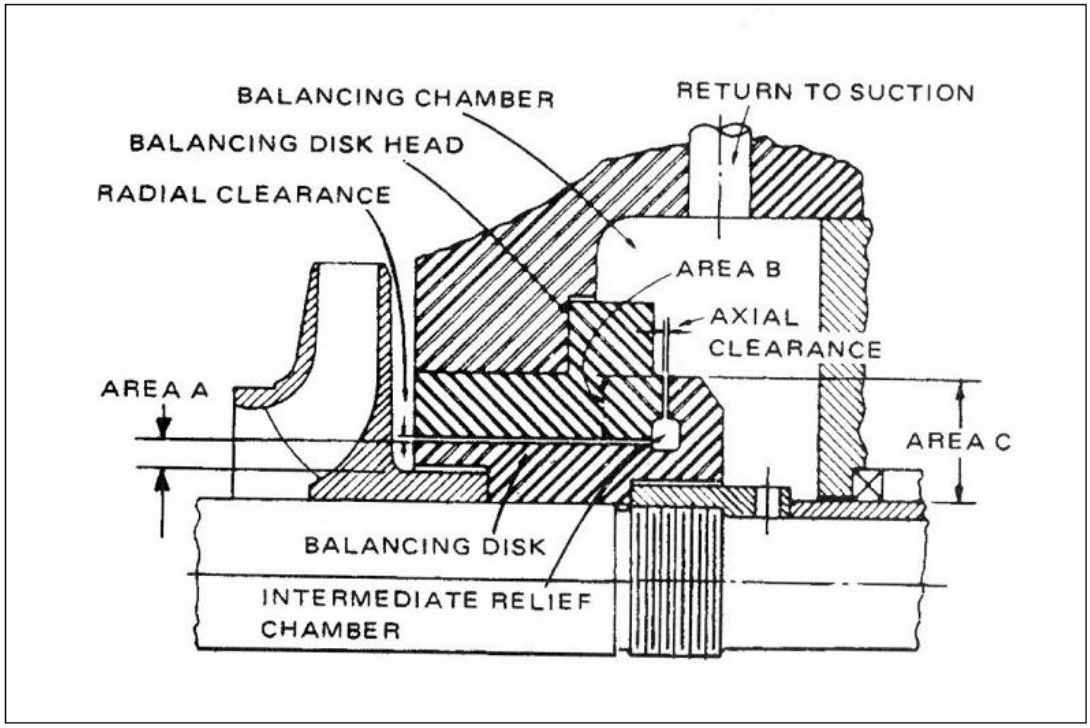

Figure 3.6 Combination of balancing disk and balancing drum, [4]

Pump-out vanes (back vanes) are used to lower the pressure at the back side of the impellers. Therefore, total thrust acting on the impeller is reduced dramatically. The liquid between back vanes (radial ribs) rotates with the same angular speed of the shaft which will reduce the pressure acting on the impeller back face. Axial clearance between vanes and pump casing should be properly adjusted to prevent wear which can cause excessive power consumption. Hence, there is an energy loss with using back vanes, diameter of vanes should not be selected too large. Pump-out vanes are generally used for handling dirty and corrosive liquids; it is not used for clean water applications, [6].

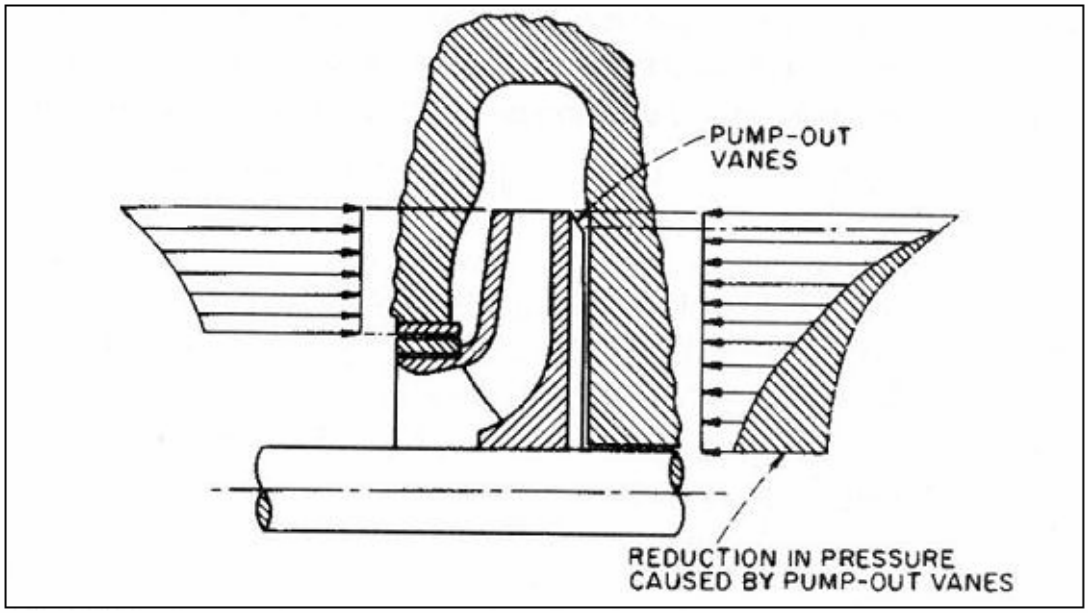

Figure 3.7 Pump-out vanes, [4]

When even numbers of impellers are present, half of them can be faced in the opposite direction. This arrangement on the impellers is named as opposed impellers. Thrust acting on half of the impellers equals to thrust acting on other half of the impellers. However, from other mechanical design features a small amount of thrust may occur on the shaft and must be compensated with thrust bearings. If uneven numbers of impellers are present, thrust acting on one of the impellers is also compensated. [4].

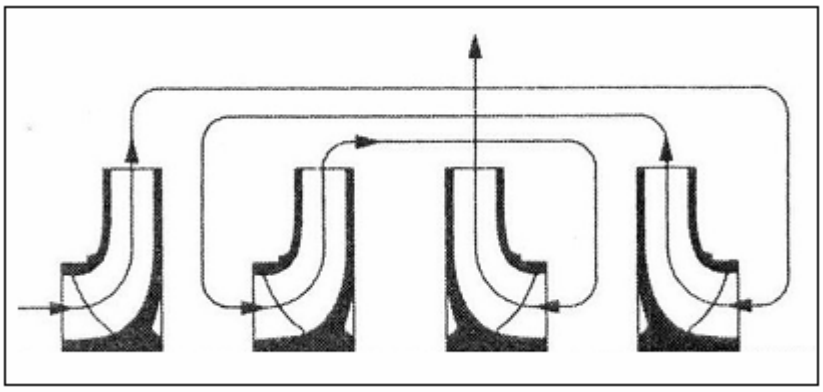

Figure 3.8 Parallel coupled opposed impellers, [11]

Another way to minimize axial thrust is using balancing holes and balancing ring on the back face of the impeller. They are used mostly in multistage vertical turbine pumps, Figure 3.9. These rings reduce the area which the higher pressure is exerted and with balancing holes; they cause a reduction in axial thrust, [20]. In some applications, back wearing ring is on the casing part or as part of the impeller. Radial clearance has an important effect on leakage flow when balancing holes are drilled at the back face of the impeller. Balancing holes are drilled to minimize the pressure at the back side of the impeller and therefore to balance axial thrust. Leakage which returns from holes to the impeller opposes the main flow which results in disturbances in the main flow. Leakage of the fluid also lowers the volumetric efficiency of the pump. The number of holes varies from 4 to 8 depending on the number of the blades and their diameter change from 3 mm to 30 mm depending on the size of the pump, [6].

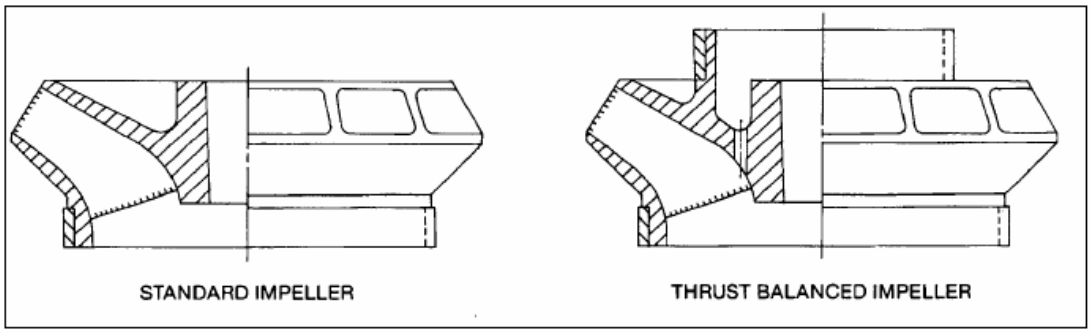

Figure 3.9 Balancing holes and impeller balancing ring, [20]

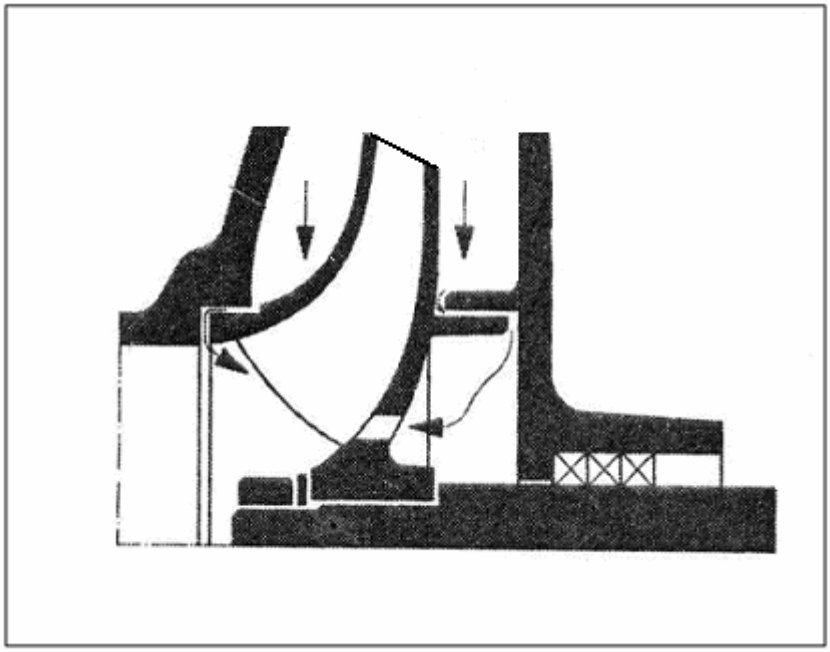

Figure 3.10 Balancing holes and leakage flow, [11]

3.3. Axial Thrust Measurement System Design

In this study, axial thrust measurements are done using load cells. Load cells used in the system are shear – beam type with a 2000 kgf capacity, [21]. They can measure loads which are applied on both sides (up and down), which give the opportunity of measuring upthrust at starting of the pump. Cylindrical compression type load cells could not be used due to small internal diameter which restrains the assembling of the head shaft inside its hole. Instead, three load cells are used in order to do tests. These load cells are mounted with equal angles between them to the additional base plate of the thrust bearing assembly, which consists of the thrust bearings. Thus, weight of thrust bearing assembly, rotating parts and axial thrust acting on the shaft are measured while operating of the pump. Axial thrust acting on the impellers is transmitted to the pump shaft, adjusting nut, thrust bearing assembly and load cells respectively.

Thrust bearing assembly is dimensionalized for the discharge head thatis used with. It is designed for maximum thrust of the pump. It is clear that maximum thrust occurs at the closed valve of the pump. Safety of coefficient is applied on the maximum thrust value and bearings are selected to compensate this amount of thrust in the axial direction. Generally, radial forces are negligible for small pumps. With the increasing dimension of pump radial forces become an important issue and a second bearing is mounted in the assembly to compensate radial forces. Inner ring of the bearings should be compatible with diameter of the head shaft. Bearings are placed inside a hole whose inner diameter is machined according to outer ring diameter of the bearing. They are lubricated and cooled with oil. Therefore amount of oil is important for cooling and lubrication of bearings. Small baffles are placed inside the assembly to provide better lubrication. Movement coupling, non-reversing plate, leak proofing sheet metal, adjusting nut and screw, thrust bearing gland and safety pins are the other parts thatconstitute the thrust bearing assembly.

Pump is driven with a 75 kW V1 type electric motor. Coupling between motor and the head shaft divides the motor and pump parts which ensures that axial thrust is only compensated with thrust bearings. Special designed motor carrying part is directly fixed on the discharge head, so weight of the motor is not measured by the load cells. On the other hand, vibration can affect the measurement of axial thrust but its effect is minimized by adjusting the settings of the load cells indicator. Besides, no strong vibrations are observed during the tests.

Calibration of the load cells are done with a hydraulic press at static load. Load cells are loaded up to 6000 kgf which is the total upper limit, Figure 3.11.

During tests, signals excited from load cells are read on an indicator and recorded on a computer. Tests are done individually with Impeller A, B, C and D at full operating range. Test results are given in section 5.4.

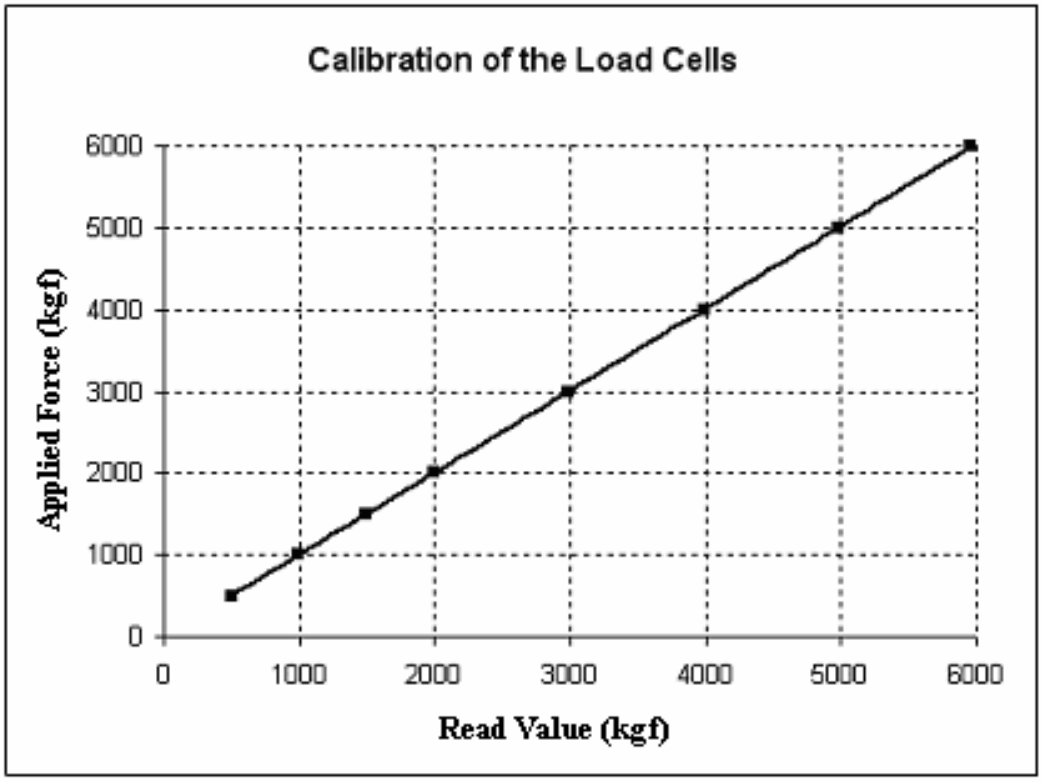

Figure 3.11 The characteristics curve of load cell calibration

3.4. Dimensional Analysis on Axial Thrust

Axial thrust, Th, on the pump shaft depends on the fluid density, ρ, specific energy, gH, flow rate, Q, angular speed, ω, and outlet diameter of the impeller, D. Dependent variable Th can be expressed in the form of,

$$Th = f_1(\rho, gH, D, \omega, Q) \tag{3.13}$$

$$f_2(Th, \rho, gH, D, \omega, Q) = 0 \tag{3.14}$$

There are 6 parameters in this physical problem. (number of parameters, k = 6) The dimensions of these parameters are,

$$[Th] = \frac{ML}{T^2} \quad [gH] = \frac{L^2}{T^2} \quad [\rho] = \frac{M}{L^3} \quad [D] = M \quad [\omega] = \frac{1}{T} \quad [Q] = \frac{L^3}{T}$$

Primary dimensions that are involved in the parameters are the mass, M, time, T, and length, L. (number of primary dimensions, r = 3) According to the Buckingham-Pi theorem, there are k – r = 6 – 3 = 3 non-dimensional parameters.

Repeating parameters are selected as fluid density, ρ (dynamic variable), diameter, D (geometric variable), and angular speed, ω (kinematic variable).

$$\Pi_1 = Th\rho^{a1} D^{b1} \omega^{c1} \tag{3.15}$$

$$\Pi_2 = gH\rho^{a2} D^{b2} \omega^{c2} \tag{3.16}$$

$$\Pi_3 = Q\rho^{a3} D^{b3} \omega^{c3} \tag{3.17}$$

Then non-dimensional parameters are found as,

$$\Pi_1 = \frac{Th}{\rho D^4 \omega^2} \tag{3.18}$$

$$\Pi_2 = \frac{gH}{\omega^2 D^2} \tag{3.19}$$

$$\Pi_3 = \frac{Q}{\omega D^3} \tag{3.20}$$

It is clear that second non-dimensional parameter is head coefficient and the third one is flow coefficient.

Therefore, axial thrust of geometrically similar pumps with different fluids and angular speed can be expressed in terms of,

$$\frac{Th_1}{Th_2} = \frac{\rho_1}{\rho_2}\left(\frac{D_1}{D_2}\right)^4 \left(\frac{\omega_1}{\omega_2}\right)^2 \tag{3.21}$$

CHAPTER 4

CFD ANALYSES OF PUMP ASSEMBLY

4.1. General Information on Analyses and Commercial Software

Computational fluid dynamics (CFD) software packages are used systematically in design of every turbomachines nowadays. The most important features of CFD softwares that introduce a designer are giving opportunity to analyze the internal flows structures better, to compare different designs with an efficient way, to shorten the design period, to reduce manufacturing of prototypes number and to decrease the overall cost of the product. Pump flow problems can be detected early in the design process and re-design can be made with the help of the CFD outputs.

Usage of commercial CFD code "CFdesign" in design of the vertical turbine pumps in Layne Bowler Pumps Company began with studies of Özgen [22] and validation of the code is achieved for some specific speed and flow rates. After the tests are done for a designed pump, test results are compared with numerical experimentation results. A correlation is tried to obtain between numerical experimentation and test results depending on specific speed, dimension, flow rate and geometry of the pump, [22]. Results of the numerical experimentation provide a database for further designs. Internal flow structure of the pump is mainly analyzed by investigating pressure and velocity distributions over the impeller blades, pathlines inside the pump and relative – absolute velocity vectors. Performance characteristics of the pump, which are flow rate – head and flow rate – efficiency curves, are achieved throughout the operating region of the pump. In brief a pump designer can investigate the design by numerical experimentation before manufacturing and test of the model pump.

CFdesign solves the Navier-Stokes equations, continuity equation and energy equation over the full three dimensional solution domain of the pump. These are the

main equations which will govern the fluid flow. Since these equations are in partial differential form, they should be discretized or algebraic equations should be used instead to do iterations on the equations. For this purpose finite element method is used in CFdesign due to its adaptivity to any geometrical model, [23]. Semi Implicit Method for Pressure Linked Equations Revised (SIMPLE-R) solution algorithm is used in CFdesign. It has an automatic mesh generator with geometry diagnostics tools. Diagnostics utility automatically finds the potential problematic areas, which came from CAD model. These areas may cause errors in assigning mesh sizes, mesh generation and convergence – stability of the analysis. Quadrilateral, triangular, tetrahedral, hexahedral, wedge and pyramid elements are available in CFdesign for numerical experimentation of fluid flows, [23]. Meshing of the solution domain gets easy with using mesh enhancement module. It constitutes layers of extruded triangle elements along walls and fluid – solid interaction areas. It also helps the user by constructing mesh elements in the boundary layer region. Sufficient amount of nodes are located in small gaps between adjacent walls and cavities with the help of the mesh enhancement. Mesh enhancement module enables the user to change boundary layer properties with boundary layer thickness factor box. The ratio of the total height of the inflation layer to the original elements and number of layers can be changed accordingly in the mesh enhancement module, [23]. The flow is assumed to be incompressible and k-ε turbulence model is used in calculations. RNG and Eddy Viscosity turbulence models are also available but k-ε turbulence model fits best for pump analysis, [22].

CFdesign V7, V8 and V9 are used in pump analyses. A computer with 3.2 GHz Pentium 4 central processing unit (CPU) and 2 GB of random access memory (RAM) is used for analyses. Numbers of elements generated, complexity of the geometrical model, numbers of iterations, CPU clock speed and amount of RAM greatly affect the analysis time. Amount of RAM enables user to use more elements on the solution domain and more clock speed of CPU enables user to make faster analyses.

4.2. Analyses Steps

4.2.1. CAD Modeling

Computer Aided Design (CAD) modeling of the geometry is the first job that should be done in order to do CFD analyses. It is important to have a clear CAD model to use in CFdesign. As mentioned earlier, problems may occur during assigning mesh sizes, mesh generation and stability – convergence of the analysis if the CAD model is improper. Avoiding from cavities or small gaps between two surfaces relative to the pump dimension may result in better convergence and stability of the analysis. Pump parts are designed in Mechanical Desktop 2007.

Solution domain of the pump includes suction reservoir, pump parts (suction intake, impeller, bowl, shaft), and exit volume which can be taught as the fluid volume inside the discharge column, Figure 4.1. Simply extruding circles at the inlet and at the exit of the pump, CFdesign automatically obtain the inner flow domain inside the pump by doing cut and boolean operations. A rotating volume (region) is also constituted around the impeller by surrounding the impeller itself. In the analyses impeller and rotating reference frame are rotated together with the same angular speed, [23]. Clearance between impeller and bowl, where the leakage flow occurs, is assumed as a solid part in all of the analysis except one of them. Same mesh sizes are assigned on pump parts when two of the analyses are performed. However, in the second case smallness of the clearance relative to the dimension of the pump causes some instability in the convergence of the analysis. While comparing different impellers, only impeller itself is changed in the assembly and all other parts are kept same.

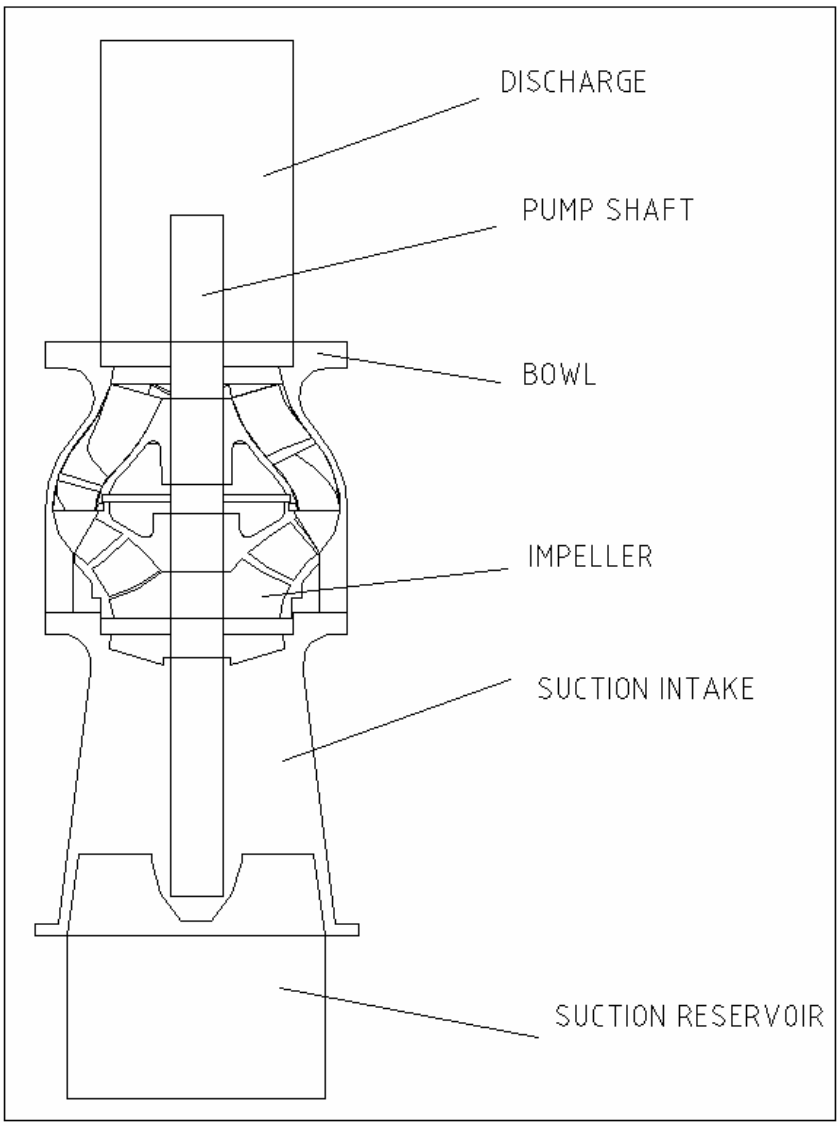

Figure 4.1 Cross sectional view of the solution domain

CAD models of the pump and analysis parts can be shown in the Figure 4.2. All of the CAD parts are a model of exact parts which are manufactured. Rotating region is seen as a solid part but when it is transformed, CFdesign performs cut and boolean operations and obtains the blade to blade volumes of the impeller, suction volume and bowl volume. If suction reservoir, discharge and rotating region is not drawn properly, desired analysis volumes could not be achieved. Finally, whole pump assembly is transferred in to CFdesign by exporting the CAD model into ACIS (sat)

file format. After transformation of the CAD model it should be checked for any defects or unwanted surfaces or volumes.

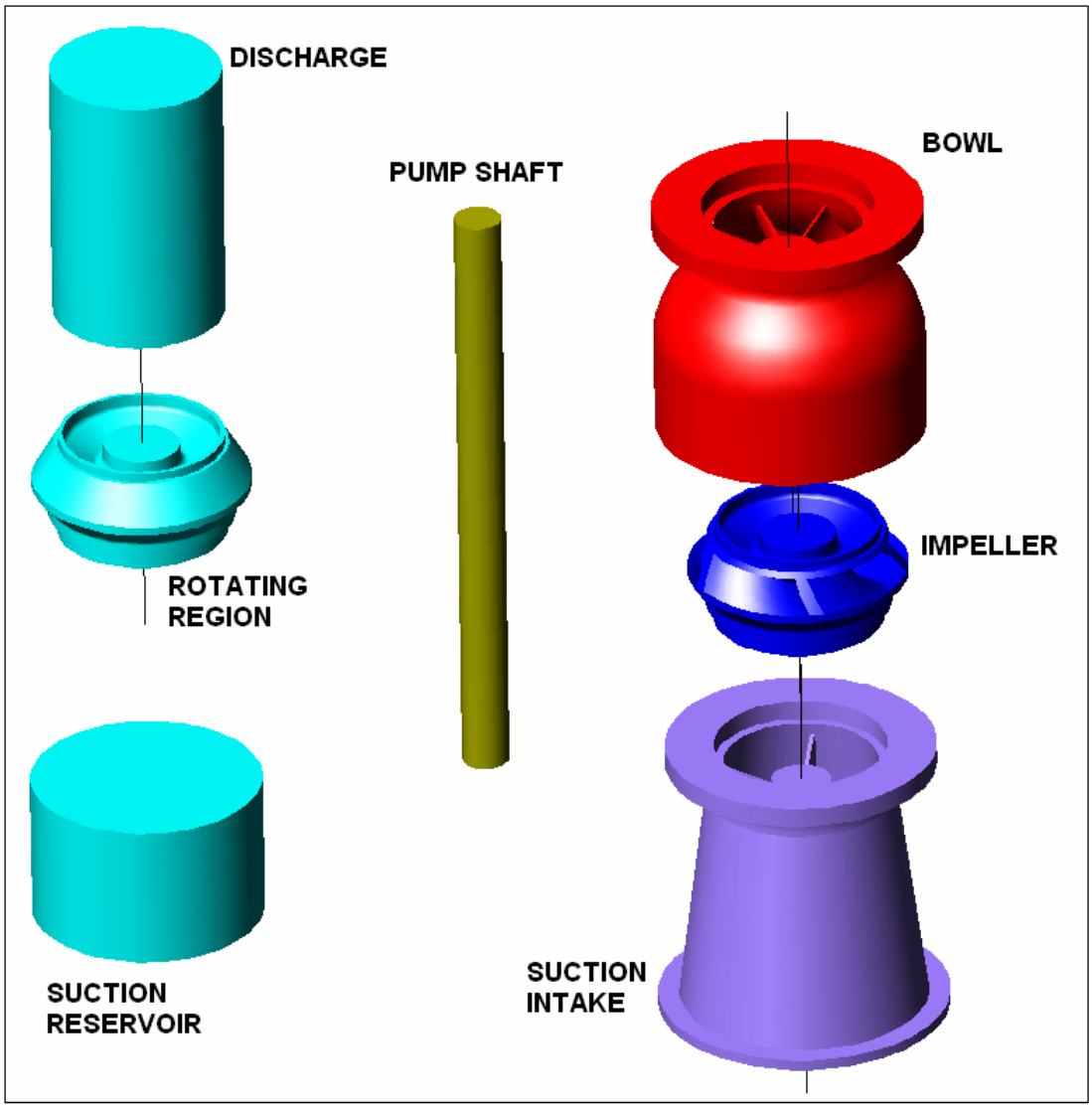

Figure 4.2 CAD models of the solution domain and pump parts

4.2.2. Boundary Condition Definitions

There are six types of boundary conditions in CFdesign which can be put on the governing equations. These are inlet, outlet, no-slip wall, symmetry line, slip wall and periodic type boundary conditions, [23]. In the analyses, volumetric flow rate is defined at the top of the pump assembly as an outlet boundary condition, zero gage

pressure is defined at the bottom surface of the suction reservoir and slip/symmetry boundary condition is defined at the lateral surface of the suction reservoir to simulate the suction. At this surface gradients that are normal to the surface are zero and therefore there is no flow across the boundary. “For incompressible flows, the most robust condition for the pressure equation is to specify a value at the exit”, [23]. This is done by specifying volumetric flow rate at the outlet and then pressure rise is read across the pump. Alternatively, analysis can begin at run-out flow rate (where the flow rate is equal to zero) to establish the flow field. In order to obtain pump performance characteristics several analyses are done at different flow rates. This is somewhat similar to adjusting the discharge valve of a pump which is installed its operation area.

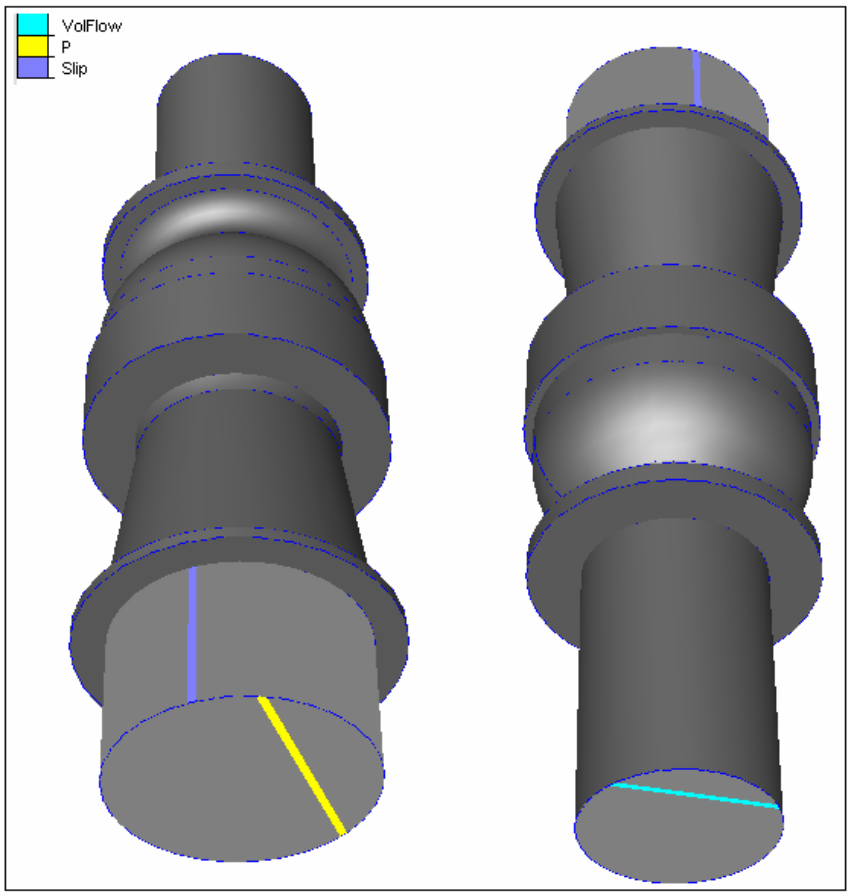

Figure 4.3 Boundary condition definitions over the pump assembly

4.2.3. Meshing of the Solution Domain

For robust and reliable CFD calculations a high quality mesh should be generated over the solution domain, [4]. A good mesh is also necessary for accurate and converged solutions. CFdesign has an automatic mesh generator and uses finite element method to discretize the flow field. Element size used in the flow field greatly depends on the experience but there are some basic guidelines. Element numbers used in the analyses are limited with the memory of the computer, so it is not possible to use so small element sizes in the solutions. On the other hand to discretize the geometry and to simulate the flow better, there is a lower limit for number of the elements used in the solutions. Ratio of the neighboring element sizes should not exceed 1.25. The mesh should be fine in the regions where pressure and turbulence gradients are mostly occur such as leading and trailing edge of an impeller. Rotating region is the most important part for the pump analyses where power is transmitted to the fluid by impeller blades. Beginning with rotating region mesh can be coarsened through bowl, suction, discharge and suction reservoir respectively. Rotating region mesh size can be chosen close to the thickness of the impeller blades in order to mesh the geometry effectively. Similarly in the bowl, mesh size should be close to thickness of the vanes but it can be coarser than rotating region mesh size because there is only fluid flow in bowl. When compared with rotating region and bowl, suction, discharge and suction reservoir have less significance on the solution. “Techniques based on geometry shape as well as anticipated flow behavior have been developed and communicated, but mesh sizing is still an area that confounds many users”, [23]. In pump analyses, that have a number of fluid elements between 1.2 million to 1.7 million, good results are obtained. On the contrary, the mesh independency could not be achieved for turbomachinery problems, [22].

Boundary layer development and separation is also important in turbomachinery solutions. Boundary layer thickness factor (ratio of the boundary layer to the original element size) and number of layers are present in the mesh enhancement dialog box

to form a proper boundary layer inside the flow domain. Default values which are 0.45 for boundary layer thickness factor and 3 for number of layers are used in the analyses.

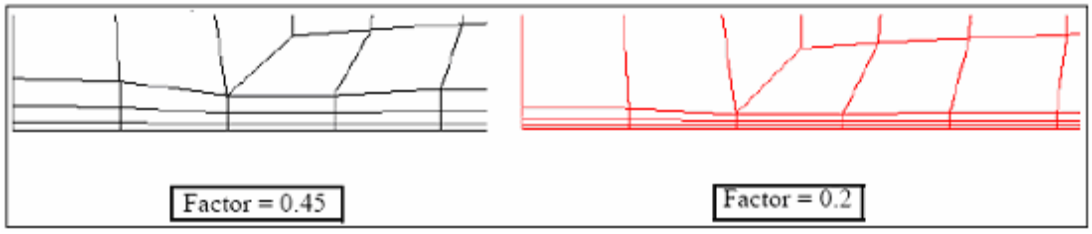

Figure 4.4 Boundary layer thickness and number of layers, [23]

Sliding mesh stator-rotor simulations are used in CFdesign. "With the rotating mesh in its new position, all scalar quantities are mapped from the rotating side to the non-rotating side of the sliding mesh interface using geometric interpolation between the two mesh systems", [23]. While in frozen rotor simulations, rotor and stator have a fixed relative position. Rotating effect is added on rotating parts with a frame transformation. Therefore it is not suitable for transient analyses.

4.2.4. Material Assignment

Material assignment is done on every volume which came from CAD model of the pump. Suction reservoir, discharge volume, volume inside the suction intake and volume inside the bowl are chosen as water. Volumetric efficiency is equal to 100% when hatched area (leakage volume) is defined as solid part, Figure 4.5. However, this volume should be chosen as water when volumetric efficiency of the pump is concerned. Volume which encloses the impeller is assigned as rotating region with constant rotational speed (2900 RPM). Revolution speed of the rotating region can also be defined variable with time like a soft starting of a pump. Rests of the parts are defined as solid which is cast iron.

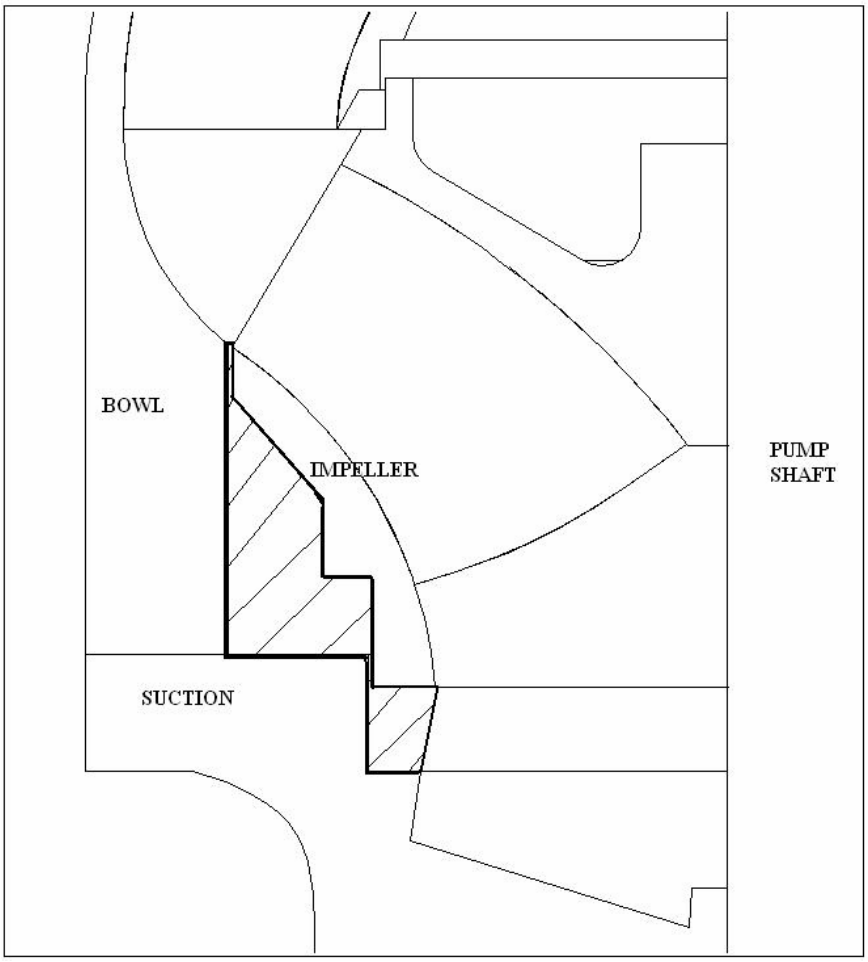

Figure 4.5 Leakage volume

4.2.5. Analyses Types and Options

Flow is assumed to be incompressible and turbulent model is k-ε. There is no heat transfer throughout the solution domain. Convergence on the pressure and other flow variables are achieved at the end of the iterations. Oscillations observed through the iterations are acceptable. Convergence of the analyses can be followed with the help of the convergence monitor that is based on average value of flow variables in the solution domain. "The primary criteria for determining convergence is that each degree of freedom is not changing with subsequent equations", [23]. Relaxation factors (α) for pressure, velocities and turbulence are assigned as 0.5 that is the default value. It represents that the new solution and old solution have the same

weights on the value of the flow property at that node. In other words, if α is equal to 0.0 new solution is ignored, if it is equal to 1.0 old solution is ignored, [23].

$$\varphi = \alpha\varphi_{new} + (1 - \alpha)\varphi_{old} \tag{4.1}$$

4.3. CFD Analyses of Pump Assembly

Effect of swept angle and stacking on the performance characteristics and effect of blade exit angle on the pump head and efficiency are investigated individually. Afterwards volumetric efficiency of the pump is analyzed on the selected model by means of meshing the leakage path. Finally, axial thrust measurements are done on the pump similar to axial thrust measurement test setup.

Comparisons are made regarding results of CFD analyses which are best efficiency point, pump head, pump efficiency and manufacturing considerations. Some design checkpoints such as velocity loading and diffusion factor, pressure and velocity distribution over the blade are also investigated. Simple blade to blade analyses are not embraced because frozen rotor mesh type is applied on the model in these types of analyses that are not suitable for transient problems. On the other hand, numbers of stator vanes and rotor blades are different from each other which make it impossible to divide the full domain into similar portions. If blade to blade flow volume of impeller is only used as a solution domain in the analyses, definition of boundary conditions become difficult due to their closeness to the rotating region area. Instability occurs in such analyses.

Analyses are nearly done with 1.2 million fluid elements. It corresponds to 265000 fluid nodes. Impeller is run at constant 2900 RPM from start to end of the analyses. Each analysis takes 38 hours to finish. In the analysis which volumetric efficiency is observed, more elements are used to mesh the volume between the impeller and bowl. This analysis is run for 46 hours. Convergence is both followed from convergence monitor and physical properties which are recorded at defined intervals

by the program. Graph of these properties are drawn versus iteration steps to investigate convergence.

To find out the head generated by pump, simply Bernoulli equation is written between two cross sections by constituting cut-planes, Figure 4.6. These cut-planes are at the pump exit and below the suction intake of the pump.

$$Head = \left(\frac{p}{\rho g} + \frac{V^2}{2g} \right)_{EXIT} - \left(\frac{p}{\rho g} + \frac{V^2}{2g} \right)_{INLET} \tag{4.2}$$

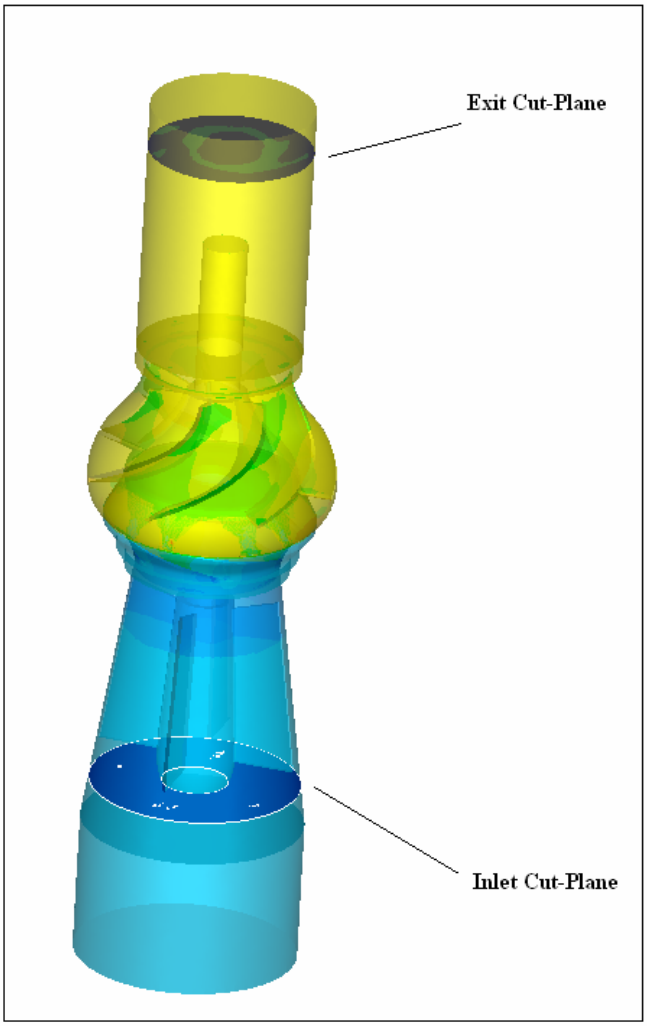

Figure 4.6 Cut-planes where pressures and velocities are read on

CFdesign generates a torque file for the rotating region volume. These file includes the magnitude of the torque in Nm which should be applied for every iteration steps. Therefore hydraulic efficiency can be calculated using these output file. If volumetric efficiency is concerned than result will be the multiplication of the volumetric and hydraulic efficiencies. With assumed mechanical efficiency overall pump efficiency can be calculated at the final step.

$$\eta_H = \frac{\rho g Q H}{\omega Torque} \tag{4.3}$$

$$\eta_{Pump} = \eta_H \eta_V \eta_M \tag{4.4}$$

Performance characteristics of the pump which are head vs. flow rate and pump efficiency vs. flow rate is achieved finally. On the other hand flow inside the pump is investigated in terms of velocity and pressure distributions. The streamline which are designed and used to model the impeller in Mechanical Desktop 2007 are transferred into CFdesign in order to find velocity and pressure distributions on these 3D streamline splines. Coordinates in 3D form are read from a file in CFdesign with XYPlot option, then velocity magnitude, U-velocity, V-velocity, W-velocity and pressure distributions are obtained respectively. Since CFdesign gives these velocities in Cartesian coordinates, they are translated into cylindrical coordinates as follows. Here x, y, z are the coordinates of the points in Cartesian system.

Radius (distance of the point from pump axis) is defined as;

$$r = \sqrt{x^2 + y^2} \tag{4.5}$$

$$\theta = atan\frac{y}{x} \tag{4.6}$$

$$z = z \tag{4.7}$$

In Cartesian coordinates,

$$\vec{V} = [V_x, V_y, V_z] \tag{4.8}$$

Unit vectors are,

In Cartesian coordinates,

$$\vec{e_x} = [1,0,0] \ , \ \vec{e_y} = [0,1,0] \ , \ \vec{e_z} = [0,0,1] \tag{4.9}$$

In cylindrical coordinates,

$$\vec{e_r} = [\cos\theta, \sin\theta, 0] \ , \ \vec{e_\theta} = [-\sin\theta, \cos\theta, 0] \ , \ \vec{e_z} = [0,0,1] \tag{4.10}$$

Absolute velocities,

$$V_r = \vec{V}\,\vec{e_r} = \cos\theta V_x + \sin\theta V_y \tag{4.11}$$

$$V_\theta = \vec{V}\,\vec{e_\theta} = -\sin\theta V_x + \cos\theta V_y \tag{4.12}$$

$$V_z = \vec{V}\,\vec{e_z} = V_z \tag{4.13}$$

Relative velocities,

$$W_r = V_r = \cos\theta V_x + \sin\theta V_y \tag{4.14}$$

$$W_\theta = V_\theta - U = -\sin\theta V_x + \cos\theta V_y - \omega r \tag{4.15}$$

$$W_z = V_z \tag{4.16}$$

Meridional velocity V_m

$$V_m = \sqrt{V_z^2 + V_r^2} \tag{4.17}$$

Fluid angle β_f ,

$$\beta_f = asin\frac{V_m}{W} \tag{4.18}$$

Circumferential velocity V_θ,

$$V_\theta = U - Wcos\beta_f \tag{4.19}$$

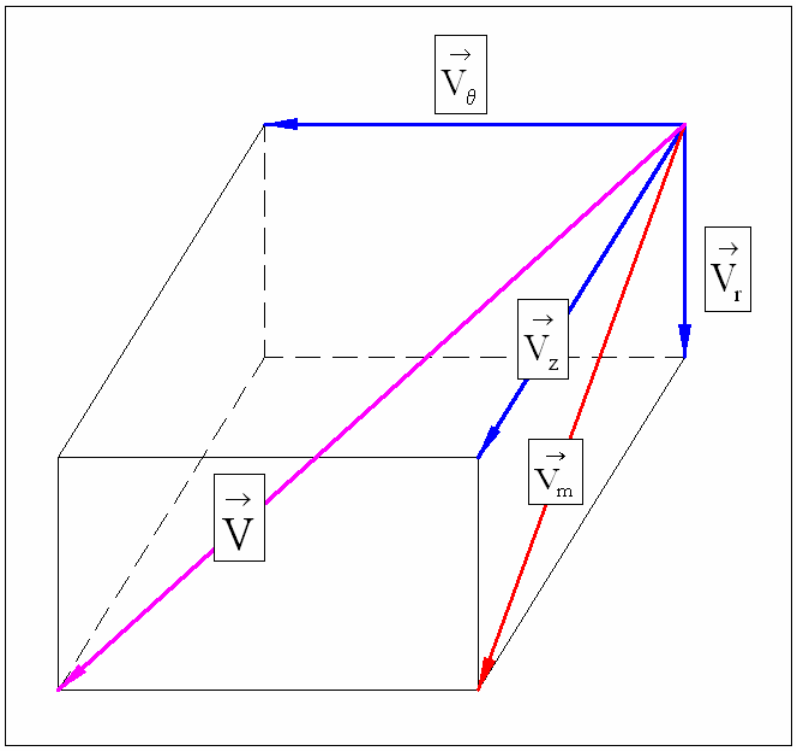

Figure 4.7 Velocity vectors

Analysis solutions for designed and manufactured pump are given below. Velocity and pressure distributions are presented for mid-streamline (AA) where the preliminary design is made. The results are given for the design flow rate 40 l/s.

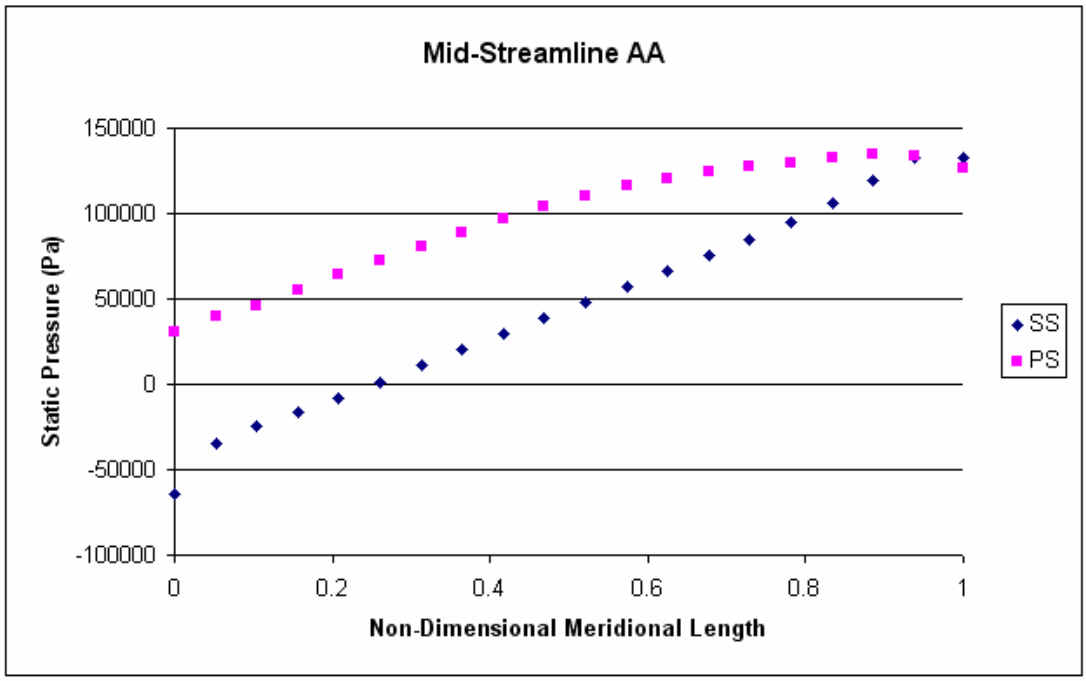

Figure 4.8 Pressure distribution along streamline AA

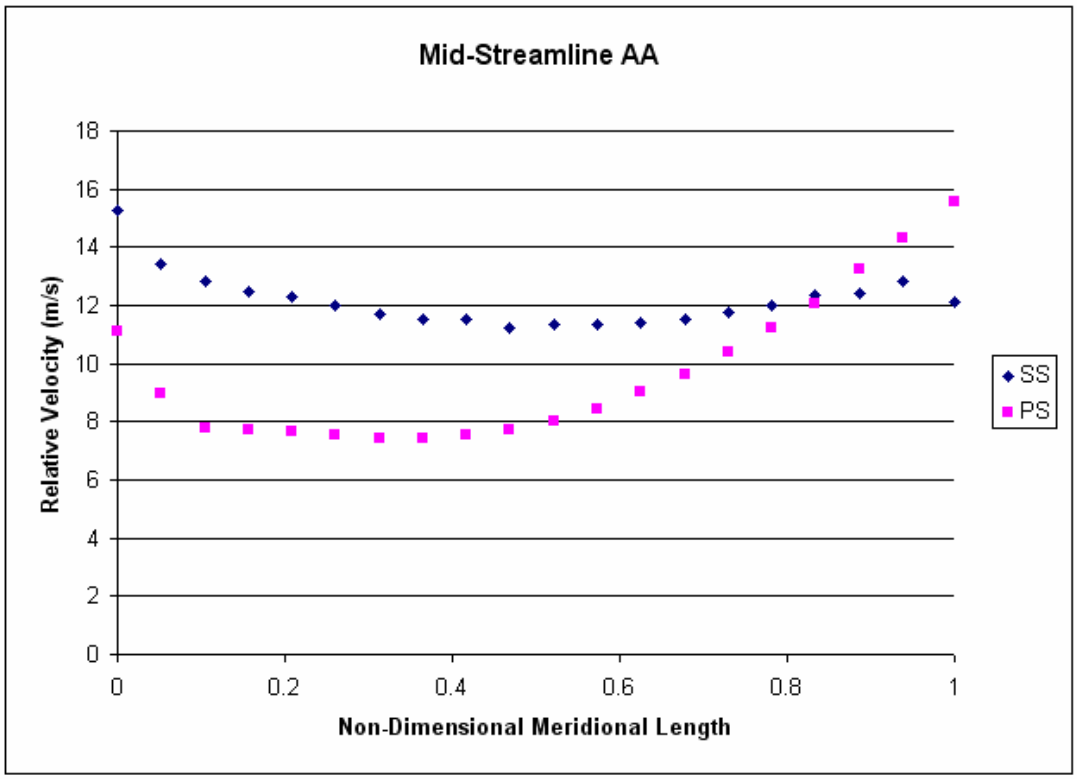

Figure 4.9 Relative velocity distribution along streamline AA

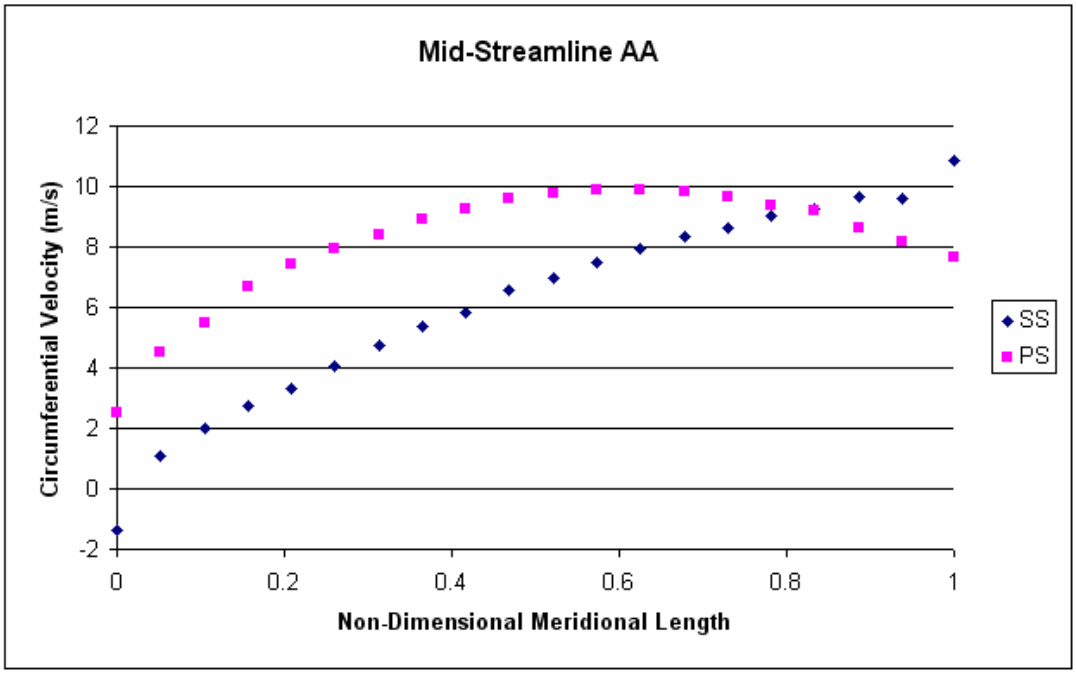

Figure 4.10 Circumferential velocity distribution along streamline AA

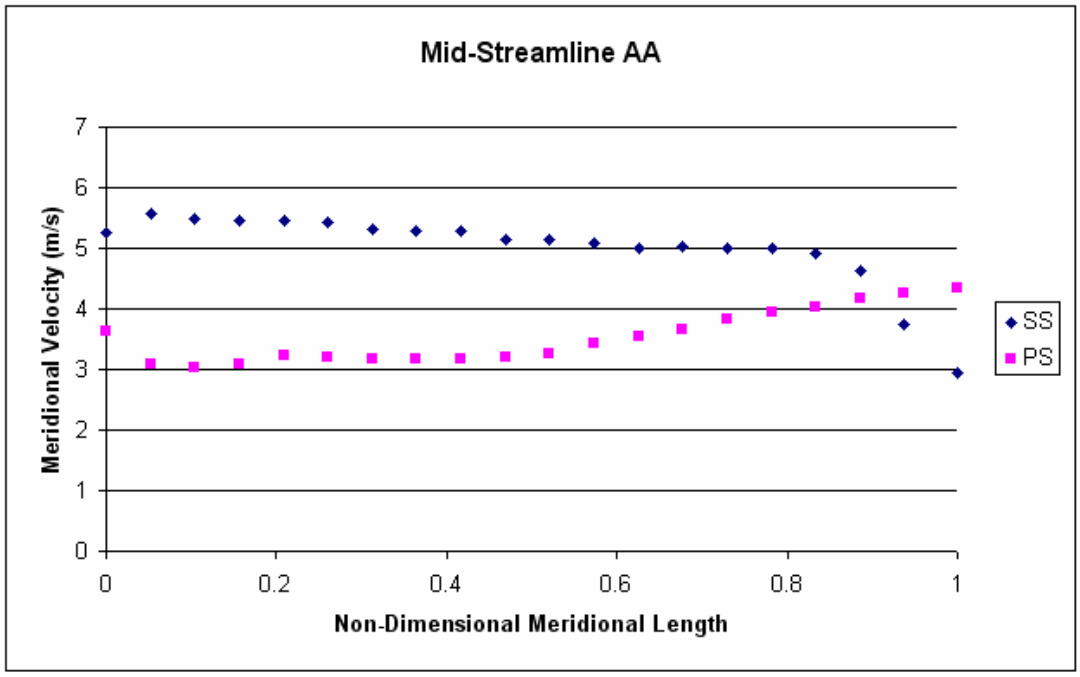

Figure 4.11 Meridional velocity distribution along streamline AA

Impeller produces the most of the pressure head. Pressure at the suction side of the impeller blade inlet is below zero that necessitates great attention to avoid cavitation. A negative geometric head is sufficient to constitute a positive pressure at the inlet of the first impeller. As a matter of fact vertical turbine pump applications are generally installed with negative geometric head.

Deceleration is observed at suction side of the blade but it is fairly slow and there is no rapid deceleration throughout the pump which can cause boundary layer separation. Relative velocities are nearly same at the inlet and at the exit of the profile. Therefore, diffusion does not take place in the impeller. On the other hand, relative velocity is considerably higher at the shroud profile because of higher angular velocity, which causes more frictional losses. Therefore, length of the shroud profile – BB is so important to minimize these frictional losses. On the contrary, relative velocity at the hub profile – EE is low due to lower angular velocities but back flow is not observed.

It is seen that at the trailing edge, relative velocity at the pressure side is higher than relative velocity at the suction side. However, it is expected that relative velocities to be same at the trailing edge of the impeller. Relative velocity at the pressure side begins to exceed the relative velocity at the suction side after 85% of non-dimensional meridional length. This is due to secondary flow formation in the impeller, [24]. Secondary flows arise due to acting of the higher Coriolis forces on the fluid particles that are present in the middle of the flow passage. However in the boundary layer, velocities are lower than the velocities of particles that are in the middle of the flow passage due to friction of the fluid. Therefore, higher Coriolis forces dragged the fluid particles towards pressure side of the blade. This phenomenon is analogous to fluid flow that is observed in 90^{o} elbow, [24]. Moreover, sharp corner of the blade, which is the suction surface of the trailing edge, is stagnation point, Figure 4.13. It also affects the distribution of relative velocity through the suction side of the impeller and secondary flow formation, [10].

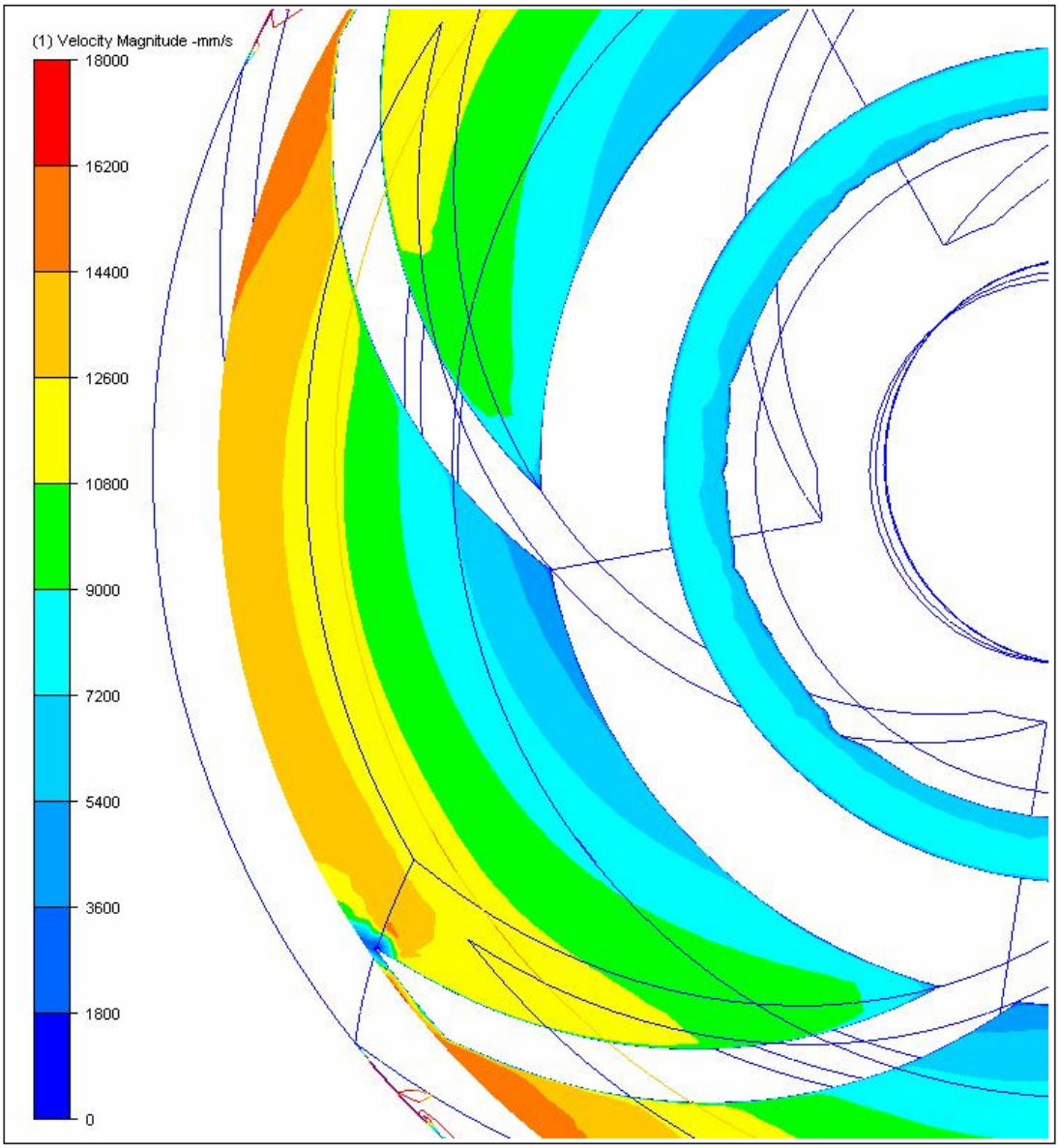

Figure 4.12 Relative velocity contours at the mid-section of impeller exit breadth length

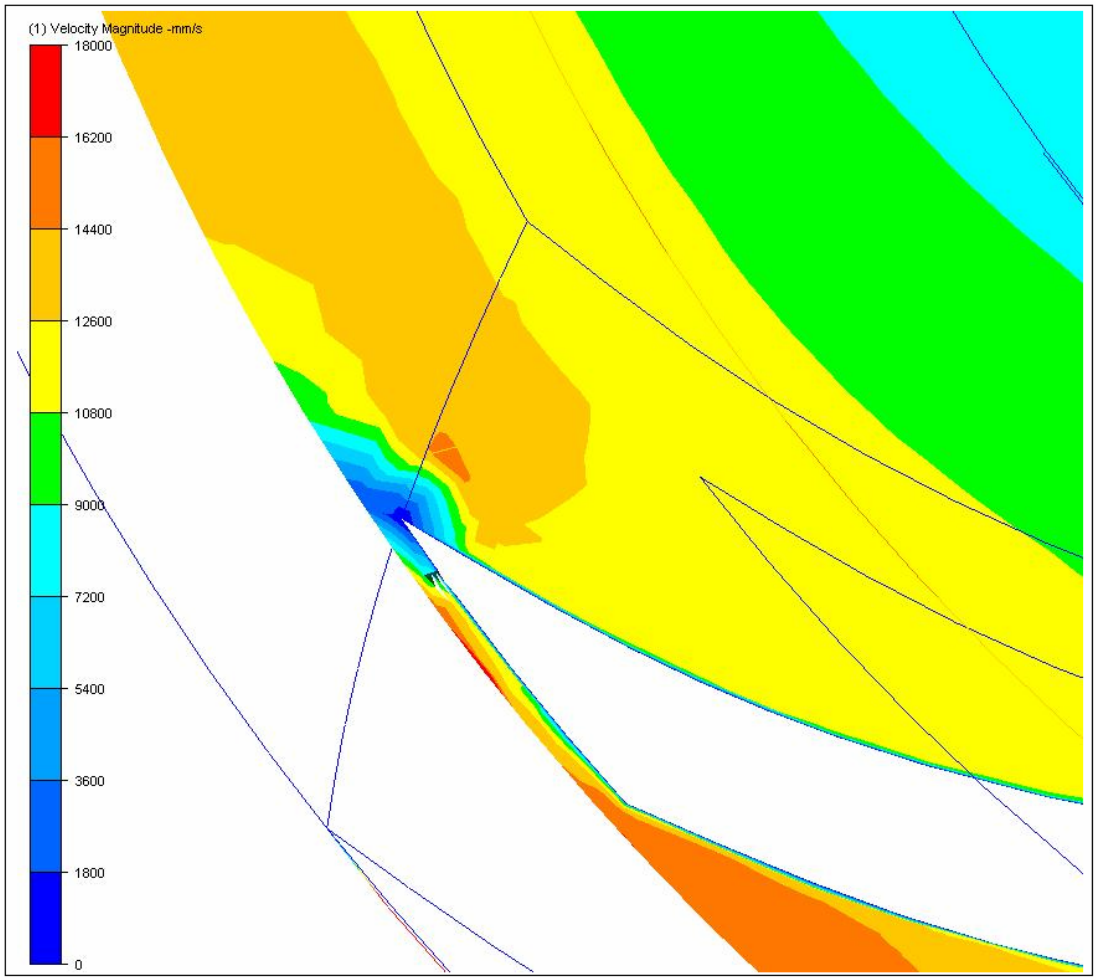

Figure 4.13 Stagnation point at the suction side of the trailing edge

Mean circumferential velocity distribution is nearly alike with that is proposed in the Figure 2.15.

On the other hand flow inside the pump can be analyzed with velocity vector representations. Pathline traces are placed on sections of the pump, Figure 4.14, Figure 4.15.

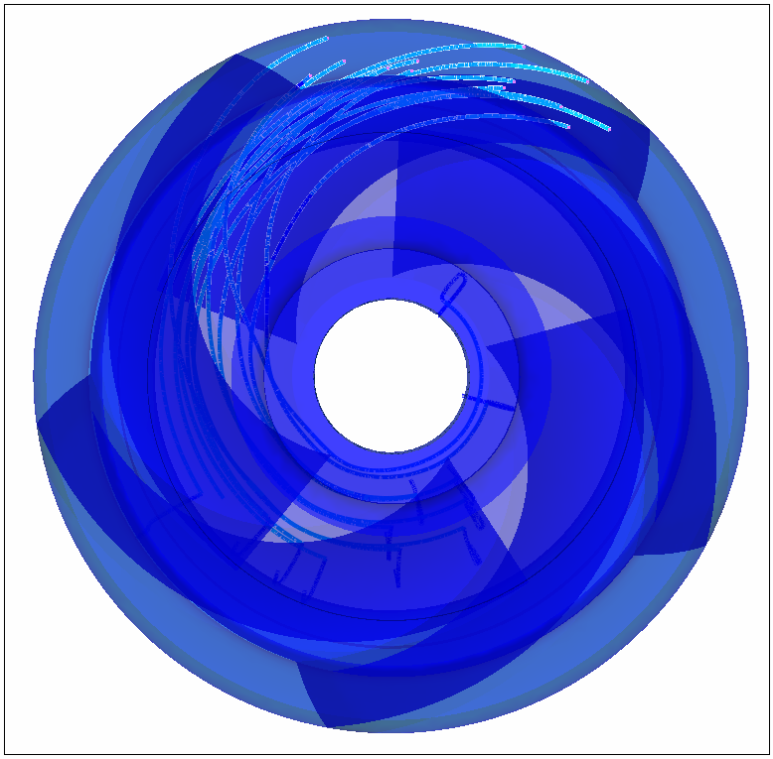

Figure 4.14 Pathlines inside the impeller

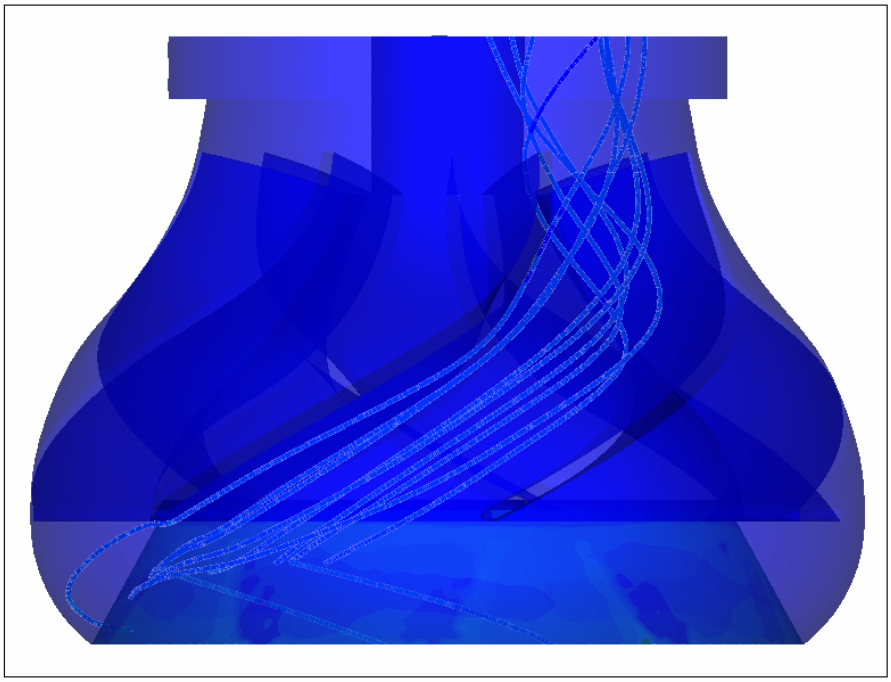

Figure 4.15 Pathlines inside the bowl

Secondary flow formation is observed inside the bowl, Figure 4.16. However there are no backflow and leading edge separation, Figure 4.17.

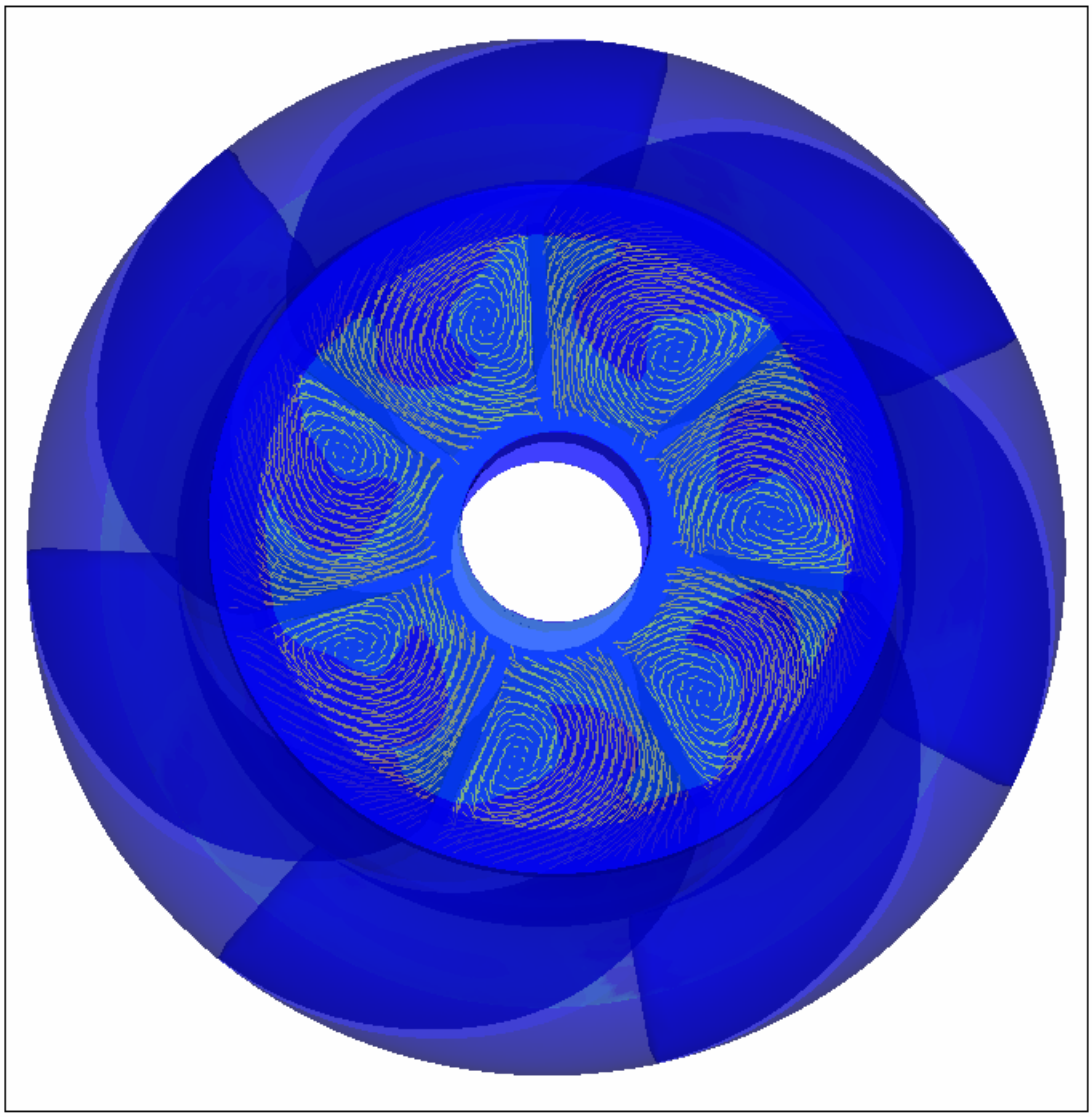

Figure 4.16 Secondary flow formation at the diffuser exit

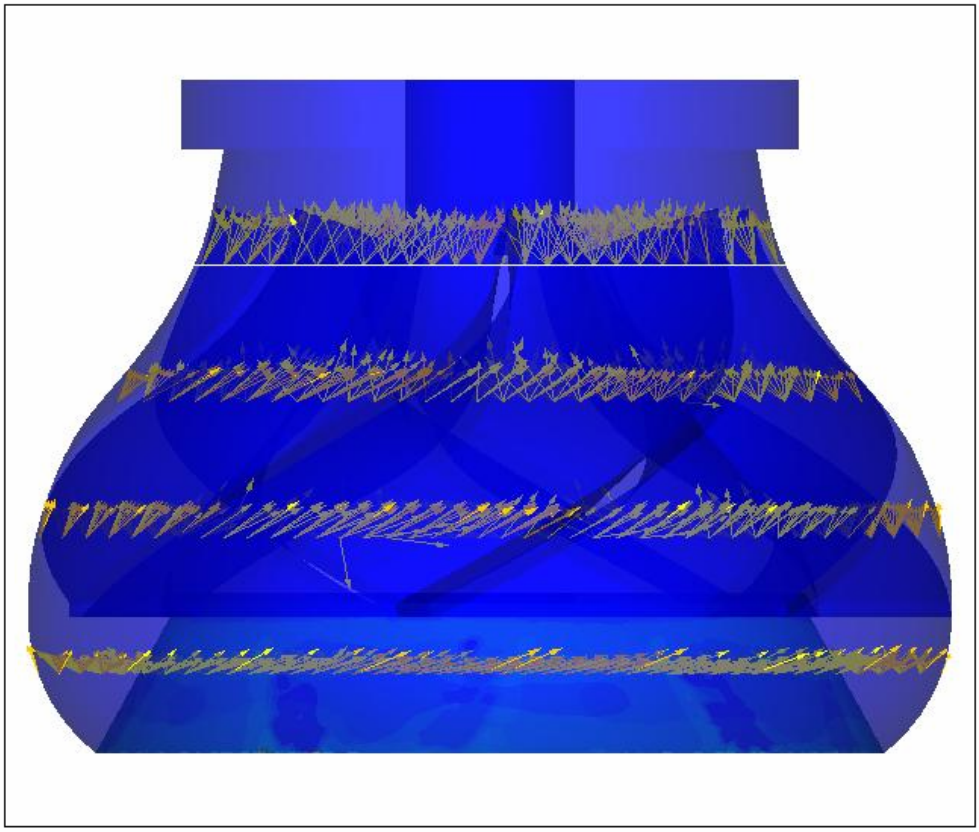

Figure 4.17 Velocity vectors at different diffuser sections

Swirling motion of the fluid tends to continue after the bowl and it is seen that flow do not enter proportionally to the inlet of the next impeller. This affects the no-prewhirl condition of the following impellers and also affects the performance characteristics. Secondary flow formation can be reduced and flow direction at the bowl exit can be corrected comparatively by changing length of the bowl and swept angle of the vanes. But vane swept angle is restricted with manufacturing abilities and length of the bowl is one of the important consideration for weight of the bowl. On the other hand long bowl vanes cause more frictional losses which will result in a drop in pump head. Therefore, an optimization should be done concerning performance characteristics of the pump, weight of the bowl, pressure recovery inside the bowl and manufacturing restrictions. On the contrary, pressure recovery is obtained with the help of the designed bowl.

Static pressure rise across the pump can be seen in the Figure 4.18. Static pressure of the pump is nearly 15 mwc at the exit of the pump bowl. To increase the desired head at the design point underfile should be done to the trailing edges of the impeller. Impeller with underfiled blades is not analyzed in the CFdesign but test results are given for underfiled impeller. If pump could not generate the desired head at the design flow rate and there is no clear errors in the analyses, design of the pump must be reviewed beginning with the impeller. Best efficiency point of the pump is at the 40 l/s which shows that pump flow passages are fairly determined and turbulence losses are kept minimum near the design point.

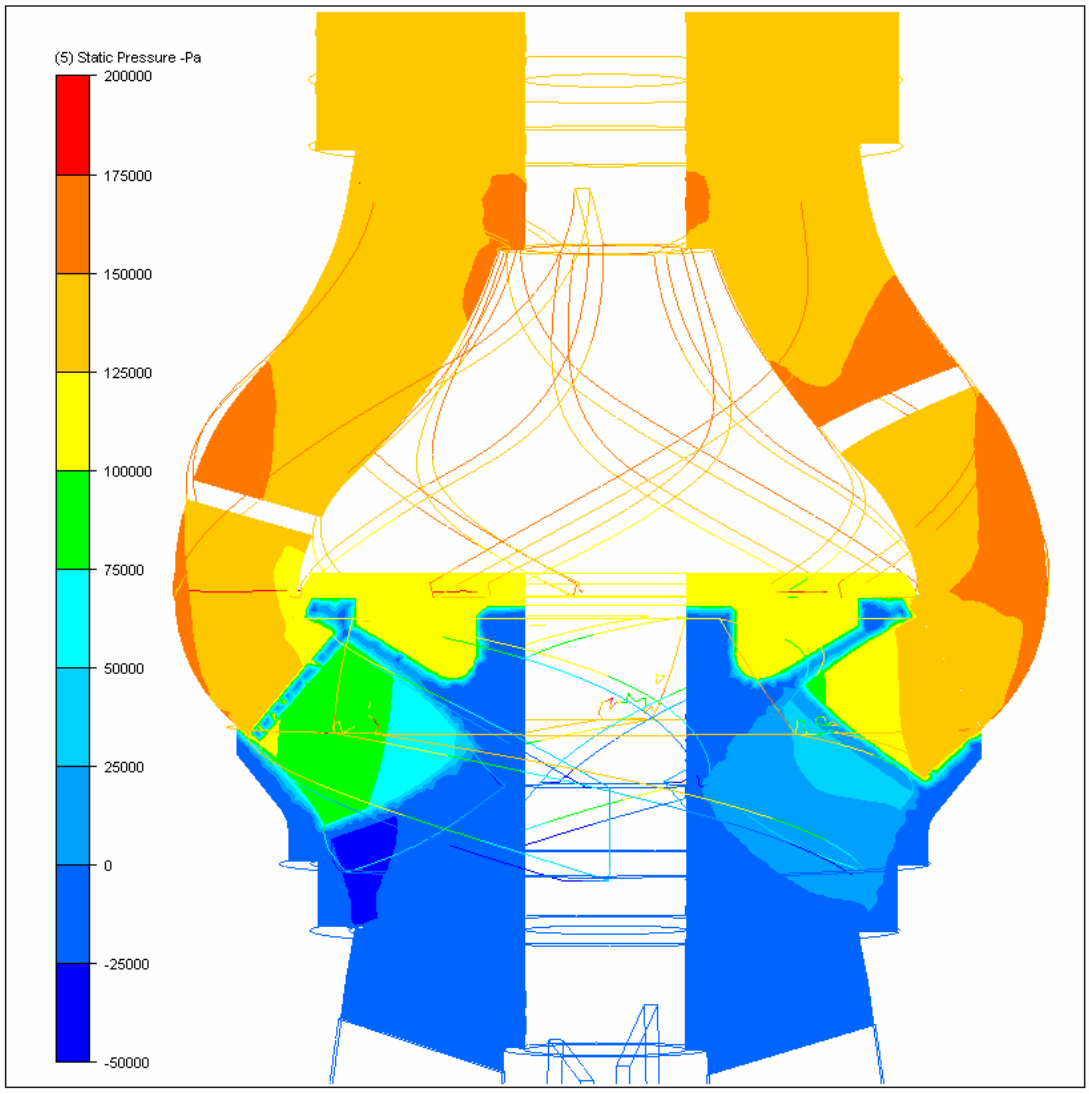

Figure 4.18 Static pressure rise across the pump

CHAPTER 5

TEST SETUP AND PROCEDURE

5.1. Test Stand

Designed pump assembly is tested in accordance to TS EN ISO 9906 “Rotodynamic Pumps – Hydraulic Performance Acceptance Tests” standard in Layne Bowler Pumps Company test stand. The test stand is accredited by Turkish Standards Institution in accordance to TS EN ISO 17025 “General Requirements for the Competence of Testing and Calibration Laboratories” standard.

Test well of the stand has a cylindrical shape which has 3 meters diameter and 9 meters depth. There are four electric controlled actuators inside the test stand to regulate the butterfly valves. These valves can be controlled with joysticks thatare present on the test panel of the test room. Three of the discharge lines are tied up with a collector at the outside of the test stand. Then four discharge lines can be used according to their diameters to discharge the water from collector. They are DN80, DN125, DN200 and DN300. Every discharge line has a gate valve installed on. On the other hand there is another discharge line which is independent from others and it is DN450. Discharge lines have U-shape at the end in order to prevent air to enter the discharge line.

Flowmeters are also installed on these discharge lines to measure the flow rate of the pump. Flowmeters are magnetic type and have maximum capacities of 30 l/s, 100 l/s, 200 l/s, 300 l/s and 700 l/s respectively. Appropriate discharge line and flowmeter is selected for pump to be tested. Flow rate of the pump at the open valve is the criterion for selection of the discharge line. Water is recirculated in to the well after the flow rate is measured.

Pressure measurements can be done either with manometers or pressure transducers. There are several manometers and pressure transducers in the test stand. Pressures up to 40 bars can be measured. Suitable pressure measurement device is selected regarding pump head at the closed valve.

Test stand electrical panel has a capacity of 250 kW. There are four main boards on the panel with power ranges of 0-15 kW, 0-45 kW, 30-185 kW and 90-250 kW. Pump motor is connected to the related electrical board considering the nominal power of the motor. Thermic relay adjustment is done in order to stop the motor if current of the motor is increased over its critical value. Also there is a frequency controlling unit which can be used up to nominal motor power of 90 kW. Motor data of the pump is read via energy analyzer which has a capacity of 1000 Amperes. Voltage, current, phase factor and total power consumption of the motor can be read individually with the help of the energy analyzer.

Geometric height measurement between pressure measuring device and water level are done manually. Rotation speed measurements can be done either optically or mechanically with a tachometer on V1 and VHS motors. These data are also collected for to determine performance characteristics of the pump.

Pressure, flow rate and motor power measurements can be done with personal computer (PC) available in the test stand. There is a programmable logic controller (PLC) panel which collects the data send from pressure transducers, magnetic flowmeters and energy analyzer. Electrical signals are converted into numerical data and transmitted to PC with the help of analogue – digital (A/D) card of PLC panel. A program running on PC converts these data into the required units and applies calibration formulas on the data. Performance characteristics of the pump are then achieved instantaneously. Calibration of the test instrumentations are done periodically by accredited calibration firms and tests are done with cold clean water that has the specific requirements described in the standard, [25].

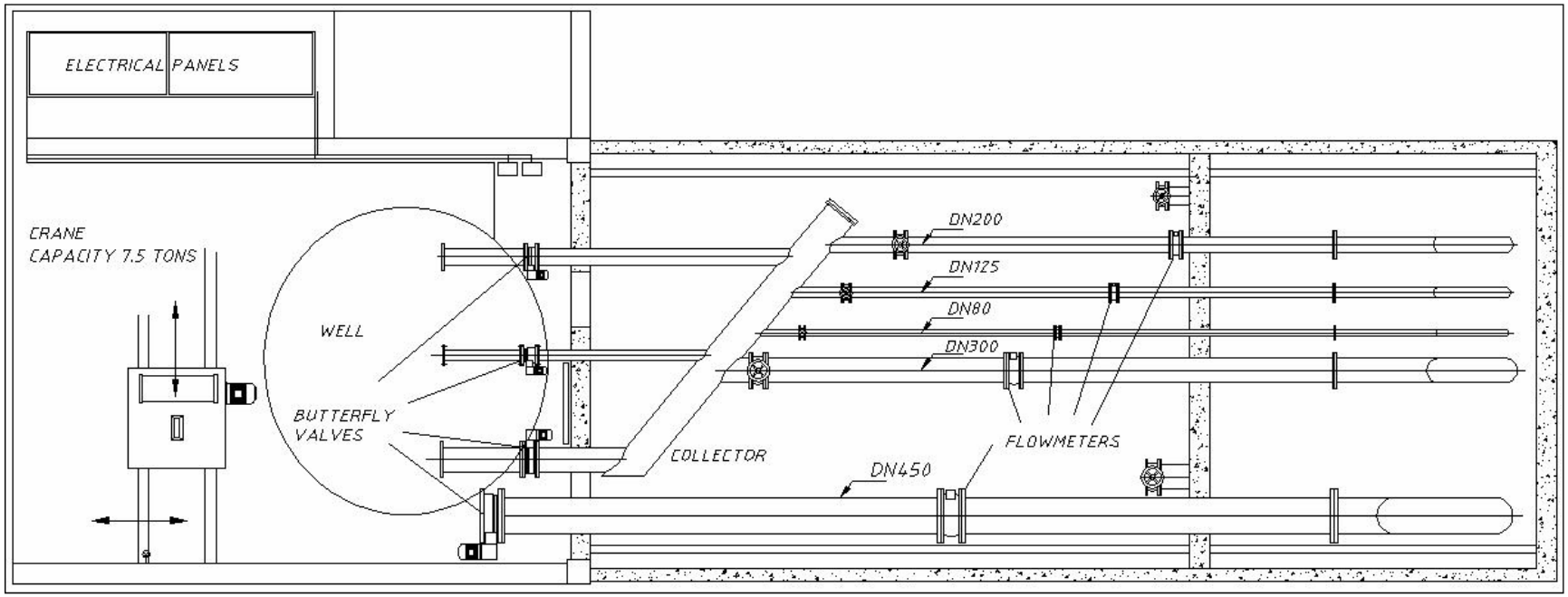

Figure 5.1 Test stand

5.2. Test Setup

Pump is assembled on the assembly line then carried into the test stand. Lateral and radial clearances should be observed after assembly process. Pump assembly is positioned in front of the valve with the help of the crane. Pump, small discharge column pipe, line shaft, discharge head, head shaft, stuffing box, special designed thrust bearing assembly with load cells, adjusting nut, motor coupling, motor carrying construction part and motor are installed respectively.

Pump assembly is tested with 75 kW V1 motor as line shaft type. Power is transmitted to pump via coupling, head shaft, line shafts and pump shaft. Shafts are lubricated with water while operating. Impellers are fixed to the pump shaft with keys. Impellers are positioned laterally inside the bowls using adjusting nut. At first they are at the lowest position inside the bowl. With the help of the adjusting nut impellers are raised and get the correct operation point. This is so important for vertical turbine pumps to get the best performance characteristics. Stuffing box is used to prevent water leakage from shaft while it is rotating. However a small portion of leakage is necessary to lubricate the stuffing material. Discharge head is connected to small discharge pipe and pipe is connected to the butterfly valve. Bolts and nuts are used at the discharge line to connect the flanges together. Threaded discharge column pipe and threaded couplings are used for assembling of pipe to the discharge head and between shafts respectively.

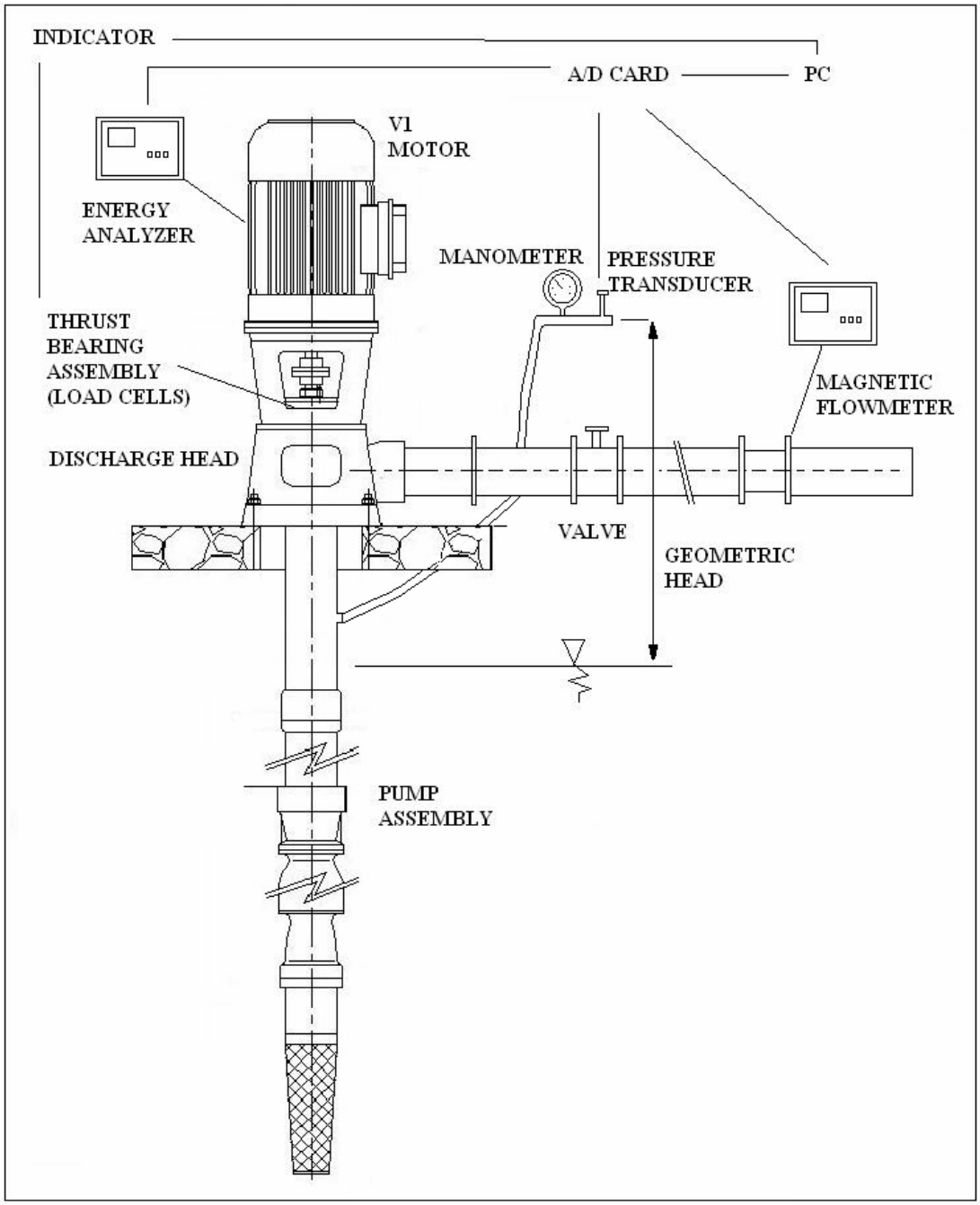

Figure 5.2 Test setup

5.3. Test Procedure And Data Processing

Test procedure followed in the pump performance and axial thrust measurement tests is given below. Processing of the collected data is expressed then.

5.3.1. Test Procedure

Following procedure is applied during the pump performance and axial thrust measurement tests.

1. Pump is assembled and installed to the discharge line.
2. Motor connections are done by electric technician to suitable board on the electrical panel and thermic relay adjustment is done.
3. Manometers or/and pressure transducers are installed on the pressure collector regarding the pump head at the closed valve.
4. Gate valve of the appropriate discharge line is opened and others are closed at the outside of the test stand. (Capacity of the flowmeter is compared with flow rate of the pump at the open valve when selecting the discharge line.)
5. Pressure hose is assembled to the columnpipe.
6. All of the emergency stop buttons and switches are opened on the electrical panel and controlling panel.
7. All of the electrical controlled butterfly valves are closed. The valve which is in front of the pump is opened with a rate of ¼.
8. Sense of rotation of the motor is controlled for a short moment.
9. If sense of rotation is correct motor is started again otherwise power connections are corrected.
10. Air which can be stucked at the end of the pressure collector is removed with the small valve.
11. Valve position is changed with joystick to get the full performance characteristics.
12. Pressure, flow rate, geometric height, power and axial thrust data are collected for every valve position after the steady state is reached.
13. Oscillations on the monitored values, noise and vibration are observed with great attention and safety regulations are followed strictly during the test. (Pump should be stopped in the presence of any abnormal situation)
14. Motor is stopped after sufficient data is acquired and pump is disassembled.

5.3.2. Data Processing

Bernoulli equation is simply written between static water level and pressure measurement location to find the pump total head.

Pressure at the discharge line which is static head, dynamic head (generated by velocity of the fluid) and geometric head take into consideration when total head of the pump is calculated. Velocity of the fluid is found dividing the flow rate into cross sectional area of the column pipe.

All of the data is processed with calibration formulae. This is either done manually or automatically with PC. Processed data is then used to find performance characteristics as mentioned in the standard, [25]. Axial thrust data is also processed with calibration formula and then weight of the rotating parts are subtracted from the measurement to find the net axial thrust, because axial thrust measurement system measures both the axial thrust and weight of the rotating parts.

5.4. Test Results

Test results for performance characteristics and axial thrust measurements of the designed pump are given below. Tests are done with 5 stage line shaft pump with 75 kW – 2900 rpm V1 motor.

Fluctuations in the measured quantities, measurement uncertainties and pump performance characteristics are in the limits that are defined in the standard, [25].

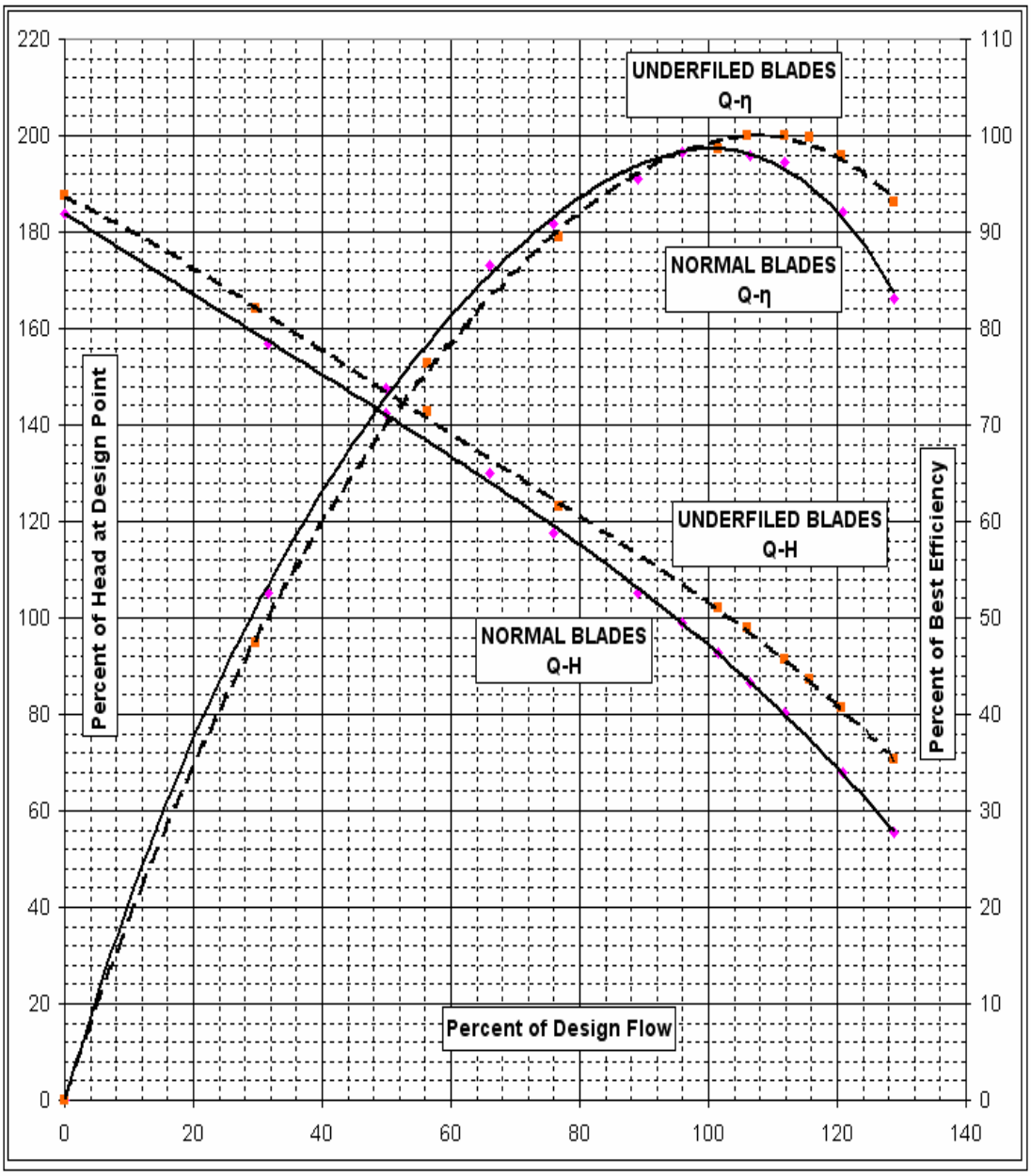

Figure 5.3 Pump performance characteristics for normal and underfiled blades

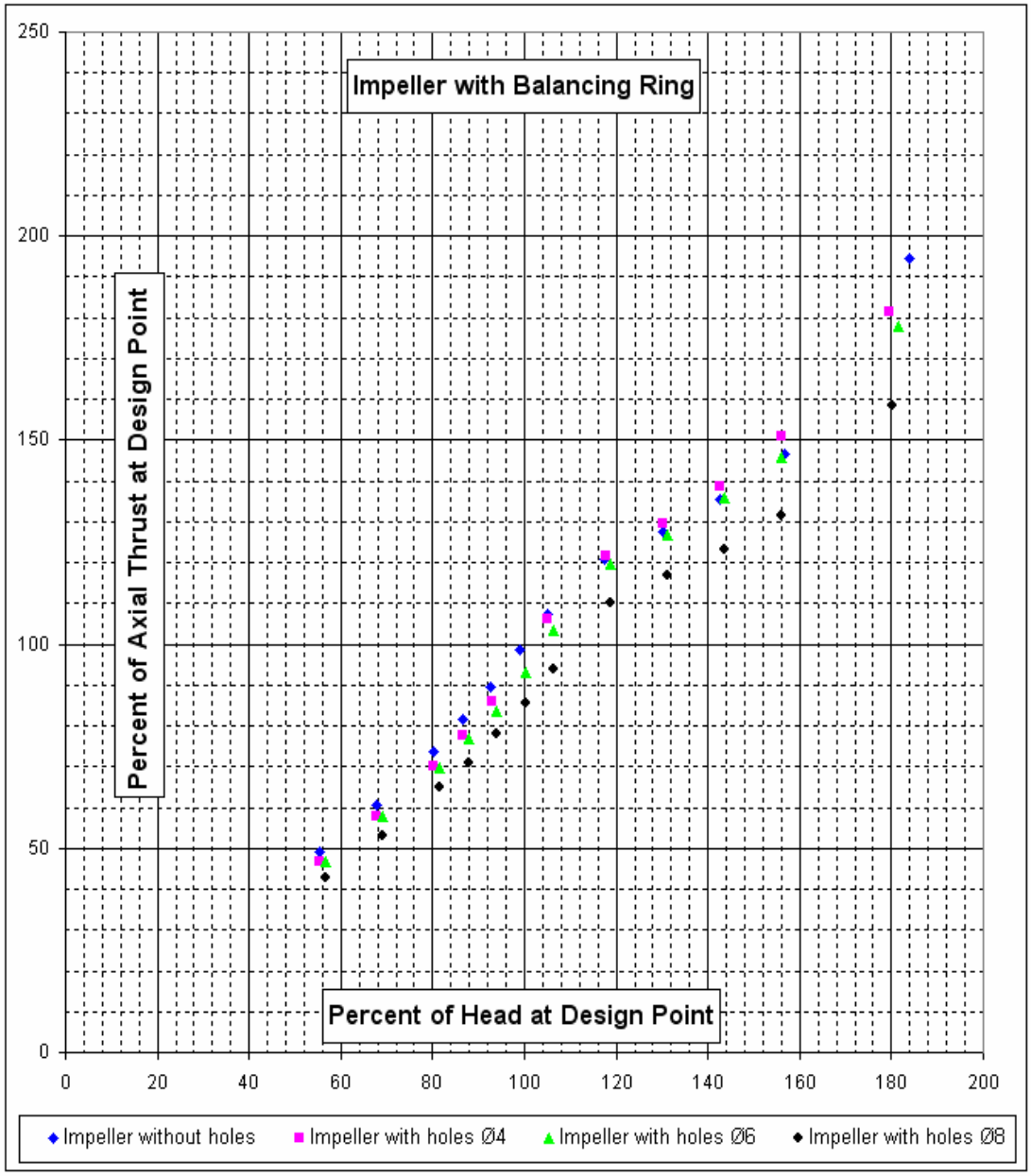

Figure 5.4 Axial thrust versus pump head for impeller with balancing ring

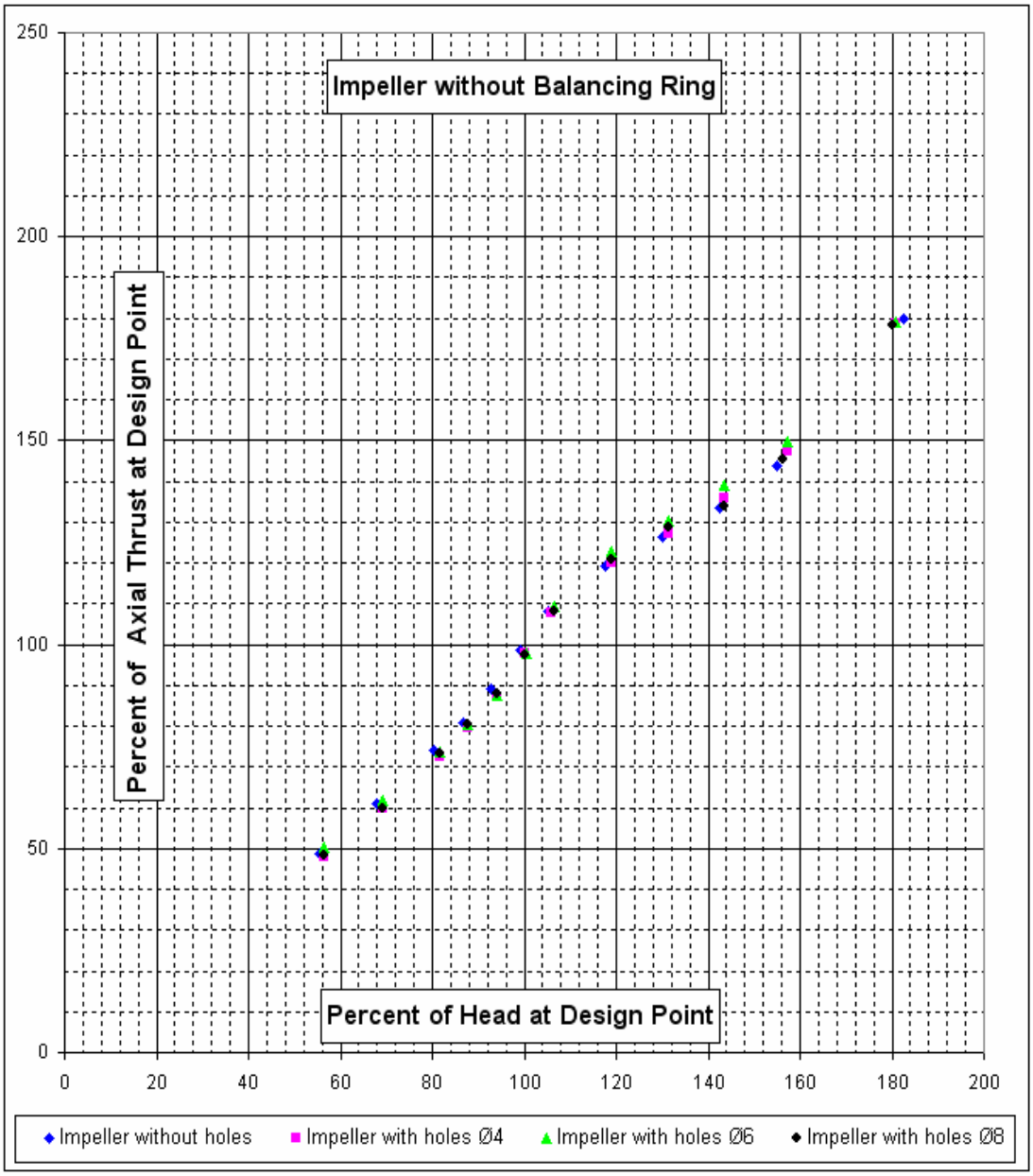

Figure 5.5 Axial thrust versus pump head for impeller without balancing ring

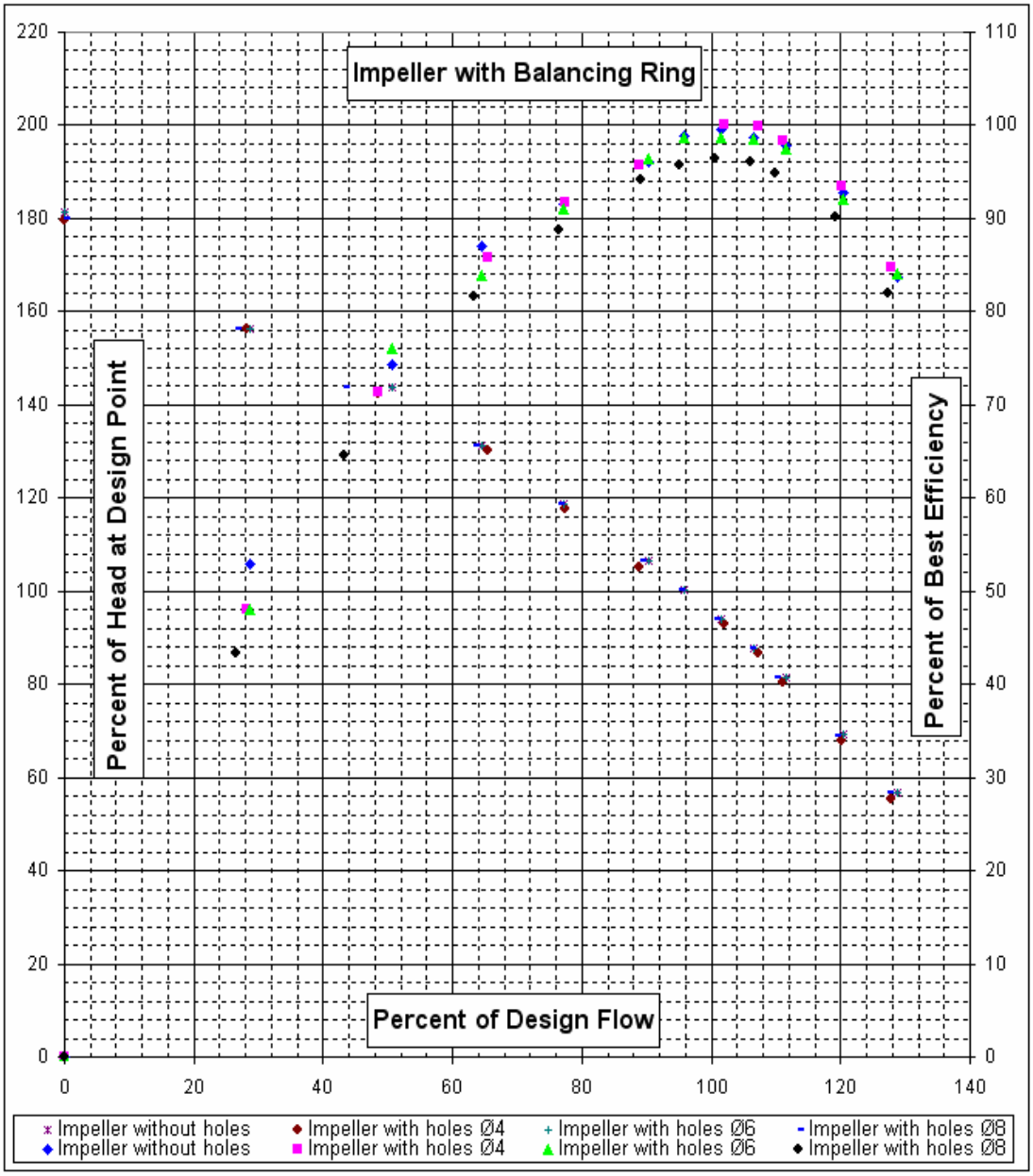

Figure 5.6 Pump performance characteristics for impeller with balancing ring

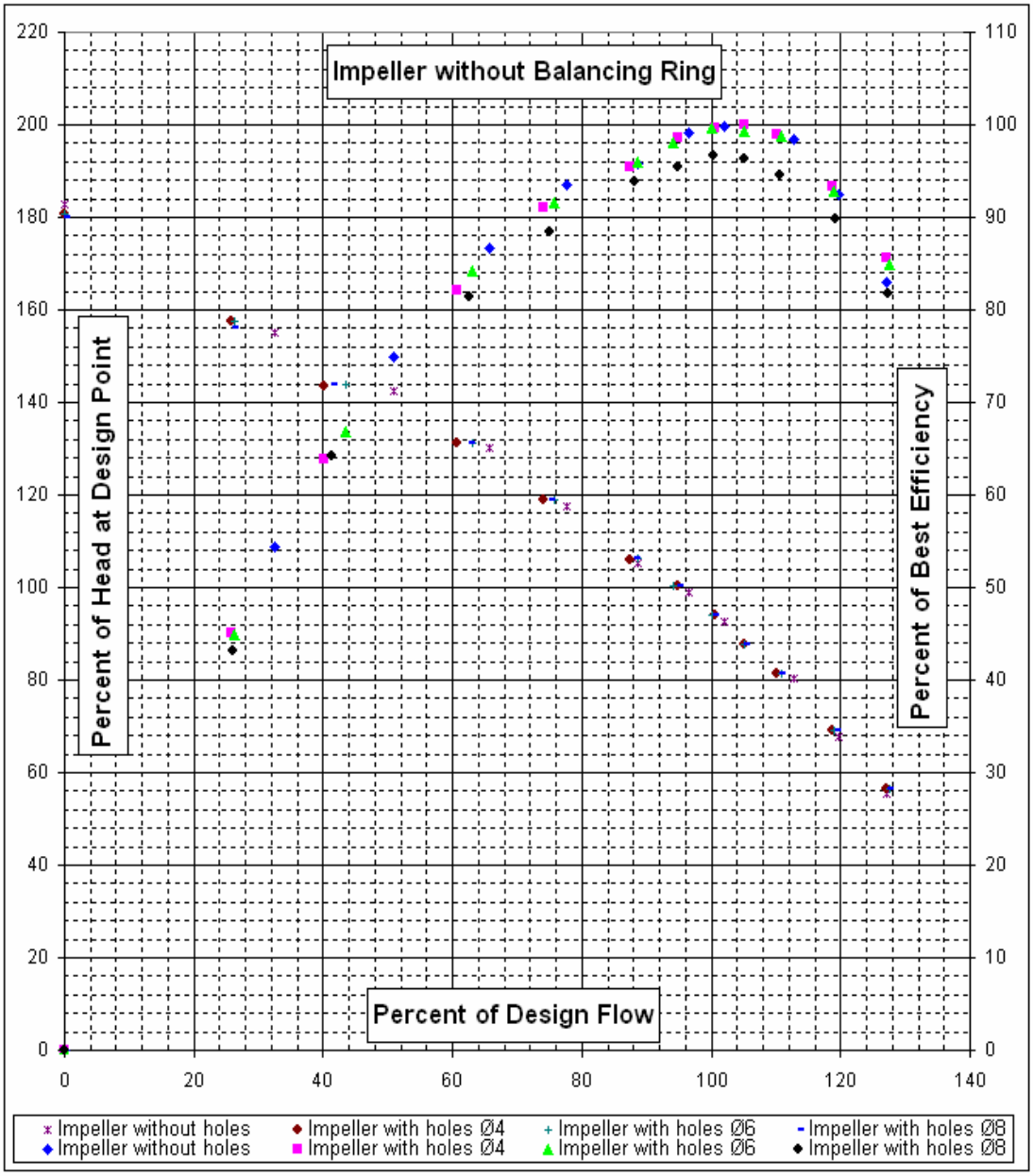

Figure 5.7 Pump performance characteristics for impeller without balancing ring

CHAPTER 6

RESULTS AND CONCLUSION

In this thesis a mixed flow vertical turbine pump is designed, manufactured and tested in Layne Bowler Pumps Company. Design is verified with CFD analyses and axial thrust measurements are also done on the pump. Comparison of test results with CFD analyses and comparison of axial thrust measurements with theoretical approaches are made. Moreover effects of design parameters on the performance characteristics of the pump, CFD analyses systematic, effects of balancing holes and balancing ring on the axial thrust and performance characteristics are also discussed.

Impeller design is divided into three main parts: Impeller meridional profile construction, determining of inlet and outlet angles and forming of the blades from leading edge to trailing edge. Two important points should be considered while meridional profile is developed. These are the head coefficient and the flow coefficient of the pump. They are effective parameters on pump head and best efficiency point of the pump respectively. Impeller exit blade angle and meridional passage area distribution from inlet to outlet are the secondary parameters that also affect these pump properties.

Determination of inlet blade angle is an iterative procedure which includes calculation of inlet constriction coefficient of the pump. Inlet blade angle should be selected correctly to minimize shock losses at the best efficiency point and fluid angle should be aligned with blade inlet angle at design flow rate. Incidence angle, which is the difference between blade angle and flow angle, should be zero for shockless flow to blades. If incidence angle is over zero, stagnation point will be on pressure side of the blade otherwise stagnation point will be on the suction side. Calculation of blade exit angle is also an iterative procedure which is coupled with slip factor (Pfleiderer correction factor – Cp) calculations. Stepanoff's master chart is

therefore a useful design material to find exit blade angle of the impeller easily. Blade number formula, Equation 2.31, is an empirical formula used to check the blade number for designed meridional profile. It is also important to find the length of the bladed region. Length of the blade should be adjusted and changed for assumed blade number. Moment of the mid-streamline and its mean radius could also be changed to achieve desired blade number. Low blade numbers are better from manufacturing point of view. Moreover, recommended blade number is decreasing with increasing specific speeds. On the other hand, if preliminary calculations are done for other streamlines, length of the se streamlines could be changed.

Swirl angle of the blade can be increased in order to increase blade area of the impeller to exert more energy on the fluid and losses due to separation can be reduced with long blades. However, it is seen that under some occasions hydraulic losses become greater than the head which is gained from long (more swirled) blades. On the other hand, high swirled blades are more difficult to manufacture when compared with low swirled blades. Swirl angle of the blades do not impede the manufacturability of the impeller and angle of overlap is selected in limits that is proposed in the references. Length of the blades, blade angle and radius of the design points are the parameters that affect the swirl when Equation 2.39 is investigated. Swirl of the streamlines also define the stacking position of the blades at the trailing edge of the impeller. Leaning the blade against the sense of rotation is a necessity to lower the secondary flows.

Meridional flow cross sectional area of the pump is important to determine the best efficiency point of the pump. Acceleration and deceleration of the fluid in the meridional passage, hydraulic losses, backflows and separations of flow inside the pump depend on meridional flow cross section of the pump. Best efficiency point of the pump could be changed by broadening or contracting the meridional flow area and other flow features can be increased or decreased by doing changes on meridional flow area. Therefore, meridional flow cross sectional area should be clearly developed and a uniform area distribution should be selected throughout the

pump. Throat area of the bowl and interaction area between rotor blades and stator vanes should be also constructed with great attention which has significant effect on pump performance characteristics. A pump family can be created with changing the meridional flow cross section of the pump (impeller or bowl) and therefore changing the best efficiency point of the pump. Meridional velocity ratios across the pump are used as checkpoints for meridional flow passage areas.

Blade thickness of the impeller greatly affects the hydraulic performance of the pump. Suitable blade thickness is advised as 2% of the impeller diameter, [4] if manufacturing abilities are available. It is seen that thinning of the impeller blades increases the efficiency and head of the pump greatly. Wall thickness of the impeller should be selected close to the blade thickness for casting requirements. Blade thickness is also considered while determining blade inlet and outlet angles. Blade outlet angle is another parameter that defines the head of the pump mainly after the diameter of the impeller, Figure 6.1.

Bowl design is a comparatively easy process than impeller design. The main objective is to form a meridional flow area that narrows down uniformly from inlet to exit of the bowl. To avoid from leading edge separation vane inlet angles should be calculated clearly. Sharp curvatures are not used especially in the hub profile where backflows may probably occur. Shroud profile is constructed like an extension of impeller shroud profile to minimize losses. Sufficient inlet area is created in order to benefit underfile operation on the impeller. Pressure recovery in the bowl is considered while determining vane swept and bowl length. Mean pressure at the bowl inlet is 13.5 mwc while it is 15 mwc at the exit of the bowl. On the contrary, vane number of the bowl (stator) is selected regarding blade passing frequency. Same number of vane and blade combinations should be strictly avoided.

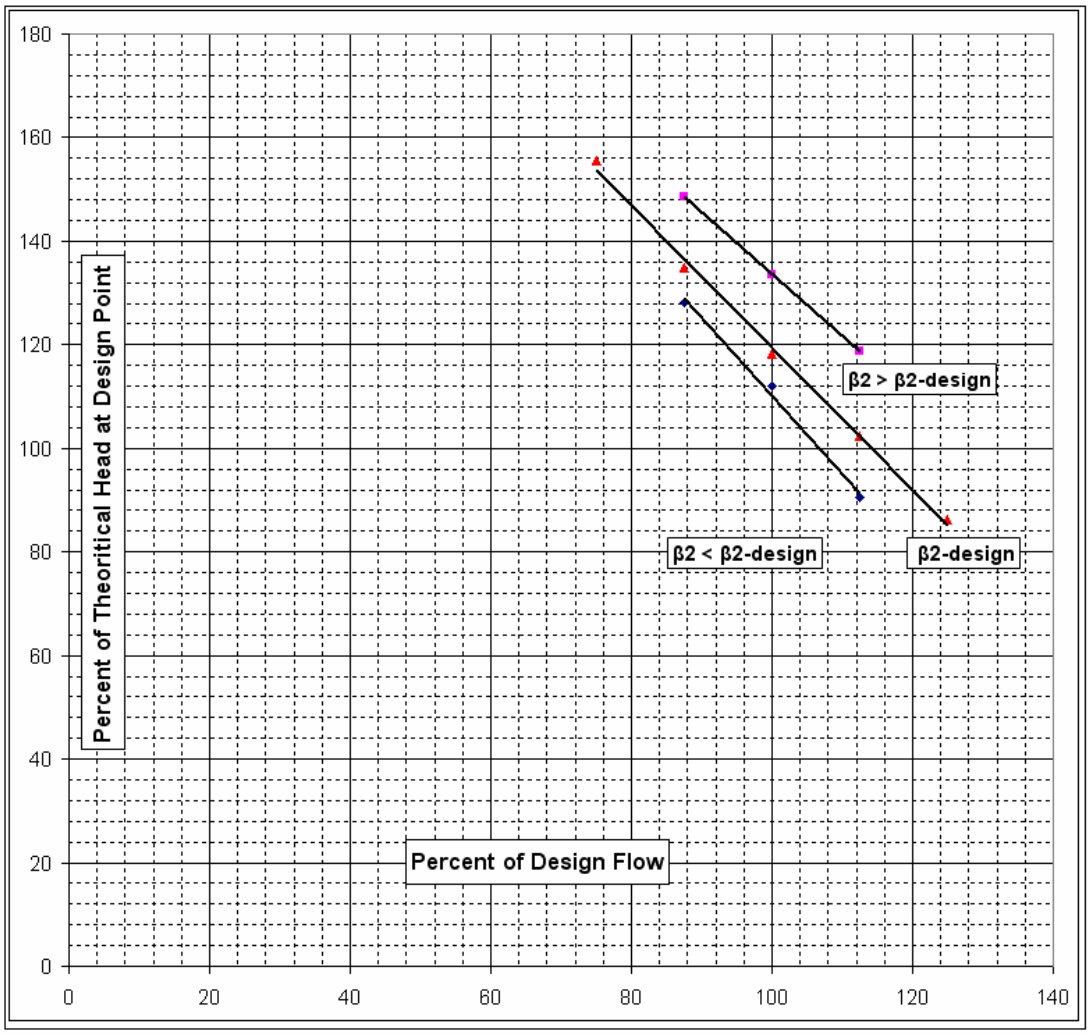

Figure 6.1 CFD results for different blade outlet angles

The degree of reaction, which is the ratio of pressure head at the impeller outlet to theoretical head of the pump, for the designed pump is found as 0.67. Therefore designed pump operates as a reaction pump and pressure energy of the water leaving the impeller takes a large portion of the energy supplied to the fluid, [6].

CFD analyses of a pump assembly require great care and several analyses options should be tried in order to get good results when compared with test results. In order to make a good CFD analysis, CAD model of the pump should be so clear. Any unwanted surface or volume may affect the solution and convergence of analysis. Controlled CAD model preparation is a necessity for this purpose. Boundary

condition definitions to the solution domain greatly affect the flow therefore suitable boundary condition definitions should be selected for pump applications. It is seen that definition of volumetric flow rate at the exit of the pump, pressure and slip – symmetry conditions at the inlet are the best choices for pump analyses. Mesh generation is the most important point for CFD analyses of any geometry. Geometry should be defined efficiently by defining accurate mesh sizes on the solution domain. Especially fine mesh sizes should be used where the gradients are mostly occurred such as rotating region of pump, impeller and bowl volume. There should not be so much difference in mesh sizes of adjacent volumes. Approximately 1.5 million elements are appropriate for pump analyses. In most of the analysis volumetric efficiency of the pump is ignored and leakage path is blocked. This is also a necessity to use fewer elements and to lower the analysis solution time because small flow gaps and crevices make meshing process and solution time excessively long. More powerful computers such as clusters or workstations enable user to use more elements and significantly decrease the analyses solution time. On the other hand, mesh independency could not be achieved for pump analyses.

Volumetric efficiency of the designed pump is investigated in one of the analyses and it is found to be 0.95. The solution is done at the best efficiency point of the pump (40 l/s) and leakage flow rate is found as 2.1 l/s. Therefore, calculated volumetric efficiency is used for other analyses to find overall efficiency of the pump. Mechanical efficiencies are assumed as 0.96. Pump efficiency is found by multiplying hydraulic efficiency (which comes from CFD analyses), volumetric efficiency (which is analyzed for best efficiency of the pump), and assumed mechanical efficiency. On the other hand, system efficiencies are measured in tests and converted into pump efficiency by dividing it into electric motor efficiency. Catalogue of the electric motor manufacturer, [26] is used for this purpose.

Hydraulic torque is the output of the program which is calculated for the rotating region where it is defined. Miscalculation of the torque by the solver results in deviation in the efficiency curve but it can be said that it resembles the original curve

and shows the same trend as that is in the test. Solution results also depend on specific speed, geometry and flow rate of the pump. Moreover, very accurate results are obtained for head characteristics of the pump. CFD analyses are done for one stage pump and multiplied by five to compare with test results of the five stages pump assembly.

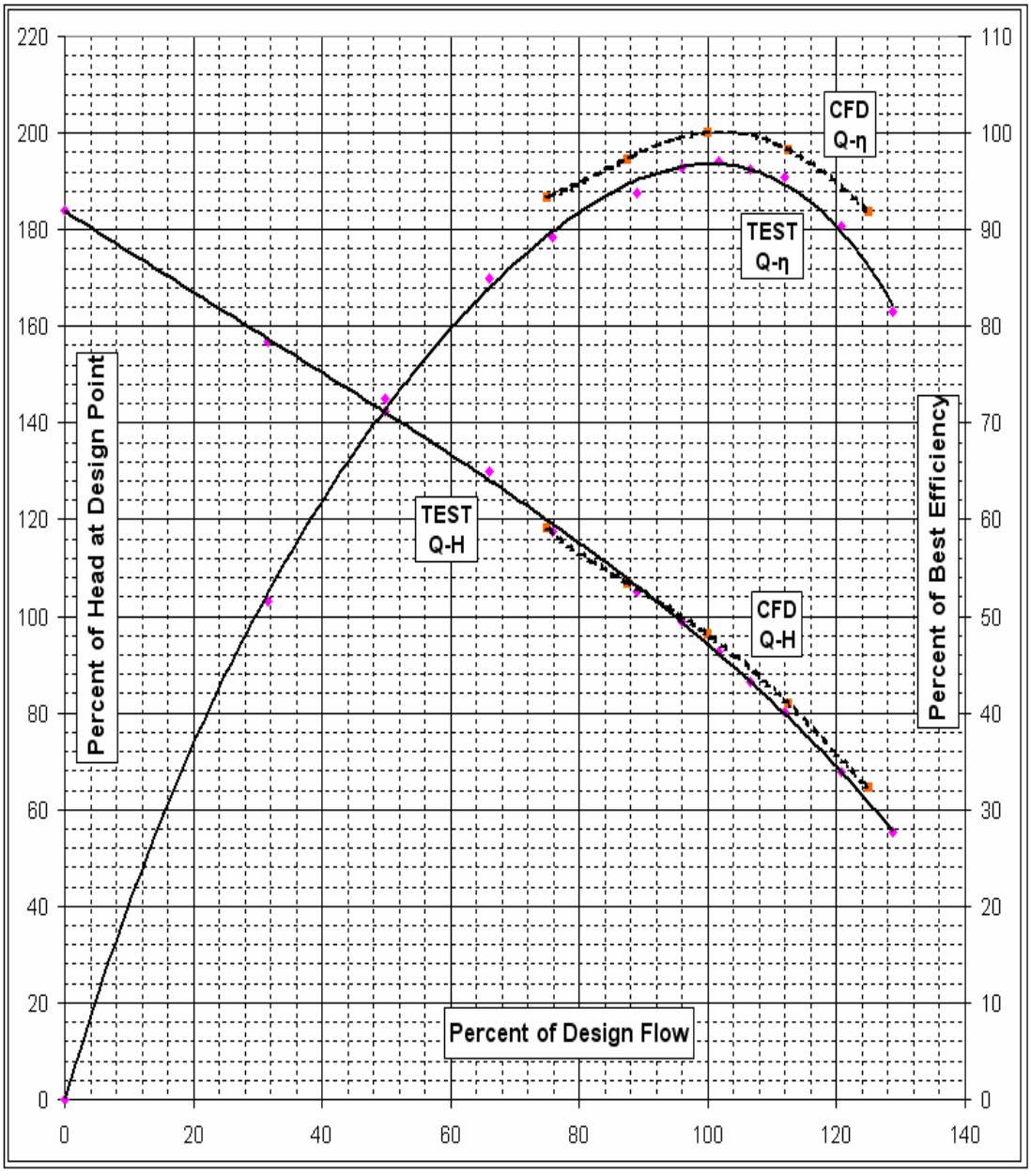

Figure 6.2 Comparison of test and numerical experimentation of pump performance characteristics

At iterations where it coincides with a full revolution (for example 120 iterations) a jump occurs due to overlap therefore analyses should be ended in non-integer revolution numbers (iteration steps). Ramping up impeller speed gradually can be considered as another analysis option but it needs much more iteration steps for convergence.

Pressure distribution over the blade seems to be uniformly distributed. Relative velocity distribution at the mid-streamline shows that velocity loading and diffusion rate ratios are quite acceptable. Diffusion in the impeller is not rapid therefore there is no boundary layer separation throughout the impeller. The impeller is mainly loaded in the forepart. Better performance characteristics could be achieved if loading is shifted towards middle part of the blades.

Diffusion rate for mid-streamline – AA,

$$DR = \frac{W_{min}}{W_{inlet}} = \frac{7.4}{11.1} = 0.67$$

Velocity loading for mid-streamline – AA at $\dot{m} = 0.1$,

$$\zeta = \left[\frac{W_{SS} - W_{PS}}{\frac{1}{2}(W_{SS} + W_{PS})} \right] = \frac{12.8 - 7.8}{0.5(12.8 + 7.8)} = 0.49$$

Diffusion rate and velocity loading values are in the limits that are proposed.

Test results for axial thrust measurements are so close to the theoretical values, Figure 6.3. Moreover, CFD analyses are not so far away from test results and they may be used with applying a coefficient on them. Since the leakage path is not

meshed, there is no pressure exerted on the front shroud of the impeller. Therefore, CFD results are 13% higher than actual test results on the designed flow rate.

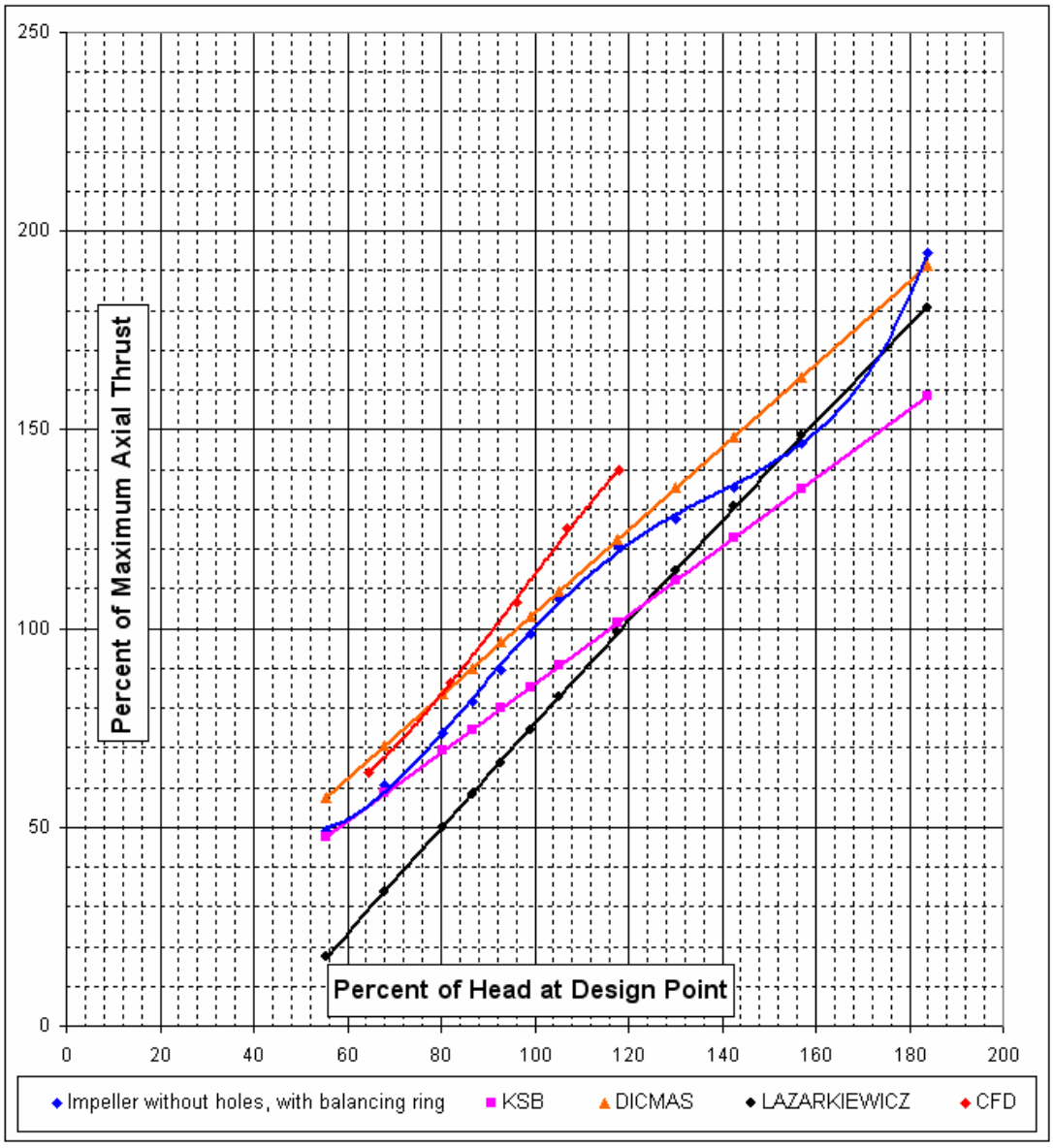

Figure 6.3 Comparison of test, CFD and theoretical results of axial thrust

It is seen that from the axial thrust measurements, considerable axial thrust decrease is not observed with balancing holes drilled at the back face of the impeller. Measured values are almost same except the one which is at the closed valve. This is because lateral surface of the balancing ring is so small to provide sufficient leak

proofing of the fluid. Therefore, radial clearance between balancing ring and stationary part should be decreased and length of the balancing ring should be increased, Figure 6.4. More lateral surface ensures less leakage to the inlet of the impeller from balancing holes and pressure in the balancing chamber is decreased considerably which results in low axial thrust. Effect of the length of balancing ring on the axial thrust is tested on another impeller which has long balancing ring length. It is observed that axial thrust is decreased 60% at the best efficiency point of the pump with balancing ring and 6 mm diameter balancing hole. However, these tests could not be done on the designed impeller because model of the pump must be changed in order to do these tests.

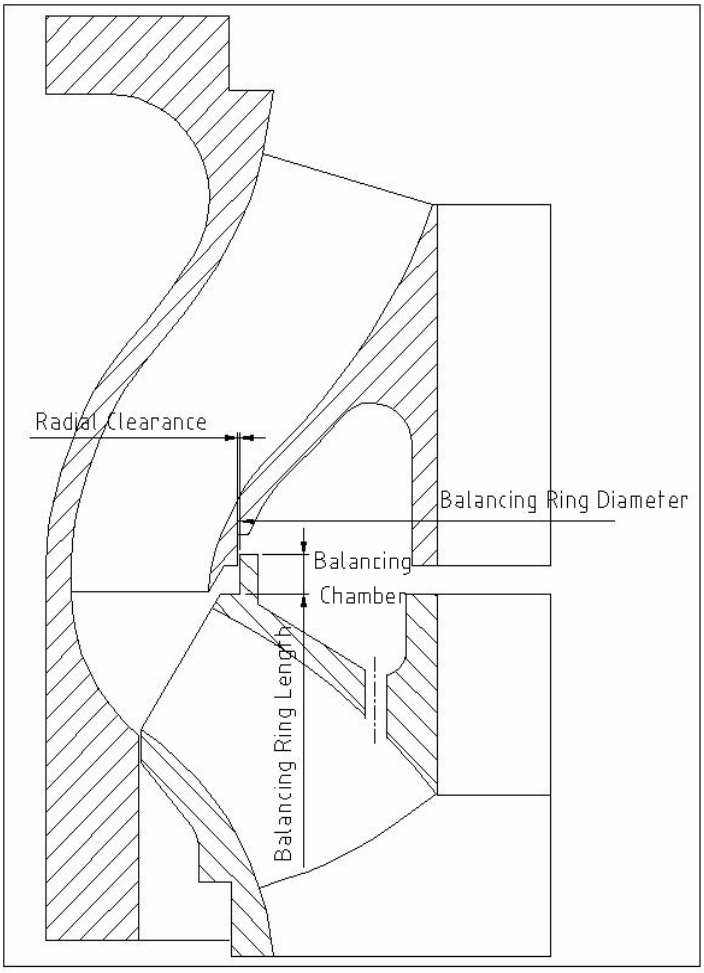

Figure 6.4 Balancing ring dimensions

Head characteristics are obtained so similar in all of the tests. The pump efficiency do not decrease until 8 mm diameter holes are drilled at the back face of the impeller. There is 2% decrease in the performance of the pump at the best efficiency point with 8 mm diameter hole when compared with the others. Diameter of the holes could not be increased more than 8 mm because bigger holes begin to impair the hub of the impeller. Finally, balancing holes without balancing ring do not have any effect on the axial thrust of the pump as seen in Figure 5.5.

In conclusion, meridional profile development is the most important step of the design and empirical formulae take great part in the design process. From this point of view composing a meridional profile library which consists of robust and efficient designs will guide further designs. Moreover, numerical experimentations help designer to understand the flow inside the pump better. Design and numerical experimentation results are in the tolerances as stated in the standard, [25]. Lastly, balancing holes with balancing ring are necessary to decrease axial thrust and to lower the cost of the pump by reducing dimension, capacity or number of the axial thrust balancing devices.

REFERENCES

1. Dicmas, J. L. (1987) *Vertical turbine, mixed flow and propeller pumps*, McGraw – Hill Inc., U.S.A.
2. *Layne Bowler pompa kataloğu* (2006) Layne Bowler Pompa Sanayi A.Ş., Ankara.
3. Anderson, H. H. (1986) *Submersible pumps and their applications*, *1st Ed*, The Trade and Technical Press Limited, England.
4. Karassik, I., Messina, J.P., Cooper, P., Heald, C.C. (2001) *Pump handbook third edition,* McGraw – Hill Inc., U.S.A.
5. Munson, B.R., Young, D.F., Okiishi, T.H. (2000) *Fundamentals of fluid mechanics,* John Wiley & Sons Inc., U.S.A.
6. Lazarkiewicz, S., Troskolañski, A. T. (1965) *Impeller pumps*, Pergamon Press Ltd., Oxford.
7. Yücel, M. (1999) *Development of axial thrust measuring techniques and effects of balancing holes for radial pumps.* M.Sc. Thesis, ODTÜ, Ankara
8. İTÜ-MAK351. (2003) *İstanbul Teknik Üniversitesi Hidrolik Makinalar Ders Notları* İTÜ, İstanbul
9. Stepanoff, A. J. (1957) *Flow pumps design, and application*, John Wiley & Sons Inc., U.S.A.
10. Japikse, D. (1997) *Centrifugal pump design and performance*, Consepts ETI, U.S.A.
11. *Centrifugal Pump Lexicon* (1990) KSB, Germany.
12. Üçer, A. (1980) *Turbomachinery*, ODTÜ, Ankara
13. Spring, H. (1992) *Affordable quasi three-dimensional inverse design method for pump impellers*, U.S.A.
14. Tuzson, J. (2000) *Centrifugal pump design,* John Wiley & Sons, Inc., U.S.A.
15. Westra, R. (2005) *An inverse design method for centrifugal pump impellers.* University of Twente, The Netherlands.
16. Zangeneh, M. (1999) *On the role of three dimensional inverse design methods in turbomachinery shape optimization,* Proc.Instn.Mech.Eng., Vol. 213, Part C

17. Van Esch, B.P.M. (1997) *Simulation of three-dimensional unsteady flow in hydraulic pumps*, Ph.D. Thesis, University of Twente, The Netherlands.
18. Spring, H. (1993) *Judge the pump hydraulic design through numbers before you buy*, U.S.A.
19. *Layne Bowler training materials* (2006) Layne Bowler Pompa Sanayi A.Ş., Ankara.
20. *Impeller engineering data*, (2007), Johnston Pump Company, USA
21. *Puls Elektronik yük hücresi kataloğu* (2006), İstanbul
22. Özgen, O. (2006) *Design improvements on mixed flow pumps by means of computational fluid dynamics.* M.Sc. Thesis, ODTÜ, Ankara
23. *CFdesign user's guide version 9.0* (2006) Blue Ridge Numerics, Inc., Charlottesville.
24. Pfleiderer, C., Petermann, H. (1978) *Akım makinaları*. Çeviren Edis K., Tekin Y., İTÜ Makina Fakültesi Yayını, İstanbul
25. *Rotodinamik pompalar – Hidrolik performans kabul deneyleri – Sınıf 1 ve Sınıf 2, TS EN ISO 9906* (2002) Türk Standardları Enstitüsü, Ankara.
26. *Gamak elektrik motorları kataloğu* (2007), İstanbul

APPENDIX A

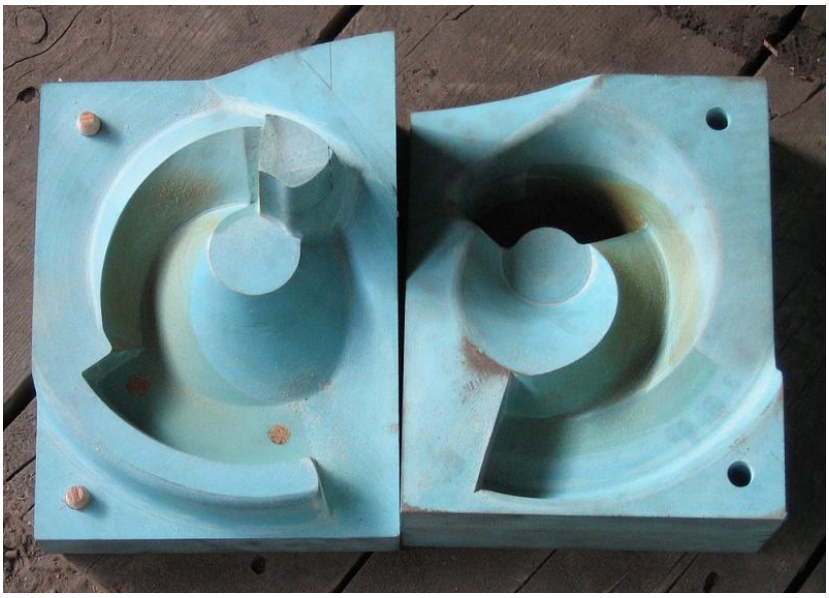

Figure A.1 Core box of impeller

Figure A.2 Core box of bowl

Figure A.3 Impeller

Figure A.4 Bowl

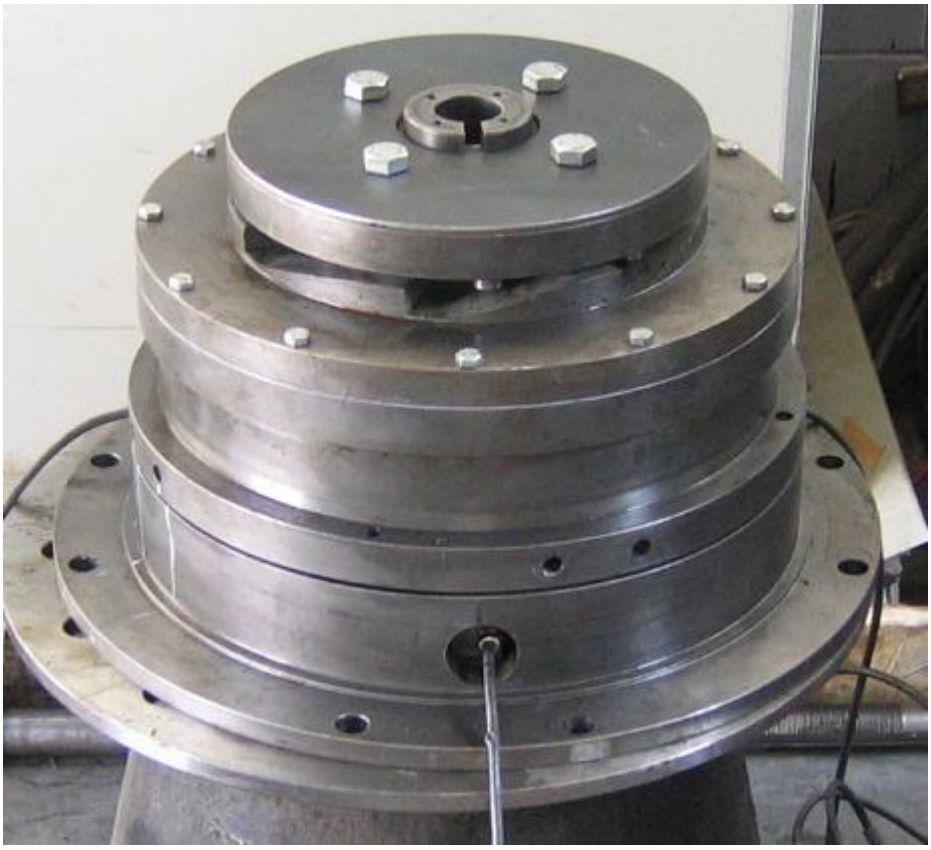

Figure A.5 Thrust bearing assembly with load cells

Figure A.6 Pump assembly and motor

APPENDIX B

SAMPLE UNCERTAINTY CALCULATION

Uncertainty calculation of the vertical turbine pump tests are done as mentioned in the standard TS EN ISO 9906, [25]. Sample uncertainty calculation is done for 20 l/s. At least 3 readings are needed for uncertainty calculation at operation point.

Table B.1 – Test data for best efficiency point

Reading Number	H_m (m)	Q (l/s)	H_{dyn} (m)	P (kW)
1	10.87	20.05	3.02	41.32
2	10.89	20.01	3.01	41.33
3	10.88	20.04	3.01	41.31
4	10.87	19.98	3.03	41.35
5	10.86	20.02	3.02	41.32
6	10.88	20.05	3.02	41.30
7	10.87	20.02	3.03	41.34
8	10.87	20.06	3.02	41.33
9	10.88	20.00	3.02	41.34
10	10.89	19.99	3.02	41.31
average	10.88	20.02	3.02	41.33

The total uncertainty of a measurement U_T is calculated using systematic uncertainty U_S and random uncertainty U_R;

$$U_T = \sqrt{U_S^{\,2} + U_R^{\,2}} \tag{B.1}$$

The random uncertainty of a measurement is defined as two times the standard deviation, [23]. The standard deviation is calculated as;

$$s = \sqrt{\frac{(x_1 - \bar{x})^2 + (x_2 - \bar{x})^2 + \ldots + (x_n - \bar{x})^2}{n}} \qquad \text{(B.2)}$$

Where $\bar{x}$ is the average value of the measurements, x_1, x_2, x_3, …, x_n are the measurement values and n is the total number of measurements. The standard deviation, the absolute random uncertainty and the random uncertainty are tabulated below for each measured quantity.

Table B.2 – Values for standard deviation and random uncertainty for each measured quantity

	H_m (m)	Q (l/s)	H_{dyn} (m)	P (kW)
Standard deviation	0.132	0.026	0.006	0.015
Absolute random Uncertainty	0.264	0.052	0.012	0.030
Random Uncertainty (%)	0.237	0.260	0.419	0.073

Systematic uncertainty depends on the sensitivity of the instrument or method used in measurements and do not change with repeating measurements, [25]. Systematic uncertainty is found by the help of calibration certificates of the instruments.

Table B.3 – Values of systematic uncertainty for each measured quantity

H_m (%)	Q (%)	H_{dyn} (%)	P (%)
2.52	0.74	0.01	1.26

Now, total uncertainty can be calculated using Table B.2 and B.3 with the formula given in Equation (B.1).

Table B.4 – Values of total uncertainty for each measured quantity

H_m (%)	Q (%)	H_{dyn} (%)	P (%)
2.53	0.78	0.42	1.26

The total head of the pump, H_t, is calculated as;

$$H_t = H_m + H_{dyn} + \frac{V_f{}^2}{2.g} \tag{B.3}$$

H_m is the manometric head, H_{dyn} is the dynamic water level and V_f is the velocity of the fluid where the pressure reading is done. Therefore V_f is calculated by dividing flow rate to the cross-sectional area, A_p, of the pipe.

$$V_f = \frac{Q}{A_p} \tag{B.4}$$

The total uncertainty of velocity of the fluid U_{T_f} is calculated using the cross sectional area of the pipe which is 0.018 m^2

$$U_{T\_f} = \frac{1}{A_p} U_{T\_Q} \tag{B.5}$$

U_{T_Q} is the total absolute uncertainty of flow rate.

$$U_{T\_f} = \frac{1}{0.018} 0.0002$$

$$U_{T\_f} = \pm 0.009 \text{ m/s}$$

Dividing the result by the nominal value of V_f total uncertainty of the velocity of pumping fluid is found to be 0.78 %.

The total uncertainty of the total head, U_{T_Ht} is calculated as,

$$U_{T\_Ht} = \pm\sqrt{U_{T\_Hm}{}^2 + U_{T\_Hdyn}{}^2 + (\frac{V_f}{g}U_{T\_Vf})^2} \quad \text{(B.6)}$$

Substituting the absolute values for each total uncertainty into Equation (B.6),

$$U_{T\_Ht} = \pm\sqrt{2.81^2 + 0.01^2 + (\frac{1.13}{9.81}0.01)^2}$$

$$U_{T\_Ht} = \pm 2.81 \text{ m}$$

Total uncertainty is calculated as 2.46% by dividing the absolute total uncertainty value of H_t to its nominal value.

The density is taken as constant throughout the experiments. A graded cylinder is used to calculate the density of the fluid. Then, density of the fluid is found by dividing mass of the fluid to its volume.

$$\rho_f = \frac{m}{V} \quad \text{(B.7)}$$

1±0.01 liter of fluid's mass is measured as 1±0.002 kg. The total uncertainty of the fluid density is calculated using the Equation (B.8),

$$U_{T\_\rho} = \pm\sqrt{(mU_{T\_V})^2 + (\frac{1}{V}U_{T\_m})^2} \quad \text{(B.8)}$$

Where U_{T_V} is the total uncertainty of the graded cylinder and U_{T_m} is the total uncertainty of the measured mass of the fluid.

$$U_{T\_\rho} = \pm\sqrt{(1\cdot 10^{-5})^2 + (\frac{1}{10^{-3}}\cdot 2\cdot 10^{-3})^2}$$

$$U_{T\_\rho} = \pm 2 \text{ kg/m}^3$$

The system efficiency of the pump-motor assembly, η_s, is calculated as,

$$\eta_s = \frac{\rho g Q H_t}{P} \tag{B.9}$$

The total uncertainty of the system efficiency (wire to water efficiency), $U_{T\_\eta s}$ is derived from Equation (B.9),

$$U_{T\_\eta s} = \left[\begin{array}{l}\left(\frac{gQH_t}{P}U_{T\_\rho}\right)+\left(\frac{\rho gH_t}{P}U_{T\_Q}\right)+\left(\frac{\rho gQ}{P}U_{T\_Ht}\right)\\ +\left(\frac{\rho gQH_t}{P^2}U_{T\_P}\right)\end{array}\right] \tag{B.10}$$

Then calculated values are substituted into Equation (B.10):

$$U_{T\_\eta s} = \sqrt{\left[\begin{array}{l}\left(\frac{9.81\cdot 0.020\cdot 114.21}{41325}\cdot 2\right)^2+\left(\frac{1000\cdot 9.81\cdot 114.21}{41325}\cdot 0.0002\right)^2\\ +\left(\frac{1000\cdot 9.81\cdot 0.020}{41325}\cdot 2.81\right)^2+\left(\frac{1000\cdot 9.81\cdot 0.020\cdot 114.21}{41325^2}\cdot 0.522\right)^2\end{array}\right]}$$

$$U_{T\_\eta s} = \pm 1.41 \ \%$$

Total uncertainty is calculated as 2.59% by dividing the absolute total uncertainty value of η_s to its nominal value.

The results are tabulated below for the uncertainty analysis and compared with the limits given in TS EN ISO 9906, [25].

Table B.5 – Comparison of total uncertainty percentages and their limits in the regarding standard, [25]

Parameters	Class – 1 Limits (%)	Class – 2 Limits (%)	Calculated Uncertainties (%)
Flow Rate, Q	± 2.0	± 3.5	± 0.78
Total Head, H_t	± 1.5	± 5.5	± 2.46
Power P	± 1.5	± 5.5	± 1.26
Efficiency, η_s	± 2.9	± 6.1	± 2.59

The calculated uncertainties satisfy the limitations of Class-2 experiments given in the standard, [25].